Amino acid dependence in acute myeloid leukaemia

Randal Leslie Stronge

The Institute of Cancer Research

And

The Royal Marsden Hospital

Thesis submitted for the degree of Doctor of Medicine

To

The University of London

Author’s declaration

I declare that I am the sole author of this thesis and that the data presented here represent my personal research conducted whilst a clinical research fellow at the Institute of Cancer Research and the Royal Marsden Hospital.

Data generated in collaboration with others is acknowledged fully within the text.

Dr Randal Stronge

December 2021

Details of collaboration

All of the experimental work described in this thesis was performed by me with the exception of the following:

General

Many of the bone marrow and peripheral blood samples were collected by the minor procedures team at the Royal Marsden Hospital. Diagnostic immunophenotyping, cytogenetic or molecular results to which I refer in the sample characteristics were performed by the relevant departments at the Royal Marsden Hospital.

PB and BM samples were processed by Dr Farideh Miraki-Moud or myself.

Chapter 5: Measuring amino acid uptake by Liquid Chromatography Mass Spectrometry

Dr Florence Raynaud, Dr Akos Pal and Yasmin Asad of the pharmacokinetics and metabolomics team helped with the experimental design of this chapter. Akos and Yasmin supervised the sample preparation for LC-MS, performed the mass spectrometry and assisted with the multivariate analysis.

Chapter 6: Proteomic interrogation of AML

Professor Jyoti Choudhary of the functional proteomics group helped with the planning of this experiment. Dr Theo Roumeliotis carried out the mass spectrometry and analysis.

Abstract

Acute myeloid leukaemia (AML) is a heterogeneous disease which remains curable in only a minority of patients. Outcome is dismal in the subgroup with adverse genetic features. Amino acid (AA) depletion is a therapeutic strategy that is used to deprive malignant cells of nutrients.

This thesis explores the dependence of AML on specific AAs. I show that primary AML cells need valine, methionine and a combination of serine and glycine to survive in culture and that this varies across AML risk groups. Depletion of these causes significantly increased apoptosis when compared to normal bone marrow cells although the combination with cytarabine chemotherapy was no more effective.

This dependence was confirmed using mass spectrometry which demonstrated increased consumption of these AAs in media following co-culture. Intracellular AA levels were difficult to measure consistently due to low cell numbers. Further analysis suggests that adverse risk AML consumes AAs more avidly than intermediate risk AML.

The enzymes of the methionine salvage pathway are strongly expressed in AML consistent with the need for methionine. Further work is needed to elucidate the role of the GCN2/eIF2α/ATF4 integrated stress response pathway.

Analysis of the AML proteome in response to valine and methionine depletion reveals that only a small number of proteins change significantly suggesting that the effect is generally at a metabolomic level. A significant increase in PHGDH, a downstream enzyme in the ISR pathway, was however seen in response to AA depletion.

These data show that AA deprivation is effective in killing primary AML cells *in vitro*. This needs to be tested in combination with other chemotherapy drugs. Potential clinical applications include combining this with conditioning chemotherapy to reduce the AML burden prior to allogeneic stem cell transplantation.

Statement of impact of interruption to study

My MD (res) was first established as a translational project based around an early phase clinical trial investigating an arginine deprivation drug in older patients with AML. Unfortunately, 8 months into my first year the company restructured and the AML portfolio was withdrawn. My project then switched to a wider laboratory based project on amino dependence in AML but a significant amount of time was lost.

Further challenges were encountered in the face of the Covid-19 pandemic. I had 2 separate redeployments to clinical practice amounting to over 6 months. Either side of these, research was further impacted by logistical difficulties mostly in collaborative work. This led to delays in both the metabolomics and proteomics chapters. Ultimately, this prevented further work from being planned and carried out within the time available.

Acknowledgements

The work described in this thesis was carried out whilst I was a clinical research fellow at the Royal Marsden Hospital and Institute of Cancer Research. I am grateful to the Armstrong Foundation who provided the funding for this. I am also thankful to CRUK who provided funding through their Poor Risk AML Programme.

I wish to thank my supervisor, David Taussig, for giving me this opportunity and guiding and supporting me through the unexpected challenges faced over the past few years. Above all I would like to thank him for prompting and fostering my interest in acute leukaemia.

I will be forever grateful to Farideh Miraki-Moud for her support throughout this project. Farideh taught me all the laboratory skills I possess and did so with endless patience. She calmly guided me through the numerous occasions when things did not go to plan in the lab providing encouragement and solutions when needed. This would not have been possible without her.

To Flo Raynaud and her team for their guidance and help throughout the metabolomics part of this project. In particular Akos Pal and Yasmin Asad for introducing me to mass spectrometry with tolerance and humour!

To Jyoti Choudhary, head of the functional proteomics team, for her input in the project design and Theo Roumeliotis for his invaluable help with analysing and understanding proteomic data.

To the minor procedures team at the RMH for helping to provide a supply of blood and bone marrow samples and to all the patients and donors who donated the samples to make this project possible.

And finally to my family.

My parents who have encouraged me to follow my dreams and have always supported me in my chosen path.

My parents-in-law for helping to manage the challenges of research and a young family with endless practical support.

And to Rohan and Aran, both of whom were born during this project. Whilst this added to the challenge at times, they invariably helped me overcome the frustrations of laboratory research and have taught me the need for time management!

Finally to Sinthiya, my wife, for her unwavering love and support throughout this project. You're the best.

Table of contents

List of figures

1: Introduction

2: Materials and methods

3: Measuring AA dependence using co-culture

4: Combining AA deprivation with chemotherapy

5: Measuring AA uptake by Liquid Chromatography Mass Spectrometry

6: Cellular control and compensation in amino acid deprivation

7: Proteomic analysis of AML

List of tables

7: Proteomic analysis of AML

List of abbreviations

AA	Amino acid
ALL	Acute lymphoblastic leukaemia/lymphoma
AML	Acute myeloid leukaemia
ANOVA	Analysis of variance
APML	Acute promyelocytic leukaemia
ARAC	Cytosine arabinoside (cytarabine)
ASXL1	Additional sex comb-like 1
ATF4	Activating transcription factor 4
ATO	Arsenic trioxide
ATP	Adenosine triphosphate
ATRA	All trans retinoic acid
BCAA	Branched-chain amino acid
BM	Bone marrow
CD	Cluster differentiation
CEBPA	CCAAT enhancer-binding protein alpha
CR	Complete remission
DA	Daunorubicin & cytarabine
EDTA	Ethylenediaminetetraacetic acid
eIF2α	Eukaryotic initiation factor 2 alpha
ELN	European LeukemiaNet
FLT3 ITD	Fms-like tyrosine kinase 3 internal tandem duplication
GAPDH	Glyceraldehyde 3-phosphate dehydrogenase
GCN2	General control nonderepressible 2
GMPB	GCSF-mobilised peripheral blood
HILIC	Hydrophilic interaction liquid chromatography

HSCT	Haematopoeitic stem cell transplant
ICR	Institute of Cancer Research
IDH	Isocitrate dehydrogenase
LC-MS	Liquid chromatography mass spectrometry
LSC	Leukaemic stem cell
MAT2A	Methionine adenosyltransferase 2A
MLL	Mixed lineage leukaemia
MR	Methionine restriction
MRC	Medical Research Council
MRD	Measurable residual disease
MS-5	Mouse stromal 5
MTA	Methylthioadenosine
MTAP	Methylthioadenosine phosphorylase
NCRI	National Cancer Research Institute
NPM1	Nucleophosmin 1
OPLS-DA	Orthogonal partial least squares discriminant analysis
OS	Overall survival
OXPHOS	Oxidative phosphorylation
PARP	Poly adenosine diphosphate-ribose polymerase
PHGDH	Phosphoglycerate dehydrogenase
PFS	Progression free survival
PS	Performance statue
PSAT1	Phosphoserine aminotransferase 1
RMH	Royal Marsden Hospital
RUNX1	Runt-related transcription factor 1
SAM	S-adenosyl methionine
TCA	Tricarboxylic Acid

TKD	Tyrosine kinase domain
TMT	Tandem mass tags
TP53	Tumour protein 53
TRM	Treatment-related mortality
VIP	Variable of importance

Chapter 1: Introduction

1.1 Acute myeloid leukaemia

1.1.1 Introduction

Acute myeloid leukaemia (AML) is an aggressive form of cancer characterised by clonal proliferation of abnormally differentiated primitive haematopoietic stem cells or progenitor cells. These cells infiltrate the bone marrow, blood and other tissues [1, 2]. Clinical presentation is variable but often relates to the extent of bone marrow failure – fatigue, haemorrhage or infection – or the degree of leucocytosis. AML can also present with organ infiltration (e.g. myeloid sarcoma or leukaemia cutis). The majority of AML cases arise *de novo* but 25-35% are secondary to prior malignancy, cytotoxic therapy or antecedent myeloid disorders (e.g. myelodysplastic syndrome) [3]. There are over 3000 cases diagnosed each year in the UK. The median age at diagnosis is 68-70 years with a 56% being male [4, 5].

1.1.2 Diagnosis

While the full blood count is often markedly abnormal changes may be subtle. Examination of appropriately stained peripheral blood and bone marrow samples is critical and forms the basis of leukaemia diagnosis. This identifies the number and morphology of the immature blasts and helps to differentiate AML from acute lymphoblastic leukaemia (ALL) whose management is significantly different.

Although not a substitute for morphological assessment, immunophenotyping by multiparameter flow cytometry has become an invaluable tool for the accurate diagnosis and classification of AML [6, 7]. In clinical practice it is also crucial in the rapid distinction of AML from ALL. Diagnostic laboratories identify the presence of blasts based on CD marker expression. The acute leukaemia panel at the Royal Marsden Hospital includes the myeloid markers CD13, CD14, CD33, CD117, HLA DR, CD64 and MPO (myeloperoxidase). CD34 and TdT are also measured along with B

and T cell markers. Immunophenotyping is also used to assess response to treatment through measurable residual disease (MRD) monitoring. MRD negativity is strongly prognostic for treatment outcome [8, 9].

Genetic and molecular results (see below) are used to define the diagnosis in further detail. A full list of myeloid neoplasms and acute leukaemia is defined by the WHO and should be used in clinical practice as it dictates management [10].

1.1.3 Classification

AML is a heterogeneous disease which is reflected in a variable clinical course and outcome. Despite the variable clinical outcome, over half of newly-diagnosed AML patients have a normal karyotype. AML genomes show fewer mutations than most other adult cancers, averaging only 13 found in genes [11, 12]. This suggests that the biology and pathogenesis of AML is driven by a more complex molecular picture. Twenty-three genes have been found to be commonly mutated with a further 237 mutated in 2 or more cases [11, 13].

1.1.3.1 MRC classification

Historically, the disease has been classified by recurrent chromosomal structural mutations which have provided the basis for diagnosis and prognostication [14, 15]. This Medical Research Council (MRC) classification is based on a large number of patients from national MRC trials and is widely used in the UK (table 1.1). Survival data are shown in figure 1.1.

Favourable	**t(8;21)** **t(15;17)** **inv(16)**	**Whether alone or in conjunction with other abnormalities.**
Intermediate	**Normal** **+8** **+21** **+22** **del(7q)** **del(9q)** **Abnormal 11q23** **All other structural/ numerical abnormalities**	**i.e, cytogenetic abnormalities not classified as favourable or adverse.** **Lack of additional favourable or adverse cytogenetic changes.**
Adverse	**-5** **-7** **del(5q)** **Abnormal 3q** **Complex**	**Whether alone or in conjunction with intermediate-risk or other adverse-risk abnormalities**

Table 1.1: MRC cytogenetic risk groups [16].

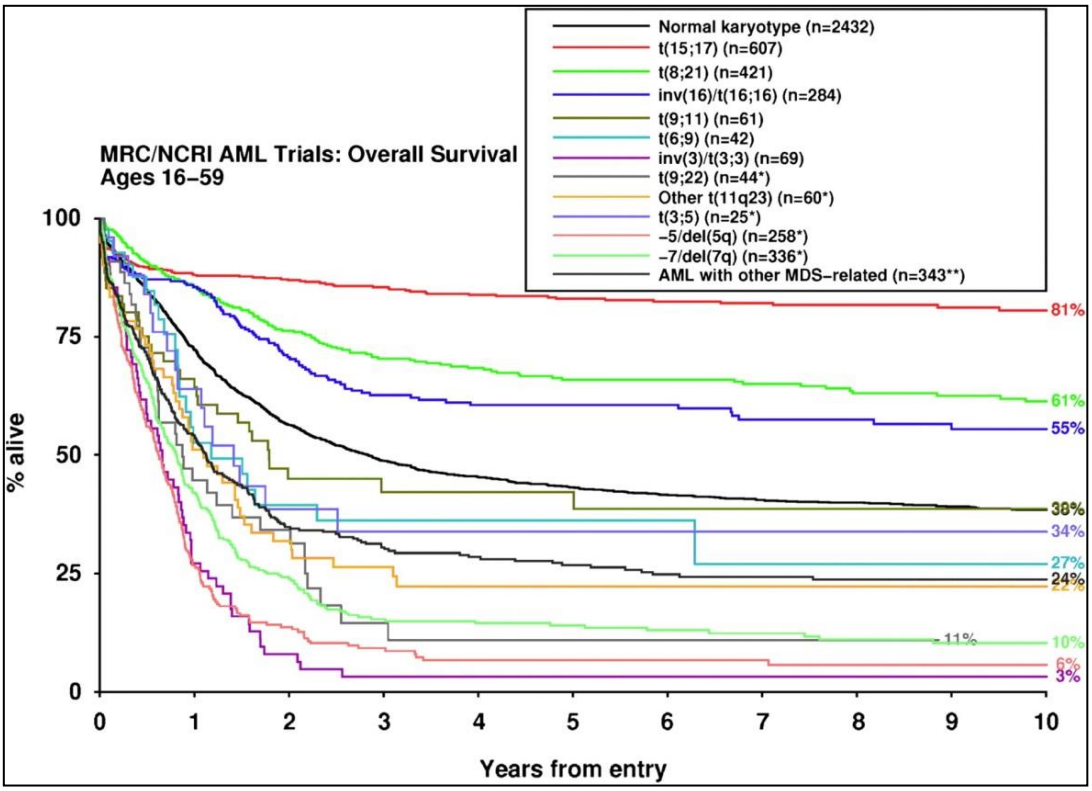

Figure 1: Overall survival according to karyotype in younger adult AML patients [15]

1.1.3.2 ELN classification

The European LeukemiaNet (ELN) has published guidelines on the management and classification of AML [14]. As outlined in table 1.2, this differs from the MRC as it incorporates molecular mutations. Initiating mutations in Nucleophosmin 1 (NPM1) and activating mutations in the *fms*-like tyrosine kinase 3 (FLT3) receptor are seen more commonly in patients with normal karyotype [17, 18].

Lesions included in the ELN classification are those that are disease defining (NPM1, CEBPA and RUNX1), those that are prognostic and targetable (FLT3) and those that are associated with adverse prognosis (TP53 and ASXL1) [19-21].

Favourable	**t(8;21)(q22;q22.1);*RUNX1-RUNX1T1*** **inv(16)(p13.1q22) or t(16;16)(p13.1q22); *CBFB-MYH11*** ***NPM1*mut without *FLT3*-ITD or with *FLT3*-ITD^{low}** **Bialleleic mutated *CEBPA***
Intermediate	***NPM1*mut and *FLT3*-ITD^{high}** ***NPM1*wt without *FLT3*-ITD or with *FLT3*-ITD^{low} (without adverse-risk genetic lesions)** **t(9;21)(q21.3;q23.3); *MLLT3-KMT2a*** **Cytogenetic abnormalities not classified as favourable or adverse**
Adverse	**t(6;9)(p23;q34.1); *DEK-NUP214*** **t(v; 11q23.3); *KMT2A* rearranged** **t(9;22)(q21.3q26.2); *BCR-ABL1*** **inv(3)(q21.3q26.2) or t(3;3)9q21.3;q26.2);** ***GATA2,MECOM(EVI1)*** **-5 or del(5q); -7; -17/abn(17p)** **Complex karyotype, monosomal karyotype** ***NPM1*wt and *FLT3*-ITD^{high}** **Mutated *RUNX1*** **Mutated *ASXL1*** **Mutated *TP53***

Table 1.2: ELN-2017 AML risk classification [14].

NPM1 is nucleolar chaperone protein found in proliferating cells and has a number of cellular functions [22]. It is overexpressed in a number of malignancies including AML. Mutations alter the DNA-binding domain resulting in aberrant nuclear export [23]. NPM1 mutations occur late in leukaemogenesis, occur in about 30% of adults with *de novo* AML and are rarely seen in secondary AML [24]. As its expression remains relatively stable in the disease course it is widely used as an MRD marker. In those with a normal karyotype NPM1 mutations have an improved overall survival (OS) and lower relapse rates [25].

FLT3 is the most common somatic mutation found in AML. FLT3 is a transmembrane ligand-activated receptor tyrosine kinase that is expressed by normal haematopoietic stem cells and progenitor cells. An extracellular ligand binds and activates cell survival and differentiation When mutated it leads to aberrant proliferation [26]. Internal tandem duplication (ITD) mutations are the most common and, together with TKD (tyrosine kinase domain) mutations, occur in around 35% of *de novo* AML cases [22]. They carry a strong negative prognostic significance [27].

1.1.3.3 Further classification

Other lesions that are frequently tested include IDH1 and 2 which are both targetable with oral chemotherapy [28]. Our knowledge of the genomic landscape of AML is evolving rapidly [29]. The 2 classification systems described above incorporate only a handful of molecular lesions. Next generation sequencing is an emerging field with the potential of identifying those who will develop AML, tailoring individual treatment regimens and monitoring responses more accurately.

1.1.4 Treatment

AML is treatable, but curable in only a minority of patients. While 80% achieve complete morphological remission (CR) after induction chemotherapy most relapse. 5 year overall survival is only 25-40% [30, 31].

Treatment decisions in AML are largely determined by risk stratification, age or 'fitness' of patient. This generally falls into 3 categories: younger patients treated with intensive therapy with or without haematopoietic stem cell transplantation (HSCT), older patients fit for intensive therapy and older patients deemed unfit for intensive treatment [32].

For those deemed 'fit', the backbone of intensive therapy, daunorubicin with cytarabine (DA), has been the standard of care induction regimen worldwide for more than 40 years. In the UK, this is generally delivered through the MRC clinical trial, the current incarnation being *AML19* (or *AML18* for those >60). For those under 60, the complete remission (CR) rate is approximately 75% but treatment-related mortality (TRM) is significant and often unacceptably high. Much of this is caused by infectious complications or organ dysfunction exacerbated by comorbidities [33].

Relapse rates are high so induction is followed by further cycles of consolidation chemotherapy, generally cytarabine with or without an anthracycline [34]. AML is the most common indication for HSCT worldwide [35]. Historically, allogeneic transplantation was reserved for high-risk patients including those requiring salvage therapy but our understanding has become more nuanced in recent years. Reduced intensity conditioning regimens, increasing donor options and a better understanding of graft-versus-leukaemia (GvL) effect has led to the transplantation of older patients or those in who it was not previously considered. Many UK centres would now consider the toxicity acceptable in those up to 75 years [36]. Advances in measurable residual disease (MRD) monitoring and accurate genomic classification have improved the selection of candidates and the optimum time to consider transplantation [35].

Therapeutic options for older 'unfit' patients, or those in whom intensive treatment is not appropriate, remain limited. Patient-related factors, such as impaired organ function, along with more frequent adverse genetic features and increased resistance to treatment render many unsuitable for conventional intensive induction regimens [37, 38]. Low-dose cytarabine, hypomethylating agents (eg azacitidine) and palliation have formed the basis of treatment. Azacitidine, for example, has a median OS of 10.4 months in those ≥65 years with newly diagnosed AML [39]. Advancements in this age-group have been limited by ineffectiveness of therapy [32]. With over half of newly

diagnosed AML cases being defined as ‘older’ there is a huge unmet need for progress in this age group.

Progress is being made however. The FDA has approved 8 new drugs for AML in the past 5 years although toxicities and low cure rates remain a problem [31, 40, 41]. In addition, venetoclax, a B-cell lymphoma (BCL)-2 inhibitor, significantly improves OS in elderly patients when used with hypomethylating agents and has also been granted FDA approval [42]. NICE has just approved this for use in those in whom intensive treatment is unsuitable. Table 1.3 gives a list of commonly used or approved drugs for AML with modes of actions and mechanisms of resistance where known.

Drug	Mode of action	Mechanisms of resistance
Daunorubicin	Anthracycline – topoisomerase II inhibitor	
Cytarabine	Pyrimidine nucleoside analogue – inhibits deoxycytidine synthesis	
CPX-351 (Vyxeos)	Liposomal encapsulation of daunorubicin and cytarabine	
Azacitidine	Hypomethylating agent – Inhibits DNA methylation	Altered expression of pyrimidine metabolism enzymes (DCK, UCK2, CDA, CAD) preventing DNMT1 depletion.
Venetoclax	BCL-2 inhibitor	Overexpression of BCL-2. Presence of FLT3-ITD mutations.
Gemtuzumab Ozogomycin (Mylotarg)	Anti-CD33 monoclonal antibody	Loss of CD33 theoretically although mylotarg given as 3 doses (max) in induction.
Gilteritinib	FLT3 inhibitor	Loss of FLT3, acquisition of new signalling pathway mutations, selection of resistant ITD clones.
Midostaurin	FLT3 inhibitor	As above
Ivosidenib	IDH1 inhibitor	Isoform switching, RTK pathway mutations, epigenetic regulation, mitochondrial metabolism
Enasidenib	IDH2 inhibitor	As above
Glasdegib	Inhibitor of Smoothened (SMO) in Hedgehog signalling pathway	Acquired SMO mutations, SUFU gene deletions, GLI2 amplifications

Table 1.3: List of commonly used or recently approved AML drugs with their mode of action. NICE approved drugs are in bold. Examples of mechanisms of resistance listed for some of the newer drugs. [43-47]

Adaptive drug resistance has been and remains a major problem in the field of AML. Kinase-activating mutations, including FLT3-ITD, and TP53 lesions have been identified as major drivers of treatment resistance in the venetoclax era [48]. With an expanding knowledge of metabolic pathways and an increasing number of targeted therapeutic options, more attention has focused on synthetic lethality. This is the concept that inactivation of 1 or other of 2 genes has little effect on cell viability but that the loss of function of both genes leads to cell death [49]. For example, glutamine deprivation has been found to sensitise multiple myeloma cells lines and patient-derived samples to BCL-2 inhibition [50]. In AML, resistance to p53 activation has been overcome by BCL-2 inhibition (and vice versa) in primary samples in vitro and a patient-derived xenograft model [51]. In another mouse model the FLT3 inhibitor quizartinib has been found to sensitise primary FLT3-ITD mutant AML cells to a PARP inhibitor by causing downregulation of DNA repair proteins. This led to a significant reduction in quiescent and proliferating leukaemia stem cells and progenitors [52].

1.1.5 Current state

There has been clear progress in the outcome of patients with AML over the last decade driven by a better understanding of the disease biology, new therapies and better supportive care. Gemtuzumab ozogamicin has improved survival when added to standard induction chemotherapy, particularly in those with favourable- risk cytogenetics (but not adverse-risk) [53]. Similarly, arsenic trioxide (ATO), in combination with all-trans retinoic acid (ATRA), has shown a survival benefit in those treated for non-high risk APML [54].

But these are 2 subgroups of AML that have consistently demonstrated the best survival data and perhaps represent ‘low-hanging fruit’. Over 20% of younger patients are refractory to primary induction chemotherapy and about half of those with primary refractory disease die within 6 months [55, 56]. TP53 mutations are associated with chemotherapy resistance and can emerge through the course of treatment. The median OS following acquisition of a TP53 mutation was 4.6 months with a 1 year OS rate of 19% in one cohort [57]. Despite therapeutic options, the 5 year OS for those with relapsed disease remains less than 10% [58]. The median OS for those that relapse following HSCT is as low as 6 months [59].

Clearly the outcome for many subgroups of AML remains dismal. We do not yet have the tools to predict accurately all of those that will be resistant to or relapse following treatment. Traditional chemotherapy has not proven to be effective and new therapeutic options are needed to manage this unmet need. Although new drug options are available their optimal use is not yet established in all cases. Questions persist about how and when to best incorporate them into current treatment paradigms and follow up data for some are short.

1.2 Amino acid dependence

1.2.1 Introduction

Cancer cells display a proliferative advantage over non-malignant cells and therefore have a higher energy demand required for survival. Amino acids are crucial to this rapid proliferation but this dependence leaves malignant cells vulnerable to exploitation [60]. Amino acid dependence is now a focus for research and therapeutic intervention.

A detailed study of the metabolism of all 20 amino acids is not within the scope of this MD thesis. Instead, I will give a brief overview of those AAs that are clinically relevant or relevant to this project.

First, a brief introduction to the work of Otto Warburg [61].

1.2.2 The Warburg effect

Metabolic reprogramming is one of the hallmarks of cancer [62]. The common feature of this rewiring in malignant cells is the increased glucose uptake and fermentation of glucose to lactate [63]. This supports rapid and inappropriate cell proliferation, growth and survival [64-66]. Normal non-dividing cells rely on ATP to maintain homeostasis. In contrast, dividing cells must acquire the building blocks for new cells, including

nucleotides, lipids and amino acids which, in turn, requires ATP and carbon and nitrogen precursors [66, 67]. They produce ATP through aerobic glycolysis, a process known as the 'Warburg effect' [61]. This circumvents oxidation through the tricarboxylic acid (TCA) cycle and mitochondrial oxidative phosphorylation (OxPhos) allowing faster glucose hydrolysis [68]. Although less efficient, this allows cancer cells to compete for glucose to sustain proliferation [69].

This rapid replication relies on a constant supply of nutrients including amino acids and has become a focus for research. However, although first developed in the 1920s, the causes and mechanisms of the Warburg effect have not been fully elucidated. It occurs even when mitochondrial functioning is maintained and, although biosynthesis is considered an important function, this requires less protein compared to glycolysis [63, 70]. Regardless of the function of the Warburg effect, simple glucose restriction is not a viable therapeutic avenue due to systemic toxicity.

Whilst cancer metabolism has long focused on carbon metabolism including glycolysis and the TCA cycle there are involved in a wide range of cellular processes including alternative fuel sources, redox balance, epigenetic regulators and as biosynthetic materials [71].

1.2.3. Control of cellular adaptations

Normal mammalian cells have well established dietary requirements. A huge number of adaptive mechanisms have evolved to detect and respond to fluctuations in nutrients [72]. In health, diets deficient in total protein, or 1 or more essential amino acids (AAs), trigger changes in gene expression leading to epigenetic and transcriptional changes including DNA methylation [72-74]. At a cellular level, an AA imbalance triggers an Amino Acid Response (AAR) involving multiple signal transduction pathways. The AAR is part of an Integrated Stress Response (ISR) that also includes the unfolded protein response to endoplasmic reticulum (ER) stress and the response to hypoxia, involved in apoptosis [75, 76]. The integrated response response (ISR) is a means for cells to maintain homeostasis when put under undue stress [77].

Gene expression is regulated at a number of steps including transcription site and rate, mRNA splicing, RNA export and turnover and translation initiation [72, 78]. Fluctuating intracellular amino acid levels are closely monitored by a number of sensory mechanisms, including mTOR and GCN2[1]. GCN2 detects a small fall in even a single type of AA whilst the mTOR pathway is inactivated in this scenario [79]. In AA starvation, mRNA binds to the GCN2 kinase leading to the phosphorylation of eIF2α[2] [80]. This pathway is ubiquitously expressed in all tissues [72]. This triggers the translation of ATF4[3] which, in turn, activates compensatory enzymes such as PHGDH, PSPH and PSAT1[4] (for the serine synthesis pathway) [81]. ATF4 has a number of functions, summarised in figure 1.2.

For example, ATF4 is highly expressed in haematopoietic stem cells (HSCs) due to low levels of eIF2α. AA deprivation results in ATF4 upregulation which promotes HSC survival [76].

[1] mTOR: mammalian target of rapamycin; GCN2: general control nonderepressible 2.
[2] eIF2α: eukaryotic initiation factor 2 alpha.
[3] ATF4: activating transcription factor 4
[4] PHGDH: phosphoglycerate dehydrogenase; PSAT1: phopsphoserine aminotransferase 1; PSPH: phosphoserine phosphatase

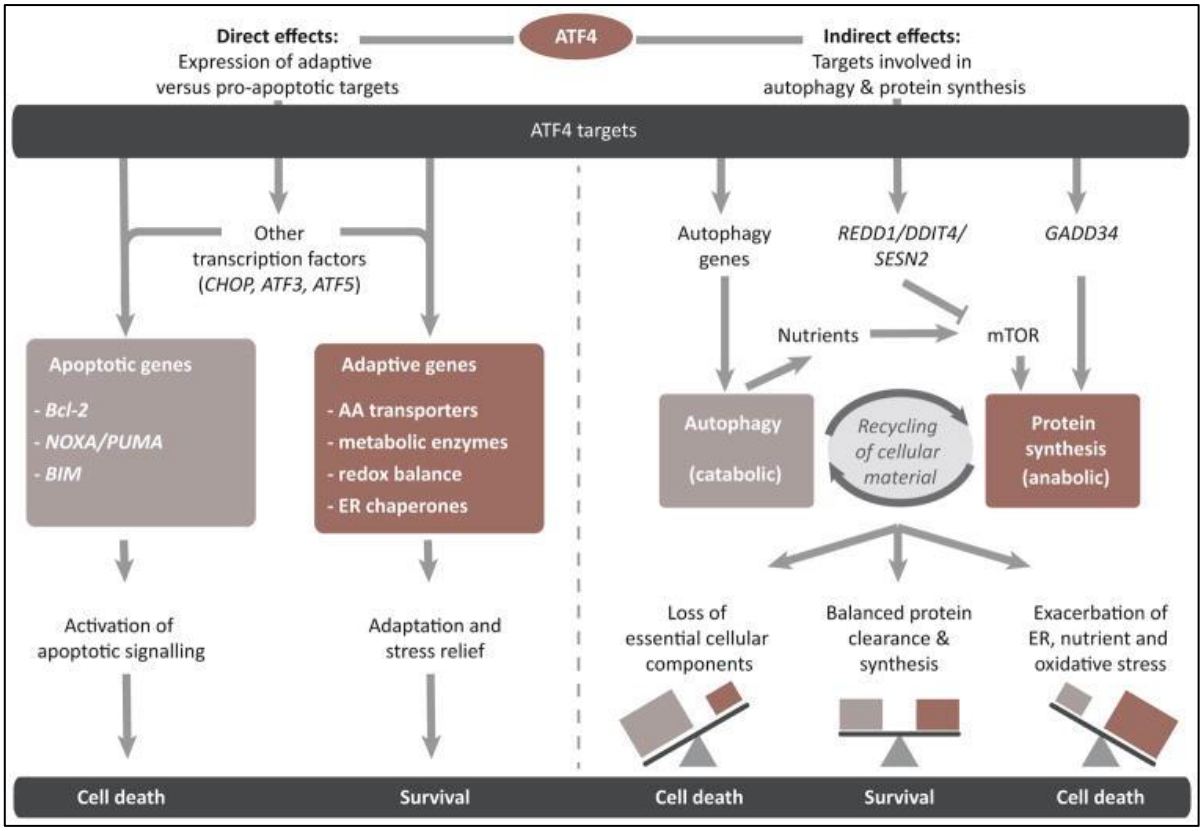

Figure 1.2: Role of ATF4 under stress conditions [78].

Serine is used to illustrate the ISR response. Depriving cancer cells of serine induces stress and leads to p53-dependent metabolic remodelling [82]. Cancer cells express the M2 isoform of pyruvate kinase (PKM2). A reduction in intracellular serine leads to a reduction in the activity of PKM2 which shunts glycolytic precursors into endogenous serine synthesis [66, 82, 83]. GCN2 detects low serine levels and upregulates ATF4 which in turn upregulates the enzymes required for endogenous serine synthesis including phosphoglycerate dehydrogenase (PHGDH). PHGDH is overexpressed in breast and pancreatic cancer suggesting that they synthesise serine [84, 85].

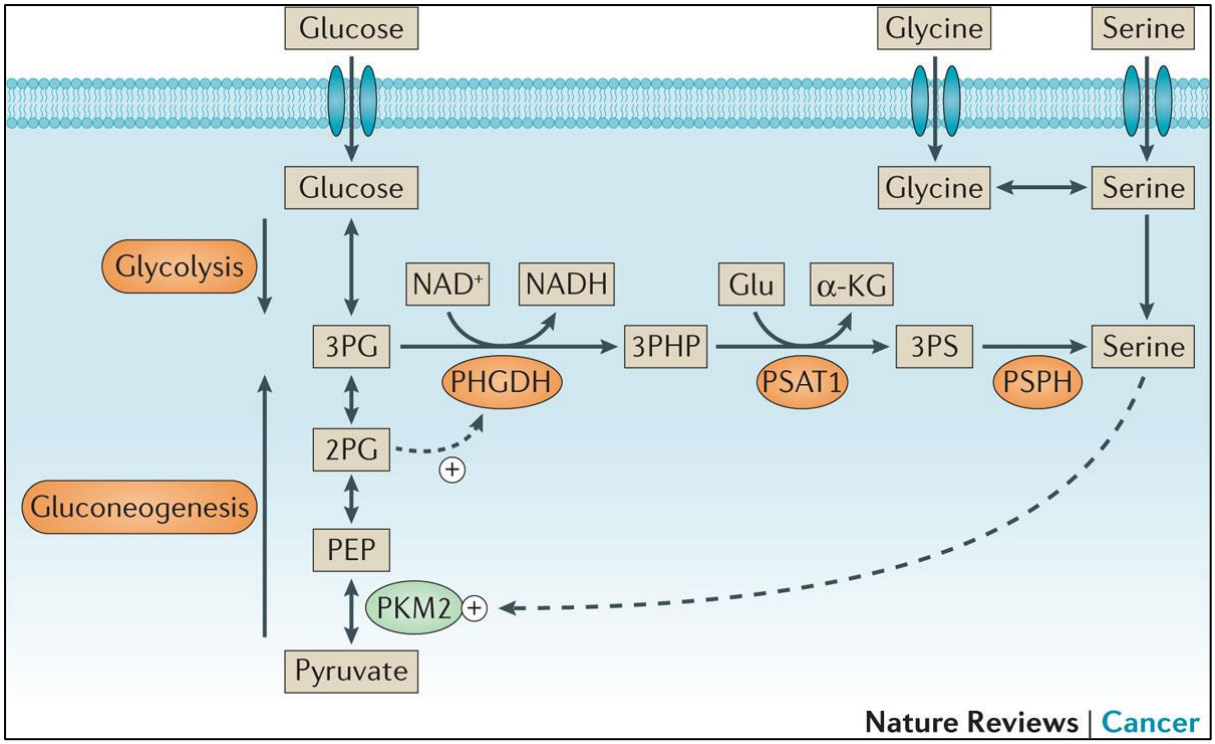

Figure 1.3: Serine synthesis pathway [86]

1.2.4 Amino acid depletion

Amino acid manipulation has been exploited in cancer treatment. L-asparaginase has transformed the outcome of acute lymphoblastic leukaemia (ALL) and is now incorporated into standard induction therapy. It catalyses asparagine, essential for ALL cell proliferation, into ammonia and aspartate [87].

AA deprivation is a strategy to deprive malignant cells of the biomass needed to proliferate and has been applied to arginine [88, 89]. Arginine is a semi-essential AA which can be either synthesised *de novo* intracellularly from citrulline and aspartate or imported from plasma. Like serine, synthesis requires critical enzymes, in this case argininosuccinate synthetase 1 (ASS1) and argininosuccinate lyase (ASL) (see figure 1.4). ASS1 is not expressed in many malignant cells meaning they rely on exogenous arginine to proliferate (auxotrophy) [88]. This is facilitated through the cationic amino acid transporter (CAT) family, although different AA transporters are involved with other AAs [90].

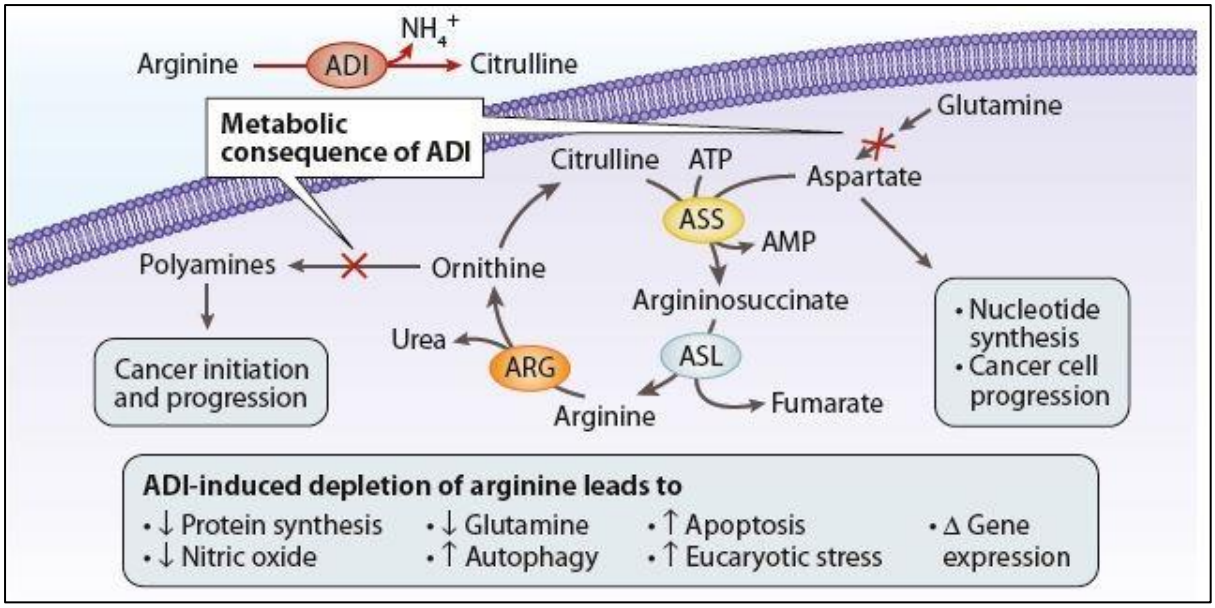

Figure 1.4: Intracellular action of arginine deprivation with ADI-PEG20 (courtesy of Polaris)

Arginine is degraded by arginine deiminase. A pegylated form of this enzyme has been developed and has been used in ASS1-deficient solid tumours including hepatocellular carcinoma, mesothelioma, melanoma and sarcoma [91-94].

Most AMLs are ASS1 deficient and this has been exploited in *in vitro* and *in vivo* experiments in AML [64]. A phase II trial has investigated ADI-PEG20 monotherapy in 43 mostly ASS1-deficient poor risk or relapsed/refractory AML patients [95]. ADI-PEG20 depleted circulating arginine levels. Of the 21 evaluable patients, a CR was achieved in 9.5% and stable disease in 33.3%, giving a disease control rate of 42.9% (CR 4.7% and SD 16.3% when evaluated on an ITT basis). Of the 2 patients that reached a CR, the durations of response were 7.7 and 8.8 months and 1 achieved a cytogenetic response. Whole transcriptome RNA sequencing was performed on the BM mononuclear cells of those that achieved CR or PD. A significant difference in both up- and down-regulation of genes associated with AML subtypes was demonstrated following ADI-PEG20 treatment between the 2 groups. Down-regulation of genes associated with STAT5A and c-MYC was seen in the 2 responders but not the non-responder group. Both of those that achieved a CR were intermediate risk by MRC classification (albeit 1 R/R and molecular lesions not stated).

Next, a phase 1 dose escalation study investigated ADI-PEG20 in combination with low-dose cytarabine (LDAC). 23 patients were included in the study with 17 in the

expansion cohort. Patients were R/R or poor risk and unfit for intensive chemotherapy or could not tolerate hypomethylating agents. Treatment was well tolerated with no dose-limiting toxicities following dose escalation to 36mg/m^2. In the ITT group most grade 3 or 4 toxicities were haematological with 1 case of anaphylaxis. Of the 18 evaluable patients the ORR rate was 44.4% with a median OS of 8 months. In the treatment-naïve subgroup the ORR was 71.4% and CR 57.1% [96].

Resistance to ADI-PEG20 has been demonstrated through the re-expression of ASS1 by demethylation of the ASS1 promoter [97].

BCT-100 is a pegylated recombinant human arginase. It was evaluated in combination with LDAC in the UK through the LI-1 trial. Patients were randomised to either LDAC (20mg bd for 10 days) or BCT-100 1600U/kg weekly in combination with LDAC. Although well tolerated and a fall in circulating arginine was demonstrated in most of the combination patients, this did not correspond to a significant improvement in either response rates or survival [98].

1.2.5 Investigation of amino acid dependence in AML

Research in the altered cellular metabolism in cancer is well established. Much of the solid cancer laboratory interrogation described previously has been performed using cell lines or xenograft models [13, 83, 99, 100]. This has been applied to AML most recently with arginine deprivation. This section contains a justification for the choice of AAs used in the co-culture work in chapter 3. It summarises the potential exploitability of each of the AAs and their clinical relevance. I have focused on the AAs relevant to this thesis.

1.2.5.1 Serine and glycine

Serine and glycine are biosynthetically linked [101]. Both are non-essential AAs and their common synthetic pathway serves as an example in the introduction of this

thesis. PHGDH, PSAT and PSPH are critical enzymes in this synthetic pathway[5]. PHGDH has been identified as a potential biomarker for cancers that are susceptible to serine deprivation. Serine (and glycine) starvation has been found to upregulate both PHGDH and PSAT in human cancer cells in vitro and in vivo [82]. PGHDH has variable expression in solid tumours and high expression has been found to promote tumour growth in vivo [85, 102]. Both serine starvation and PHGDH inhibition suppress tumour growth in susceptible cells, including those with p53 mutation [82, 100, 103].

In AML, serine is critical to cell growth in vivo. Both PSAT and PHGDH were found to upregulated in response to glutamine deprivation, suggesting the role of serine as in the TCA cycle [104].

1.2.5.2 Valine

Valine is one of the branch-chained essential amino acids (BCAAs). Valine depletion has been investigated as a potential treatment for cancer as long as 4 decades ago [105]. Murine leukaemia cell lines demonstrate increased apoptosis when cultured in valine-deplete media for up to 24 hours [106].

More recently, Taya and colleagues have explored the role of valine in maintaining haematopoietic stem cells (HSCs) [107]. HSCs ($CD34^{-}Kit^{+}Sca^{+}Lin^{-}$ cells) showed reduced proliferation when cultured in media lacking valine (Val^{-}) but haematopoietic precursor cells (HPCs; $CD34^{+}Kit^{+}Sca^{+}Lin^{-}$) showed normal growth. Valine requirements for HSC maintenance were then determined with a repopulation assay whereby HSCs grown in Val^{-} media were transplanted into irradiated mice. No engraftment was documented.

Next, mice were fed either a complete or a Val^{-} diet for 4 weeks. The mice fed the Val^{-} diet had a significant reduction in both white and red cell numbers. PB and BM valine concentrations fell by 90% over the same period. PB and BM cell types were then quantified using immunophenotyping to evaluate the Val^{-} effect further. HSCs, B and T cell numbers all fell and systemic effects were noted histologically in some tissues.

[55] PHGDH: Phosphoglycerate Dehydrogenase; PSAT: Phosphohydroxythreonine aminotransferase; PSPH: L-3-PhosphoserinePhosphatase

When the mice reverted to a complete diet half recovered haematologically (HSC, HPC and lineage numbers) while the other half died of refeeding syndrome.

HSCs from mice fed a Val^- diet for 4 weeks and BM cells were then injected into mice that had been lethally irradiated (to mimic a myeloablative HSCT). Donor chimerisms were slightly reduced up to 8 weeks but then fell rapidly after 12 weeks suggesting that the Val^- diet depletes HSCs but has a lesser effect on HPCs. The team repeated this model in non-irradiated immunodeficient (NOD/Scid) mice to determine if valine restriction could effectively replace the role of highly toxic irradiation pre-HSCT. All mice fed the Val^- diet survived with good engraftment and blood cell reconstitution. Finally BM cells were transplanted into non-irradiated congenic mice that had been fed a Val^- diet for 3 weeks. Valine was gradually reintroduced to the diet over 2 weeks to avoid refeeding syndrome. These mice demonstrated long-term donor chimerism and survival without significant toxicity. Similar findings were observed when a Val^- diet was tested on human haematopoiesis using mice reconstituted with BM $CD34^+$ cells.

This highlights the importance of valine in HSC homeostasis although the mechanism is unclear. Jones and colleagues have also investigated the demand for AAs of both LSCs and blasts. They did not find valine critical to LSC survival although they did use 3 day culture rather than 7 (of Taya) which may explain the difference [108].

With regard to AML, doxorubicin-resistant AML cell lines have been found to have significantly higher concentrations of valine [109]. The importance of the interplay between the BM niche and AML warrants further investigation.

1.2.5.3 Methionine

Methionine is an essential amino acid and, as such, acts as a substrate for other AAs. Methionine restriction (MR) has been the focus of health research for decades following the discovery it prolongs the life of Drosophilia, mice and rats [110-112]. Methionine has many cellular functions which have been shown to be relevant to cancer pathogenesis and MR has been exploited in several tumour groups [113].

It has been found to inhibit cell migration and invasion in triple negative breast cancer cell lines in vitro and reduce metastases in vivo [114, 115]. In shorter term restriction (than performed by Taya and colleagues with valine), methionine metabolism was found to be altered within 2 days of mice being fed an MR diet [116]. This was then applied to 2 treatment-resistant patient derived xenograft models of RAS-driven colorectal cancer. Mice were then given either a replete or a methionine-restricted diet and the latter inhibited tumour growth in the KRAS-mutated mice and an inhibitory effect in the NRAS-mutated mice.

When applied to MLL-rearranged leukaemia cell lines, disruption of the methionine metabolic pathway by MR reduced cell numbers and increased apoptosis in the acute leukaemia cell lines but not BCR-ABL driven cell lines. When combined with chemotherapy in an MLL-rearranged cell line xenograft model, this significantly increased survival [117]. Methionine levels have been found to be lower in AML patients than controls suggesting there may be increased uptake [118].

L-methioninase, an enzyme isolated from Clostridium sporogenes, was found to lead to a growth inhibition of blasts in primary AML samples in culture 40 years ago [119]. As was the case with asparaginase development, immunogenicity has been put forward as a reason for the lack of therapeutic exploitation in the intervening period [120, 121].

Much of the focus of MR in cancer research has revolved around the methionine salvage pathway, including MTAP[6]. In order to avoid repetition this is discussed in more detail in chapter 7.

3.2.4 Asparagine

Asparagine is a non-essential AA that can be synthesized from aspartate and glutamine by asparagine synthetase (ASNS) and hydrolysed to aspartate by asparaginase. This latter enzyme is exploited in ALL treatment. Given the success of asparaginase in ALL regimens, the focus on asparagine has been extended to AML.

[6] MTAP: Methylthioadenosine phosphorylase.

AML with monosomy 7 (-7) has a dismal outcome. It has been found to lead to the downregulation of ASNS rendering AML cells more susceptible to asparaginase. AML cell lines and primary paediatric AML cells with -7 have been found to be more sensitive to asparaginase treatment [122].

In further AML cell line work, Michelozzi and colleagues found asparaginase to be effective against leukaemic stem cells ($CD34^+$ $CD38^+$ and $CD34^+$ $CD38^-$) and AML blasts but not mesenchymal stromal cells or monocytes [123].

The response of AML to asparaginase has been augmented with the addition of chemotherapy. Asparaginase alone was found to inhibit proliferation and induce apoptosis in 3 AML cell lines but this was enhanced with the addition of mitoxantrone and cytarabine [124].

Higher asparagine levels are significantly associated with anthracycline resistance in AML cell lines by multivariate analysis of a metabolomic profile [109].

3.2.5 Glutamine

Glutamine is the most abundant AA found in human plasma. Its role as an energy source in the altered cancer metabolism is well documented [125-128]. Glutamine is included here to act as a model for comparison for the other amino acids.

However, the impact of glutamine deprivation on oxidative phosphorylation has also been investigated in AML [129, 130]. Targeting glutaminolysis has a potential role in AML therapy. Glutamine levels control OXPHOS in AML. Its catabolism is controlled by glutaminase C (GAC). GAC inhibition with a small molecule has been found to increase apoptosis in AML cells [129]. Inhibition of another glutaminase isoenzyme has been found to reduce AML cell growth, increase apoptosis and induce differentiation in IDH mutant AML [62]. Glutaminolysis is a metabolic dependency of FLT3-ITD mutant AML which is unmasked with FLT3 inhibition meaning it is a potential therapeutic target [131].

1.2.6 Quantifying AAs in AML

Plasma AA concentrations have been found to differ in AML patients when compared to other solid tumours with baseline methionine, serine and taurine found to be significantly lower when measured at presentation by ion-exchange chromatography [132].

Our own group has previously investigated the effect of arginine deprivation using a pegylated arginine deiminase (ADI-PEG 20) in primary AML cells *in vitro* and *in vivo* [64]. ADI-PEG 20 led to a fall in plasma arginine levels. Both plasma arginine and citrulline were measured using liquid chromatography mass spectrometry (LCMS). Attempts were made to measure intracellular arginine in BM samples but no corresponding increase was documented. The lengthy extraction process for marrow involving multiple washes may have affected the intracellular results (personal communication, DC Taussig). The cellular uptake of arginine was however demonstrated using labelled $^{13}C_6$ arginine.

Similar work has been performed using the arginase BCT-100 in AML cell lines and primary AML samples [133]. Plasma arginine levels fell following *in vitro* culture for 72 hours with BCT-100. Intracellular arginine was quantified using a combination of ELISA and fluorescently labelled BCT-100 with a corresponding fall over the same period [107].

More recently LCMS has been used to interrogate AA levels in AML cells [108]. Relative levels of reactive oxygen species (ROS) were used to differentiate leukaemic stem cells (ROS_{low}) and AML blasts (ROS_{high}). Global metabolic profiling was then used to compare the two. A range of metabolites were investigated but 16 of the AAs were found to have a higher concentration in the LSC group. Flux experiments at up to 60 minutes again demonstrated higher AA uptake in the LSC group. Deprivation of all AAs is not a viable approach in clinical practice but this elegantly demonstrates the use of LCMS and measuring AA concentrations.

Metabolomic and AA changes have been investigated as a means of predicting response to cyatarabine and doxorubicin in AML cell lines [109]. A cellular metabolic profile was examined in 7 cell line samples with varying degrees of chemosensitivity. Cell pellets were washed and processed using ultra-high performance liquid

chromatography mass spectrometry (UHPLC-MS). In this small cohort asparagine, glutamine and glycine were all found to be more abundant in the doxorubicin-resistant samples.

Further AML cell line work has been performed comparing the metabolomic profile with CD34+ haematopoetic stem cells derived from cord blood [134]. Only 3 AML cell lines and 1 CML cell line were cultured and then the media/supernatant processed and measured using gas chromatography mass spectrometry. Of the AAs, glycine, serine, threonine, alanine, aspartate, proline, ornithine and lysine had a significantly different profile in the leukaemia cell lines.

Attempts have been made to apply this clinically. Zhou and colleagues used gas chromatography and mass spectrometry to measure plasma and BM supernatant AA concentrations in AML patient samples [118] They identified that altered taurine and lysine levels were associated with adverse outcome in the M2 (acute myeloblastic leukaemia with maturation) subgroup of AML and could potentially be explored as a biomarker.

This is by no means an exhaustive review of AA measurement but does demonstrate the focus and methodology of some of the work carried out in AML and potential clinical applications. It also raises some points: AML cell lines are frequently used as a proxy for AML although may not be representative of 'real life' AML behaviour and media/supernatant changes are often assumed to be an inverse surrogate for cellular changes when this may not be the case.

1.2.7 Current state

It is established that cancer leads to a remodelling of cellular metabolism. Demand for AAs is increased to fuel cell replication. This has been exploited therapeutically with asparagine deprivation now used in ALL and arginine deprivation across a number of tumour groups [92, 135, 136]. Fluctuations to AA concentrations lead to compensatory metabolic mechanisms which are mediated by the GCN2/eIF2α/ATF4 pathway. These fluctuations are known to alter gene expression and other epigenetic changes. This understanding has more recently been brought to AML with glutamine,

valine and serine all being investigated with the use of cell lines, primary AML samples and xenograft models. Our understanding of AA metabolism in AML is growing.

Many questions remain unanswered. Although attempts have been made to stratify the disease, AML is characterised by its heterogeneity. We do not fully understand the metabolic differences underlying this. Due to its relative lack of genetic lesions, AML is well suited to epigenetic analysis [11-13].

1.3 Hypotheses and project aims

1.3.1 Hypotheses

1. Different AML risk groups have different amino acid dependencies.

2. Different AML risk groups will respond differently to AA deprivation.

1.3.2 Project aims

1. Determine AA dependency in different AML risk groups by measuring cellular and media changes in AA concentration following culture.

2. In selected AAs investigate the effect of deprivation using modified culture media.

3. For those AML samples that do not respond to AA deprivation check for synergism with chemotherapy.

4. Where there are significant AA dependencies investigate their role within the cell.

5. For selected AAs investigate mechanisms and cellular adaptations to AA deprivation.

Chapter 2: Materials and methods

2.1 Samples and ethical approval

2.1.1 Primary samples

The majority of the peripheral blood and bone marrow samples were collected from AML patients at the Royal Marsden Hospital, Sutton. Samples were collected at either untreated presentation or relapse. Written informed consent was obtained prior to collection using the hospital *Tissues for Research (TFR)* consent form. Additional samples were obtained from the hospital's regional Haematological Malignancies Diagnostic Service (HMDS).

Overall ethical approval for the MD(res) project falls within the *Laboratory Studies into the pathology of leukaemia study* (CCR4508) which was approved by the East of England – Cambridge South Research Ethics Committee (REC reference 16/EE/0266). All studies complied with the rules of the Review Board and the revised Helsinki protocol.

2.1.2 Control samples

Bone marrow control samples were obtained from the Royal Marsden Hospital. Samples for patients with lymphoma were used. Those with confirmed or suspected current or prior bone marrow involvement (on histology or imaging) were excluded. Due to the required cell numbers for some experiments, further volunteer BM samples were purchased (Lonza, Stem Cell Technologies).

GCSF- mobilised peripheral blood (GMPB) was obtained from those donating for sibling or haplo-identical haematopoietic stem cell transplant. Samples were collected at the Royal Marsden Hospital following written consent.

2.1.3 Sample processing

Samples were collected in tubes containing either EDTA or heparin sodium and processed by Dr Miraki-Moud or myself as quickly as feasibly possible. In short, samples were diluted in PBS and layered on Lymphoprep™ (Stem Cell Technologies), either 5ml in 15ml or 15ml in 50ml Falcon tube depending on volume. Samples were then centrifuged for 30 minutes at room temperature (1500rpm, no brakes). The mononuclear layer was removed using a pipette, resuspended in PBS and centrifuged for 5 minutes (1500 rpm). Pelleted cells with heavy red cell contamination were resuspended in 10ml ammonium chloride (Stem Cell technologies) for 10 minutes at 4ºC, deactivated in 2ml FBS and centrifuged for 5 minutes (1500rpm). Cell pellets were then resuspended in 2% FBS for counting. Cell number and viability were recorded using a Luna II automated cell counter (Logos Biosystems). Cells were added to freezing mix (95% FBS and 5% DMSO) and transferred to cryotubes (Sigma). Cryotubes were placed in Coolcell™ containers (Sigma), stored at -80ºC overnight and then transferred to liquid nitrogen until required. The RMH tissue Biobank is regulated by the Human Tissues Act 2004 (Licence No. 30000).

2.2 Tissue culture methods

2.2.1 MS-5

All primary AML samples were co-cultured in murine stromal cell line (MS-5, DSMZ (German Collection of Microorganisms and Cell Cultures)) as previously described [137]. In summary, all liquids were pre-warmed to 37ºC in a water bath. Cells from the MS5 cell line (DSMZ) were thawed, washed and resuspended in 10mls 10% MEM alpha (Thermo Fisher) for counting. Antibiotics (1% penicillin and streptomycin (P/S), Sigma) were added to all media to prevent cell-line contamination. $0.1x10^6$ cells were resuspended in 20mls media and added to a $75cm^2$ flask (Corning) and incubated at 37ºC, 5% CO_2.

Cells were inspected regularly and divided twice weekly before confluence was reached. Cells were first washed twice using 10mls PBS. 2mls trypsin-EDTA (Sigma) was added to the flask and incubated for 5 minutes at 37ºC. The flask was tapped gently to loosen adherent cells and 7mls 10% MEM added to prevent further trypsin activity. Cells were then centrifuged (1500rpm for 5 minutes), resuspended in 10% MEM and cultured at the same concentration.

When required for AML co-culture, MS5 cells were irradiated with gamma irradiation at 7.5Gy by the Biological Services Unit at the ICR. MS5 cells were cultured for at least 2 weeks prior to being used as a feeder layer. Cells were passaged no more than 25 times before being discarded.

2.2.2 AML cell lines

AML cell lines were obtained from DSMZ (German Collection of Microorganisms and Cell Cultures) and grown as recommended by the supplier. FKH-1 and Kasumi-1 were grown in 80% RPMI 1640 (Thermo Fisher), 20% heat-inactivated foetal bovine serum (FBS) and + 1% P/S. HL-60 was grown in 90% RPMI 1640, 10% heat-inactivated FBS and 1% P/S. Further culture methods are detailed in the chapter specific co-culture methods sections.

2.2.3 Primary AML cells

AML samples were thawed in a water bath at 37ºC for 5 minutes. Cells were then transferred to a 50mL Falcon tube (Corning), 500µL DNase added and the samples warmed at 37ºC for a further 5 minutes and 10mls PBS then added. Samples were centrifuged at 1500rpm for 5 minutes and filtered using a 70µM cell strainer (Fisher) before counting. Precise culture methods and details of washes and media are outlined in the relevant sections below.

2.2.4 Control samples

Bone marrow and peripheral blood control cells were cultured in the same way as outlined above with one exception. Due to increased cell clumping and death, 1ml DNase was added following thawing. Samples were then incubated at 37ºC for 5 minutes followed by RT for 10 minutes. Cell viability was significantly improved with the addition of these steps.

2.3 Chapter specific co-culture methods

2.3.1 Chapter 3: Measuring AA dependence using co-culture

2.3.1.1 Co-culture media

For cost reasons 'modified' MEM alpha media deplete of all 6 AAs specified in table 3.4 (Thermo Fisher) was used throughout this experiment. Dialysed FBS (Thermo Fisher), with a dialysis cut-off of 10kDa, was used to minimise AA contamination. Individual AAs were used to supplement the modified media: L-Serine (105.09kDa), L-Glycine (75.07kDa), L-Valine (117.15kDa), L-Methionine (149.21kDa), L-Asparagine (150.1kDa) and L-Glutamine (146.14kDa, all Sigma). These were reconstituted, aliquoted and stored as recommended by the manufacturer until required.

When required, 500mL 'modified' MEM was supplemented with 1% penicillin streptomycin and passed through a 0.22µm vacuum filter (Starlab). This formed the 'Zero' media used for washing and counting cells. For each of the 8 conditions, 5mL dialysed FBS was added to make 50mL aliquots (ie 10% FBS). AAs concentrations were then calculated (using the Graphpad Prism molarity calculator) and supplemented appropriately. Aliquots were stored in 50mL Falcon tubes at 4ºC until required and for no longer than 6 weeks.

2.3.1.2 Co-culture method

MS-5 cells were used to support the primary AML and control samples.

Cells were cultured in 24 well plates. On day 1 cells were irradiated with gamma irradiation at 7.5Gy. Following irradiation, cells were washed in 5mls customised 'Zero' media 3 times, resuspended in 2mls '0' media and counted. MS-5 cells were cultured at a concentration of $0.025x10^6$ cells in 500µl customised media per well. Each AA condition was cultured in triplicate at 37ºC, 5% CO_2. Generally 2 plates were cultured, 1 for counting and 1 for annexin V, caspase 3/7 and Ki-67.

At 24 hours AML or control samples were removed from liquid nitrogen and thawed as described in chapter 2. Cells were washed 3 times in 'Zero' media, filtered and counted in either 2 or 5mls 'Zero' media depending on pellet size. Cells were then added to each customised media at a concentration of $0.4x10^6$ cells in 500µl customised media per well. Several samples had fewer cells in which a concentration of $0.3x10^6$ cells per well was used. Each AA condition was cultured in triplicate at 37ºC, 5% CO_2 for 72 hours. A summary schematic of the protocol is shown chapter 3.

2.3.1.3 Dose response experiment

Aliquots of 'customised' media were made for the –Val and –Met conditions only. The aliquots were then supplemented with Val or Met at different doses (details in chapter 3). Control samples contained the valine and methionine concentrations found in standard MEM alpha media. Samples were co-cultured in triplicate using an MS-5 feeder layer as described above.

2.3.2 Chapter 4: Combining AA deprivation with chemotherapy

2.3.2.1 Co-culture method

Cytarabine (ARAC; Selleckchem) is one of the 2 agents used commonly in induction treatment and was therefore selected here. The effective therapeutic doses were established by our team in other experimental work. The drug was reconstituted in DMSO following the manufacturer's instructions. The equivalent volume of DMSO was used in the 'control' arm so as to mitigate against its effect on AML cells.

The method for making the 'customised' MEM alpha media deplete of valine and methionine is described in section 2.3.1.1. Briefly, MS-5 cells were cultured as described previously. At 24 hours primary AML cells were thawed, washed 3 times and counted in 'Zero' media. Cells were then added to each customised media (Control, -Val and –Met) at a concentration of $0.4x10^6$ cells in 500µl customised media per well and the cytarabine added. Each AA condition was cultured in triplicate at 37ºC, 5% CO_2 for 72 hours.

2.3.3 Chapter 5: Measuring amino acid levels by Liquid Chromatography Mass Spectrometry (LC-MS)

2.3.3.1 Co-culture method

MS-5 cells were used to support the primary AML cells.

Cells were cultured in 6 well plates with standard 10% MEM alpha media. On day 1 cells were irradiated with gamma irradiation at 7.5Gy. Following irradiation cells were cultured at a concentration of $0.1125x10^6$ cells in 3mL media per well.

At 24 hours AML samples were removed from liquid nitrogen, thawed and placed in a 50mL Falcon tube. After incubation with DNase, 20mL PBS was added and the cells

centrifuged. Cells were then resuspended in media and cultured at a minimum of $4x10^6$ cells per well. Samples were cultured in quadruplicate.

The remaining cells were then washed twice with 20mL ice cold PBS and counted. $1x10^6$ cells were placed 1.5mL Eppendorf tubes (Starlab), topped up with ice-cold PBS and centrifuged at 7000rpm, 4ºC for 7 minutes. The supernatant was then aspirated manually to minimise disruption of the cell pellet and samples snap frozen. Again this was performed in quadruplicate.

Cells were co-cultured for either 24 or 72 hours. At the determined endpoint the contents of each well was collected in a 50mL falcon tube and centrifuged for 5 minutes. 500µL supernatant was aspirated from each tube, placed in an Eppendorf tube and snap frozen. 2mL ice-cold PBS was immediately added to each well, agitated and the contents added to the Falcon tube. This step was repeated twice (3 x 2mL washes). The contents were then centrifuged at 1500rpm for 5 minutes and then washed again with 20mL ice-cold PBS. Cells were counted and $1x10^6$ pellets prepared as above. Therefore each AML subject generated 16 samples (4 at baseline and after culture for both cell pellets and media/supernatant). Samples were stored at -80ºC until analysis.

2.3.4 Chapter 6: Cellular control and compensation in AA deprivation

2.3.4.1 Co-culture method

Selected samples were co-cultured in 2 media conditions: control (all AAs) and –Met (without methionine only). An MS-5 feeder layer was set up in 6 well plates and the primary AML samples added at a concentration of at $1.2x10^6$ cells per well at 24 hours. Cells were cultured at 37ºC, 5% CO_2 for 24 hours as previously described. At 24 hours the contents were aspirated and centrifuged and the pellets washed in 1mL PBS, centrifuged, snap frozen and stored at -80ºC until required.

2.3.5 Chapter 7: Proteomic analysis of AML

2.3.5.1 T cell depletion and co-culture method

The sample was removed from liquid nitrogen and thawed as described in previous chapters. The sample was then divided into 3 and each sample topped up with 3 different media conditions: control (containing all AAs), -Val (without valine) and –Met (without methionine).

T-cell depletion was first performed on each sample to optimise the purity of the sample using an EasySep™ Human CD3 positive selection kit (Stemcell Technologies). Briefly, mononuclear cells were added to the tube provided. 100µL/mL selection cocktail was added and the contents mixed and incubated at RT for 3 minutes. Rapidspheres (magnetic beads) were added to the sample (60µL/mL) and again the contents mixed and incubated for 3 minutes at RT. The tube was then placed in the magnet and incubated at RT for a further 3 minutes. The supernatant was then carefully poured into a 50mL Falcon tube and the purity assess by flow cytometry. Samples were topped up with the appropriate media and counted.

Samples were then co-cultured in an MS-5 feeder layer as described above. Cells were cultured at a minimum of $6x10^6$ cells per well in duplicate. For each media condition (control, -Val and –Met), cell pellets were stored at 4 time points (baseline and 24, 48 and 72 hours). Cell pellets were prepared by washing cells twice with 40mL ice-cold PBS. Cells were then resuspended in ice-cold PBS and counted. $2.5x10^6$ were transferred to an Eppendorf tube, topped up to 1mL with ice-cold PBS and spun at 7000rpm at 4ºC for 7 minutes. Supernatant was aspirated off manually and the cell pellets snap frozen and stored at -80ºC until required for analysis.

2.4 Flow cytometry

2.4.1 Introduction

Flow cytometry is a widely used technique that provides rapid multi-parametric analysis of single cells in solution. Flow cytometers use lasers to produce both scattered and fluorescent light signals that are read by detectors [138]. The analysis of the expression of cell surface and intracellular molecules allows the characterisation of cell types. A variety of fluorescent reagents are used including fluorescently conjugated antibodies and viability dyes.

The bound antibody-fluorochrome absorbs the laser energy and then releases it in a specific wavelength as the cells pass the laser in single file. This emitted light is identified by the detector which is sensitive to specific wavelengths, which is in turn determined by optical filters. The light signal is then converted into an electrical signal which is plotted graphically.

2.4.2 Specific uses for this study

Although flow cytometry was used extensively, its application was limited to cell counting, detection of apoptosis and assessment of cell cycling.

2.4.2.1 Cell counting

Co-cultured primary AML cells from each well was transferred to a 5mL FACS tube (BD) and each well washed with 800µL PBS. 90µL 0.5% trypsin/EDTA (Thermofisher) was added to each well and the plate incubated at 37ºC, 5% CO_2. At 5 minutes, the plate was tapped to loosen cells, 500µL 2% PBS added to each well to deactivate the trypsin and the contents added to the FACS tube. Samples were centrifuged at 1500rpm for 5 minutes and then the contents discarded and the tubes dried quickly on paper. 2.5 µL CD45PE (BD) was added to each tube and the tubes vortexed and incubated in the dark at room temperature (RT) for 20 minutes. Cells were then washed with 2mL 2% PBS, centrifuged and again the contents discarded before drying

the tubes on paper. 300µL DAPI (1/2000 from 500µg/mL stock, Sigma) and 25µL CountBright Absolute Counting Beads (Biolegend) were added to each tube.

Samples were counted on the FACS Canto II (BD) with a stopping gate for beads of 1000 events. The following formula was used to calculate cell number:

Absolute count (cells/µL) = A/B x C/D

A = Number of cell events
B = Number of bead events
C = bead count concentration (beads/25µL)
D = volume of sample (µL)

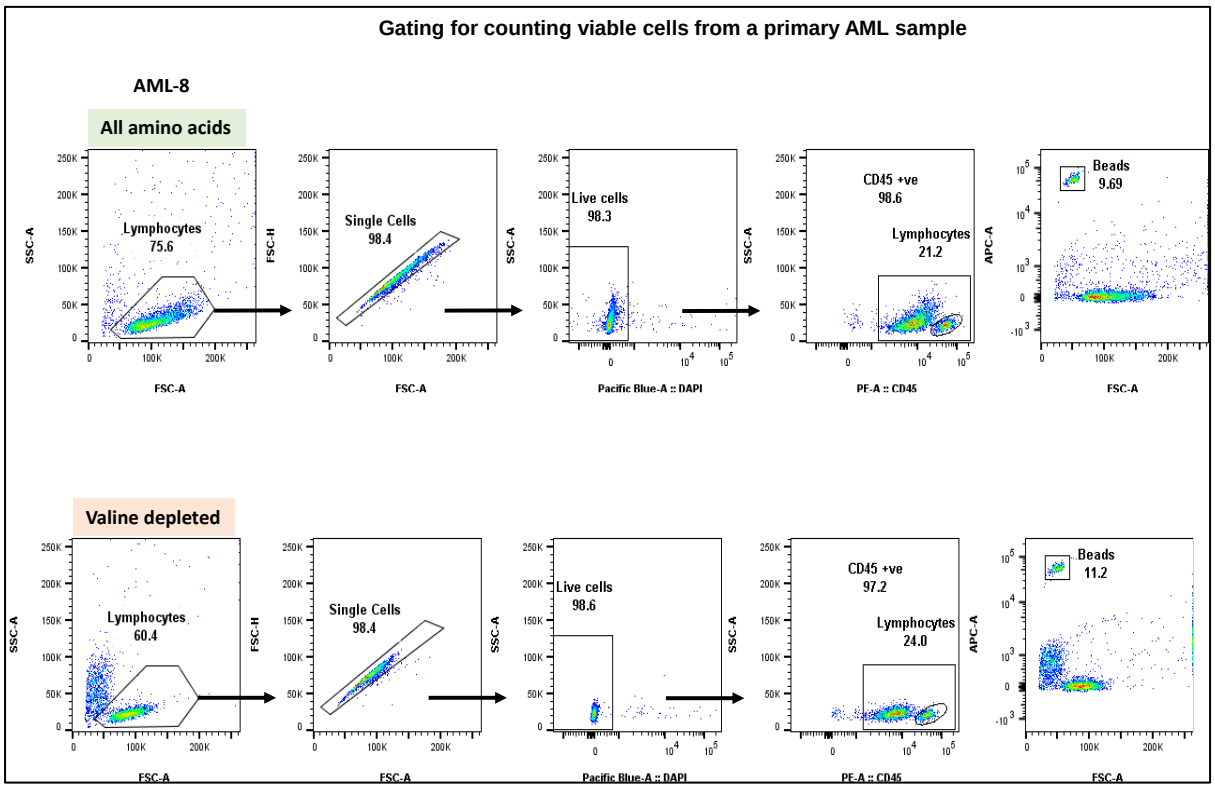

Figure 2.1: Gating for counting of control and valine depleted samples – AML8 used as an example.

Samples were gated on both CD45+ cells and lymphocytes, the latter providing an internal 'normal' control for each sample.

2.4.2.2 Caspase 3/7

The assay is based on fluorochrome-labelled inhibitors of caspases (FLICA). The FLICA reagent interacts with a 4 amino acid peptide (DEVD). DEVD inhibits the ability of the FLICA reagent to bind to DNA. However, once caspase 3/7 is activated in apoptotic cells, the DEVD is cleaved allowing the FLICA reagent to bind to the DNA producing a fluorescent response.

Co-cultured primary AML cells from another plate were trypsinised as before and divided into two tubes, one for checking annexin V and the other for measuring caspase 3/7 activity. Tubes for caspase 3/7were then centrifuged at 1500rpm for 5 minutes, the supernatant discarded and the tubes dried quickly on paper. 2.5µL CD45PE was added and the tubes incubated and centrifuged as above. After discarding the supernatant and drying, 5 µL FLICA (diluted as recommended, Life Technologies) was added. The samples were incubated at 37ºC for 1 hour, with mixing before and at 30 minutes. Cells were then washed in 1mL caspase wash buffer (BD), centrifuged at 1500rpm for 5 minutes and the cells resuspended with 300µL DAPI (4µL DAPI in 8mL 2% PBS).

.

2.4.2.3 Annexin V

Annexin V is a marker of early apoptosis. Annexin V is a member of the phosholipid-binding annexin family and binds to phosphatidylserine (PS). As annexin V can bind to PS specifically, it is considered a selective probe for identifying and quantifying apoptotic cells. PS is restricted to the inner leaflet of the plasma membrane but during apoptosis the plasma membrane undergoes structural changes and PS is translocated to the outer leaflet of the plasma membrane.

Initial steps were performed as outlined above. Once centrifuged (1500rpm for 5 minutes), and the supernatant discarded, cells were washed with 1mL annexin binding buffer (BD) and again spun at 1500rpm for 5 minutes. After the supernatant was discarded and tubes dried, 2.5µL CD45APC and 2.5µL annexin V FITC (both BD) were added, mixed and incubated at RT in the dark for 15 minutes. Cells were then washed

with 1mL annexin binding buffer, centrifuged and resuspended in 300µL DAPI (4µL DAPI in 8mL annexin binding buffer).

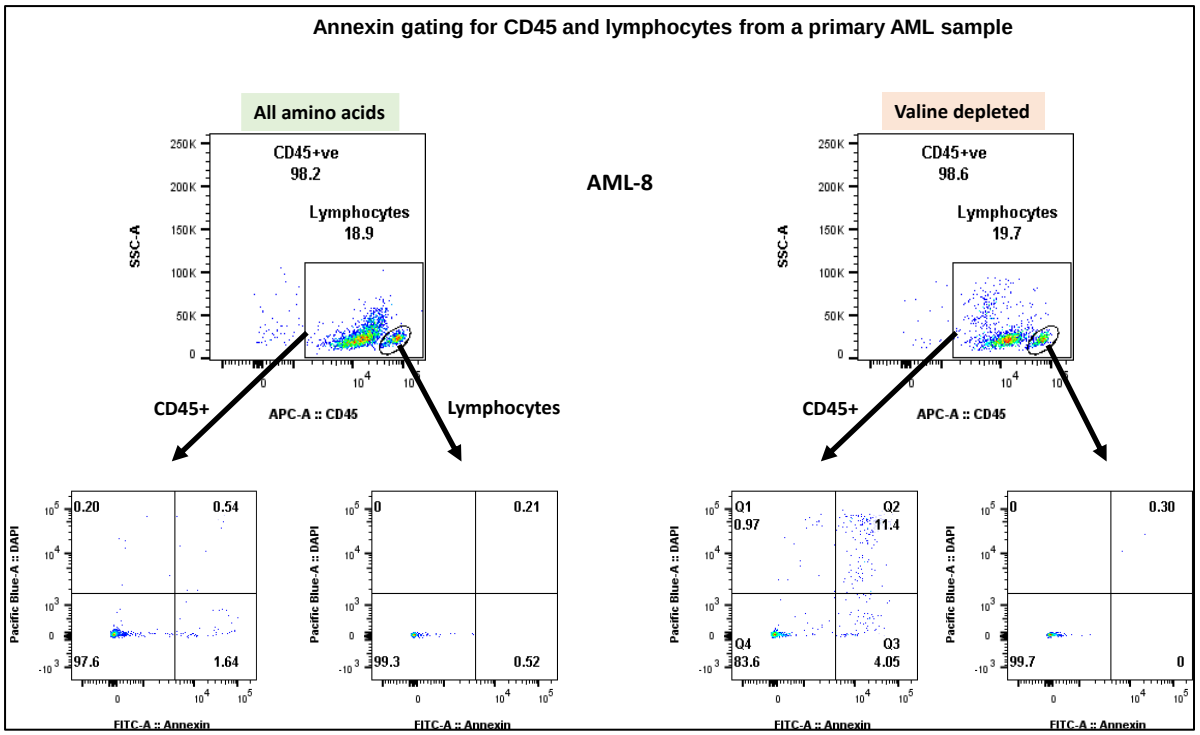

Figure 2.2: Gating for annexin V for control and valine depleted sample – AML8 is used as an example.

2.4.2.4 Ki-67

The Ki-67 protein is strictly associated with cell proliferation. During cell cycling (G_1, S, G_2 and M) it is detected within the cell nucleus but is absent in during G_0.

Initial steps were performed as above. Once centrifuged and dried, 2.5µL CD45PE was added to each tube. Tubes were mixed and incubated at RT in the dark for 20 minutes. Cells were washed with 2% PBS, centrifuged and dried quickly and 0.5mL Fixable Viability Dye eFluor® 780 added (diluted as recommended, eBioscience). Cells were incubated at 4ºC in the dark for 30 minutes and then washed with 2mL 2% PBS. After mixing, 100µL fixation medium A (Nordic-MUbio) was added and the cells incubated at RT for 15 minutes. Cells were then washed with 2mL 2% PBS and 100µL permeabilization medium added before incubating at RT in the dark for 30 minutes.

Cells were then washed again in 2mL 2% PBS, resuspended in 300µL DAPI (3µL DAPI and 1.5mL 2% PBS) and incubated at 4ºC for 10 minutes.

3.4.2.5 Combined cell counting and annexin V

In order to allow faster sample analysis, cell counting and annexin V were later performed from cells for the same 24-well plate. After the initial steps as outlined above, cells were washed in 1mL annexin V binding buffer and centrifuged. 2.5 µL CD45PE (rather than APC) and 2.5µL annexin V were added and the cells incubated at RT in the dark for 15 minutes. They were then washed again with 1mL annexin V binding buffer, centrifuged and resuspended in 300µL DAPI *and* 25µL counting beads. This technique was validated in our lab.

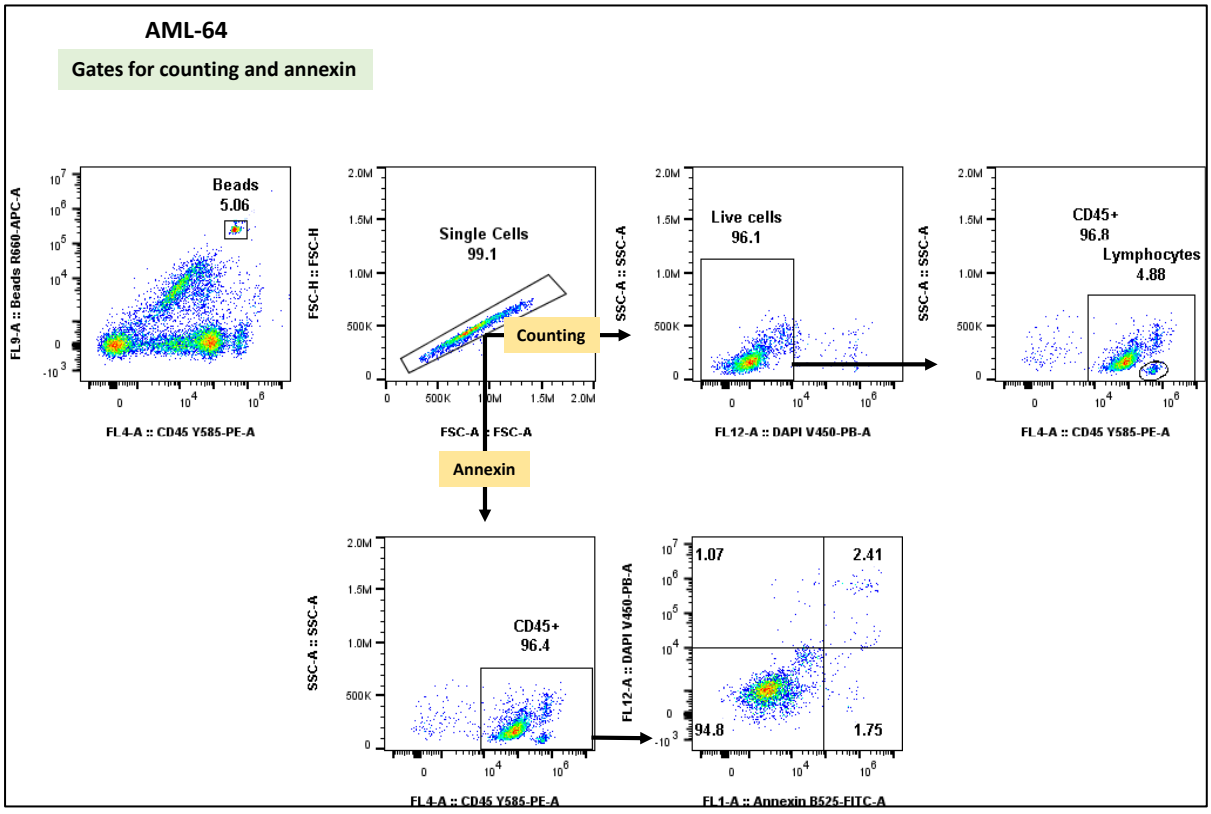

Figure 2.3: Gating for both counting and annexin V for control sample – AML64 is used as an example.

2.3.3 Sample processing and analysis

Compensation was performed although fluorescent spill over was minimal due to the limited number of antibodies and fluorochromes required. Samples were initially measured on a FACS Canto II flow cytometer (BD Sciences) and later a Cytoflex LX flow cytometer (Beckman Coulter).

All samples were analysed using Flowjo software.

2.5 Liquid chromatography mass spectrometry (LC-MS)

2.5.1 Introduction

LC-MS involves the physical separation of compounds or analytes followed by their detection based on mass. The LC component involves an analyte being injected into a flowing stream of solvent (mobile phase) which is then pumped through a column containing silica (stationary phase). The components then separate depending on their affinity to the stationary phase. When the mobile phase flows out of the column it passes through a detector which recognises the different physical and chemical properties of the analytes. The time at which this happens is the retention time which enables the differentiation of the analytes. This is combined with MS to improve accuracy. MS ionises molecules to help their separation and detection based on their mass and charge. When the two interact The MS component ionises molecules to facilitate their separation and detection.

2.5.2 LC-MS method for Biocrates

Samples were processed in accordance with the manufacturer's protocol. Briefly, the stored pellet/media samples were thawed on ice and mixed thoroughly. 200µL 100% ethanol was added to each sample, before incubating on ice for 30 minutes and centrifuging at 4ºC for 5 minutes.

The AbsoluteIDQ® p180 plates were prepared with 10µL internal standard mix and 15µL sample added to each well. The plate was then dried under a nitrogen evaporator for 30 minutes. Derivatization was then performed using 5% PITC (phenylisothiocyanate) and the samples incubated for 20 minutes and then dried under nitrogen flow for a further 60 minutes. 300µL extraction solvent was then added to each sample and the plates agitated at 450rpm for 30 minutes. Samples were then filtered by centrifugation for 2 minutes at 500g. 150µL was then transferred to a second 96-well plate and diluted with 150µL water.

Plates were then run on a TQ-S mass spectrometer (Waters). Data were acquired and analysed using MassLynx and TargetLynx software and processed/evaluated using MetIDQ software (Biocrates Life Sciences). Data are shown on Graphpad Prism. Multivariate cluster analysis was performed using SIMCA (Umetrics/Sartorius).

Details of the collaboration and the degree of assistance received is outlined at the beginning of the thesis.

2.5.3 LC-MS method for initial optimisation experiments

Metabolites were extracted from AML cells with methanol at -80ºC, dried under nitrogen and reconstituted in acetonitrile-water (1:1) before LC-MS/MS analysis.
Targeted, non-quantitative LC-MS/MS was carried out on a QTrap6500 mass spectrometer (AB Sciex) with a Shimadzu Nexera UPLC system using HILIC chromatography and a positive/negative ion-switching method [139]. Chromatography was performed on an XBridge® Amide 3.5 µm HPLC column (100 mm x 4.6 mm i.d.) (Waters) using a gradient mobile phase of acetonitrile and 20 mM ammonium acetate at pH 9. The flow rate was 0.3 mL/min and the run time 23 mins [139]. Analyst® software (AB Sciex) was used for data acquisition.

2.5.4 MS for proteomics project

Analysis of the AML proteome was performed by the Functional Proteomics team at the ICR using isobaric labelling through tandem mass tags (TMT) [140]. A schematic of the workflow is shown in figure

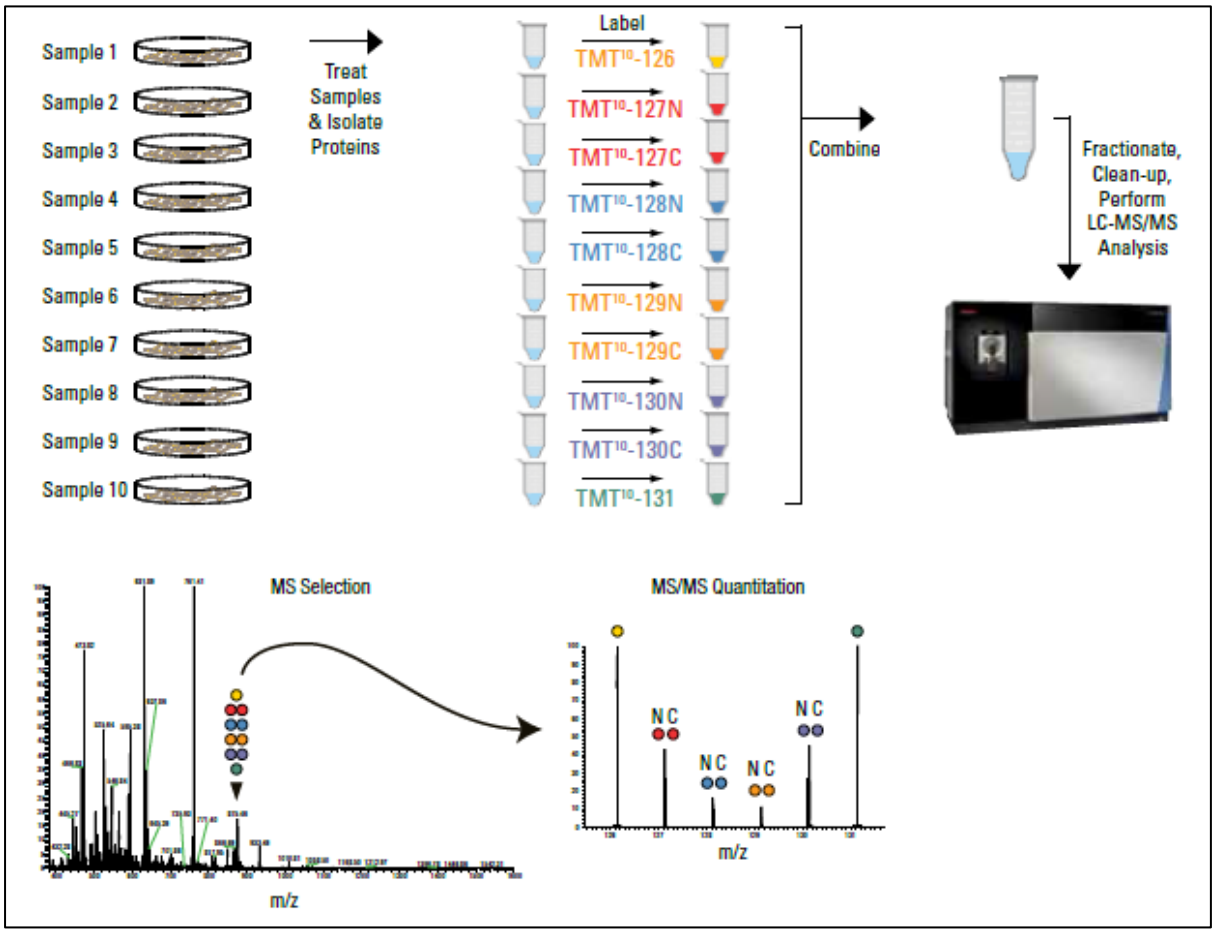

Figure 2.4: Schematic showing an overview of the TMT workflow (courtesy of Creative Protemoics).

2.6 Molecular techniques

2.6.1 Western Blotting

Western Blotting allows visualisation and examination of the expression levels of proteins extracted from cells. Proteins are separated from one another based on their molecular weight using SDS-PAGE. The detergent SDS linearises proteins and coats them in negative charges, meaning molecular weight is the only difference between the proteins. An electrical current is applied to the gel and the negatively charged proteins migrate towards the anode based on their molecular weight – smaller proteins migrate faster, larger proteins migrate slower. Separated proteins are then transferred to a PVDF membrane which allows the protein of interest to be detected using specific antibodies.

Western blot analysis was performed using the NuPAGE Bis-Tris electrophoresis system (Invitrogen). Cells were lysed with CelLytic M cell Lysis Reagent (Sigma) supplied with protease and phosphatase inhibitor cocktails (Sigma) for 20 minutes on ice. After centrifuging at 12000g for 15 minutes, protein concentrations were determined by Bicinchoninic Acid (BCA) method. Bicinchoninic Acid is a highly specific chromogenic reagent for Cu (I) forming a complex with an absorbance maximum at 570 nm. The total protein concentration is exhibited by a colour change of green to purple in proportion to protein concentration, which can then be measured using colorimetric techniques. This assay uses defined BSA (bovine serum albumin) concentrations to produce a standard curve from which unknown protein concentrations can be calculated by linear regression.

50µg of extracted proteins were mixed with NuPAGE LDS Sample Buffer (Invitrogen) and boiled for 5 min. The denatured proteins were subjected to 4–12% NuPAGE gels (Invitrogen) and transferred onto polyvinylidene fluoride membrane (PVDF) using the iBlot dry blotting system (Invitrogen). Membranes were blocked with 5% nonfat dried milk in PBS Tween-20 (0.2%) for 1 hour at room temperature and then incubated with primary antibodies (listed in chapter 7) overnight at 4°C. Unbound primary antibody was washed off with TBS-T (3 × 10 minute washes) after which membranes were probed with anti-rabbit/anti-mouse HRP (horse radish peroxidase) conjugated

secondary antibodies for 1 hour at room temperature with agitation. Unbound secondary antibody was washed off with TBS-T (3 ×10 minute washes). Membranes were coated in Pierce ECL Western Blotting Substrate to allow exposure of bands which were visualised using LI-COR developer. Membranes were washed and stripped with TBS-T and stripping buffer and re-probed if needed. For loading controls ß-actin antibody were used.

Semiquantification of the bands was carried out by optical densitometry and analysed using the ImageJ software. The expression of each protein analysed was normalised with ß-actin.

2.6.2 mRNA expression by real-time PCR

Total RNA was extracted from primary samples with an RNeasy Mini Kit (Qiagen). Prior to cDNA synthesis genomic DNA was removed from total RNA using an RNase-free DNase set (Qiagen). The RNA concentration and purity were checked by Nanodrop 1000 (Thermo Fisher Scientific). 2µg of total RNA was used for synthesising complementary DNA (cDNA) using a high capacity RNA to cDNA kit (Applied Biosystems) according to the manufacturer's instructions. Expression level of genes (listed in chapter 7) were measured using Taqman real-time PCR assay. The 20x FAM dye labelled probe-primer mix and the 2x Universal Master Mix were purchased from Applied Biosystems. The reactions were performed in 96-well plates in triplicates using StepOne Real-Time PCR system (Applied Biosystems) in accordance with manufacturer's guidance. Data were analysed using the $2^{-\Delta Ct}$ method after normalisation to GAPDH, an endogenous control. All quantities were expressed as number of folds relative to the expression of GAPDH.

Each sample was analysed in triplicate and normalised to GAPDH (delta CT). Delta CT values were standardized to a calibrator value generated from the average delta CT of all values. The relative expression was calculated using the comparative CT method with fold change (2-delta delta CT).

2.6.3 Immunofluorescence

Immunofluorescence staining for antibodies (listed in chapter 7) was performed on mononuclear cells from AML patients. $0.5x10^6$ cells were attached to SuperFrost Plus microscope slides (Life Technologies) using cytospin centrifugation. Cells were washed with PBS, fixed with 4% paraformaldehyde for 10 min and permeabilised with 0.5% Triton X-100 for 10 min. After washing, cells were blocked with 2% FBS containing 0.05% of Tween-20 (TPBS). Antibodies were diluted in blocking buffer and incubated on slides overnight at 4°C. AlexaFluor-conjugated secondary antibody (diluted 1:500) in blocking solution was then added and the slides incubated at 37°C for 1 h in a humidified chamber. The slides were then washed with TPBS and mounted with antifade mounting medium with DAPI (Vectashield; Vector Laboratories). Images were captured on an LSM510 Meta confocal laser microscope (Carl Zeiss) in XY mode using a 40 x 1.3 oil immersion objective with the image size set at 512 × 512 pixels. HeLa cell line were used as positive control.

Chapter 3: Measuring AA dependence using co-culture

3.1 Introduction

3.1.1 Challenges

The focus of this research project was originally the investigation of arginine deprivation in AML within the context of a clinical trial. For reasons beyond our control, the clinical trial around which the experimental laboratory work centred, did not proceed in the UK and the project changed to a broader laboratory based investigation of amino acid dependence. Ideally, results from chapter 5 would have informed the choice of AAs selected for the deeper analysis described in this chapter but this was not feasible due to time constraints caused by this delay. This was compounded by prolonged interruptions to study caused by the COVID-19 pandemic.

3.1.2 Rationale for selection of amino acids

The 6 amino acids studied in this chapter were therefore selected because of the potential susceptibility of AML to their restriction. The reasons for their selection is justified in the chapter 1.

3.2 Aims and objectives

The primary aim of the work in this chapter was to determine the effect of selected AA deprivation on AML cells. Based on the knowledge that cancer cells show increased uptake of amino acids the hypothesis was that AML cells would demonstrate a susceptibility to AA deprivation. This objective was achieved by co-culturing AML cells

in media lacking in specific AAs and analysing cell death and markers of apoptosis and proliferation.

The first objective was to investigate the effect in AML cell lines.

The second objective was to determine the significance of any effect in primary AML samples when compared to normal controls.

A third objective was to compare any effect across different AML risk groups: i.e. are adverse risk AMLs more dependent on AAs.

3.3 Summary of specific methods

Detailed methodology is described in chapter 2 but a brief overview is provided here.

3.3.1 Samples

A summary of the characteristics of the AML cell lines, primary AML samples and BM control samples used in this chapter are provided in tables 3.1, 3.2 and 3.3 respectively. Peripheral blood AML samples were used to ensure an adequate sample number, sufficient cell number for co-culture and to maintain consistency. Samples were generally processed on the same day or, when not feasible, the following day. Bone marrow rather than peripheral blood controls were used in line with our team's previously published work [64, 141].

Cell line	Description	Origin	Karyotype
FKH-1	Secondary AML (Ph. Negative CML)	35 female	t(6;9)
HL-60	Acute promyelocytic leukaemia (APML)	61 male	Complex
Kasumi	Relapsed post HSCT	7 male	Complex

Table 3.1: Cell line sample characteristics

ID	1˚/2˚	Sex	Age	Timing	Cytogenetics	MRC Risk	ELN Risk	NPM1	FLT3-ITD	Ratio	TP53
AML38	Primary	M	72	Diagnosis	Complex	Adverse	Adverse	No	No	n/a	Yes
AML39	Primary	M	59	Diagnosis	Complex	Adverse	Adverse	No	No	n/a	Yes
AML37	Primary	M	47	Relapse	7q-	Adverse	Adverse	No	No	n/a	NK
AML41	Primary	M	56	Relapse	Complex	Adverse	Adverse	No	No	n/a	NK
AML42	Secondary	M	80	Diagnosis	t(3;3)	Adverse	Adverse	No	Yes	0.78	No
AML49	Secondary	F	21	Relapse	Complex	Adverse	Adverse	No	No	n/a	NK
AML58	Primary	M	73	Diagnosis	Complex	Adverse	Adverse	No	No	n/a	No
AML27	Primary	F	25	Relapse	Complex	Adverse	Adverse	Yes	No	n/a	No
AML64	Primary	M	24	Diagnosis	Normal	Intermediate	Adverse	No	Yes	0.56	No
AML20	Primary	M	72	Diagnosis	Normal	Intermediate	Adverse	No	Yes	0.36	No
AML24	Primary	F	69	Diagnosis	-16, -18	Intermediate	Adverse	No	Yes	0.28	Yes
AML43	Primary	M	71	Relapse	t(1;11), +8	Intermediate	Adverse	No	No	n/a	No
AML25	Secondary	F	82	Diagnosis	i(22q)	Intermediate	Intermediate	No	No	n/a	NK
AML8	Primary	F	71	Diagnosis	Normal	Intermediate	Intermediate	No	No	n/a	NK
AML35	Secondary	F	64	Relapse	1q-	Intermediate	Intermediate	No	No	n/a	No
AML44	Secondary	F	39	Diagnosis	t(9;11)	Intermediate	Intermediate	No	No	n/a	No
AML5	Primary	F	81	Relapse	Normal	Intermediate	Intermediate	No	No	n/a	NK
AML31	Primary	M	59	Diagnosis	Normal	Intermediate	Adverse	Yes	Yes	2.17	No
AML29	Primary	F	67	Diagnosis	3 way	Intermediate	Intermediate	Yes	Yes	n/a	NK
AML30	Primary	F	69	Diagnosis	Normal	Intermediate	Intermediate	Yes	Yes	0.87	No
AML28	Secondary	M	65	Diagnosis	+8	Intermediate	Intermediate	Yes	No	n/a	No
AML4	Primary	F	22	Diagnosis	Normal	Intermediate	Intermediate	Yes	No	0.61	NK
AML3	Primary	M	47	Diagnosis	Normal	Intermediate	Favourable	Yes	No	n/a	NK
AML7	Primary	F	57	Diagnosis	Normal	Intermediate	Favourable	Yes	Yes	0.04	NK
AML45	Primary	M	72	Diagnosis	Normal	Intermediate	Favourable	Yes	Yes	0.48	No
AML46	Primary	M	65	Diagnosis	Normal	Intermediate	Favourable	Yes	Yes	0.37	No
AML40	Primary	F	40	Diagnosis	Normal	Intermediate	Favourable	Yes	No	n/a	No
AML47	Primary	F	55	Diagnosis	Normal	Intermediate	Favourable	Yes	No	n/a	No
AML21	Primary	F	34	Diagnosis	inv(16)	Favourable	Favourable	No	No	n/a	No
AML22	Primary	M	60	Diagnosis	inv(16)	Favourable	Favourable	n/a	n/a	n/a	NK

Table 3.2: Primary AML sample characteristics showing both the MRC cytogenetic and ELN risk classifications (red=adverse, orange=intermediate, green=favourable).

Control number	Source	Age	Sex
BM1	Lymphoma staging	65	M
BM2	Lymphoma staging	41	M
BM3	Healthy volunteer	41	F
BM4	Healthy volunteer	38	F
BM5	Healthy volunteer	36	F
BM6	Healthy volunteer	41	M
BM7	Lymphoma staging	54	M
BM8	Healthy volunteer	44	F

Table 3.3 Characteristics of BM controls.

3.3.2 Synopsis of co-culture method

Table 3.4 summarises the co-culture conditions used throughout the experiments described in this chapter. A schematic summarising the co-culture method described in chapter 2 is shown in figure 3.1.

3.3.3 Statistical analysis

All statistical analysis was performed using Graphpad prism software. A student t test was used unless otherwise stated ($p<0.05$).

Number	Condition	Description
1	Control	Contains all AAs
2	-Ser	Without serine
3	-Ser/Gly	Without serine, glycine
4	-Val	Without valine
5	-Met	Without methionine
6	-Asn	Without asparagine
7	-Gly	Without glycine
8	-Gln	Without glutamine

Table 3.4: Modified AA conditions

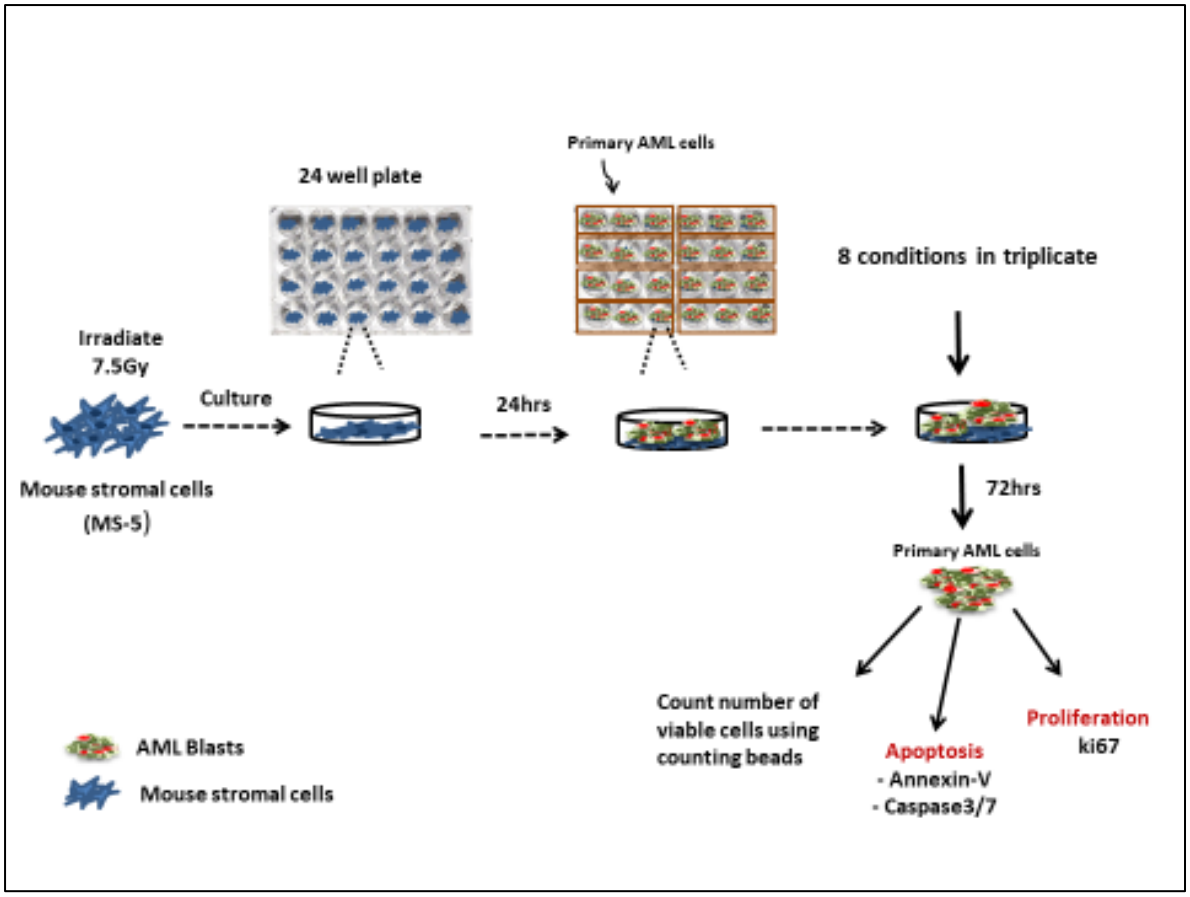

Figure 3.1: Schematic of the co-culture protocol used for primary AML and control samples. Note an MS-5 feeder layer was not required for support of AML cell lines.

3.4 Results

3.4.1 Sample characteristics

A total of 3 cell lines, 30 primary AML PB samples and 8 BM control samples were co-cultured successfully. A summary of the sample characteristics of the primary AML samples is shown in table 3.2. 15 (50%) were male and the mean age 57 years (range 21-82). By MRC cytogenetic classification 27% (8/30) were adverse risk, 67% (20/30) intermediate risk and 6% (2/30) favourable risk. By ELN classification, 13/30 (43%) were adverse, 9/30 (30%) intermediate and 8/30 (27%) favourable risk.

Of the 8 controls half were male and half female. The mean age was 45 (36-65).

3.4.2 Amino acid requirements of AML cell lines

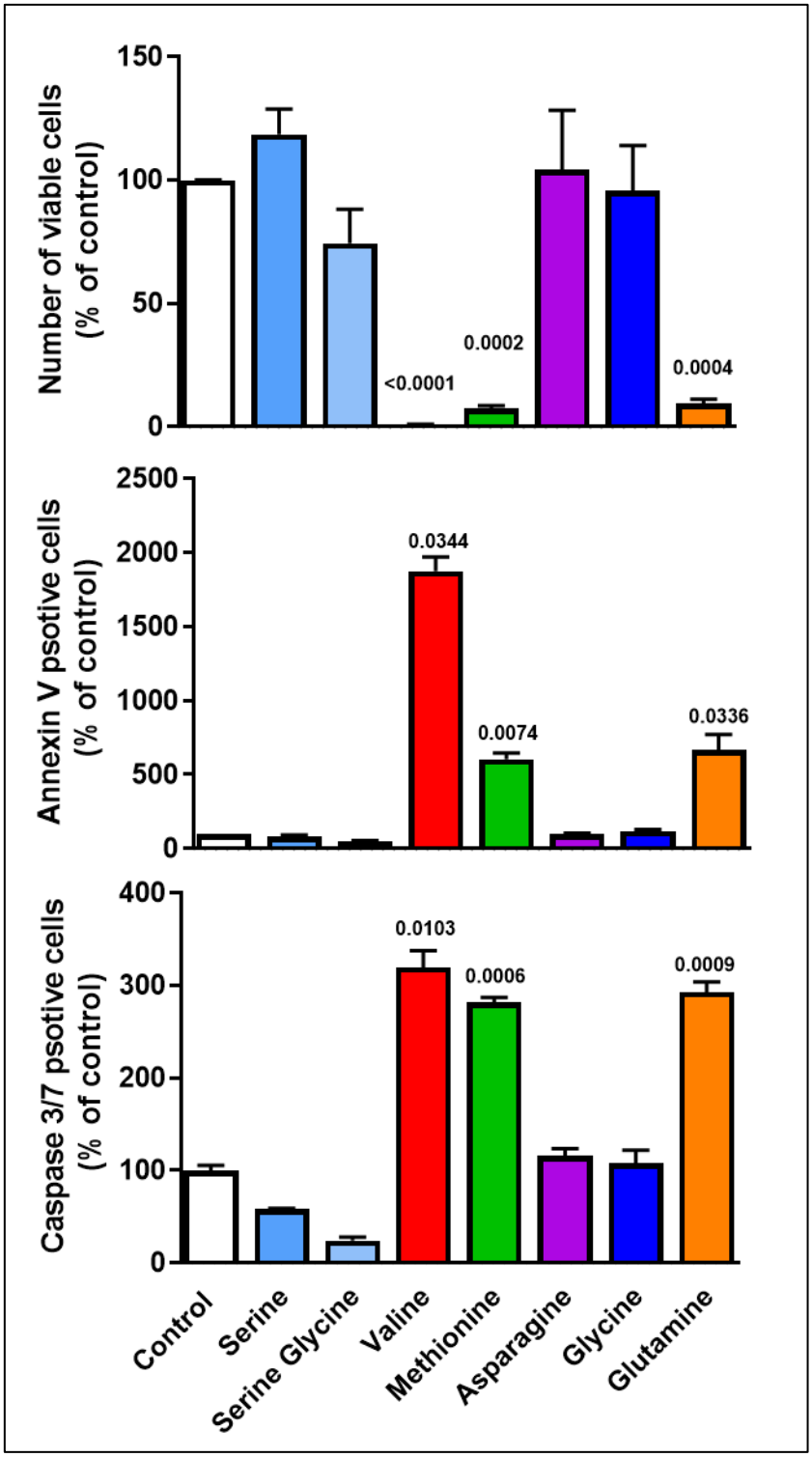

Figure 3.2: Bar chart showing the results for the HL-60 cell line - number of viable cells, and % of annexin and caspase 3/7 positive cells. Control = all AAs, Serine=serine deplete etc.

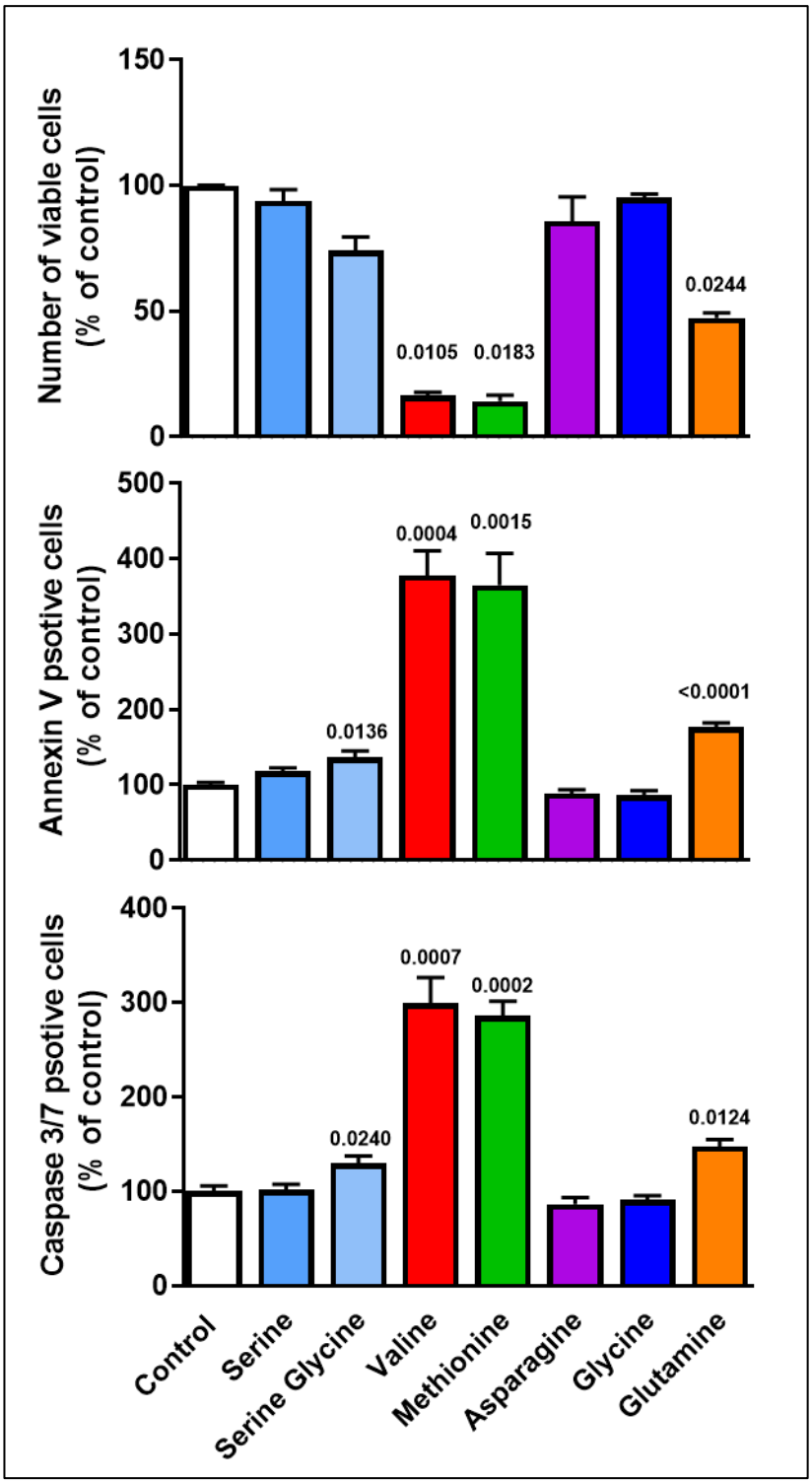

Figure 3.3: Bar chart showing the results for the Kasumi cell line - number of viable cells, and % of annexin and caspase 3/7 positive cells. Control = all AAs, Serine=serine deplete etc.

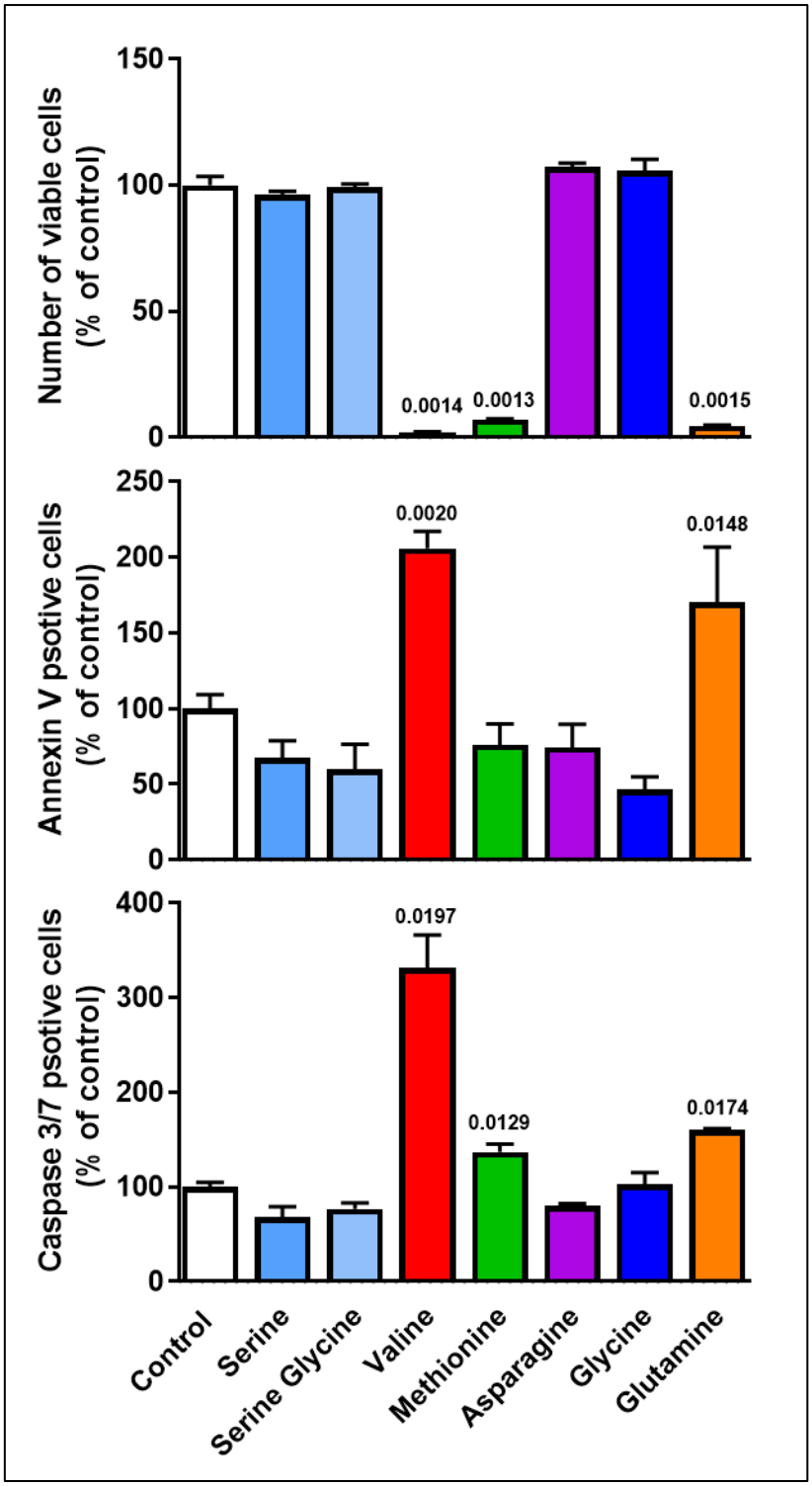

Figure 3.4: Bar chart showing the results for the FKH-1 cell line - number of viable cells, and % of annexin and caspase 3/7 positive cells. Control = all AAs, Serine=serine deplete etc.

Figures 3.2 to 3.5 show the results for the 3 AML cell lines (HL-60, Kasumi and FKH-1). There was a significant reduction in viable cells following depletion of valine, methionine and glutamine. This was mirrored by a significant increase in markers of apoptosis. Figure 3.3 shows that there was a significant increase in the percentage of cells in GO following depletion of serine/glycine, valine, methionine and glutamine.

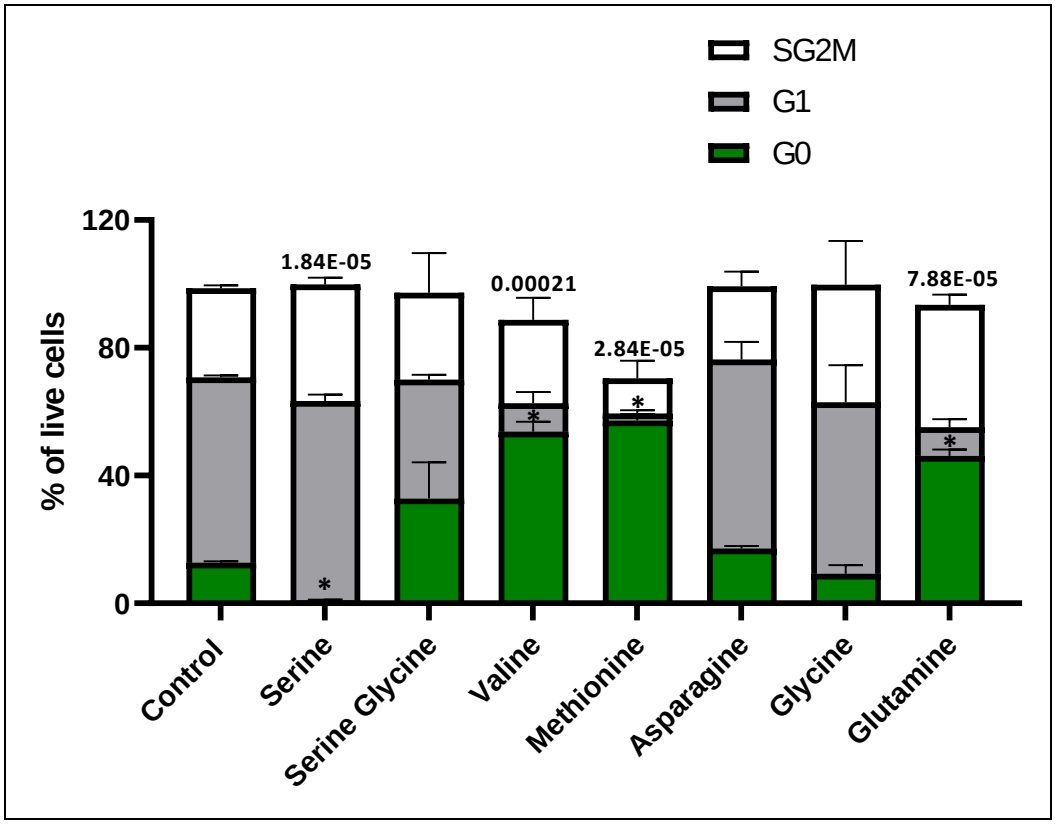

Figure 3.5: Bar chart showing the combined results for the HL-60 cell line for Ki-67. There is a a significant increase in the number of cells in G0 following depletion of serine/glycine, valine, methionine and glutamine. Control = all AAs, Serine=serine deplete etc.

Next I looked at primary AML samples. Ki-67 analysis showed that cells were in G0 so this was not routinely performed for the AML samples.

3.4.3 Example of a primary AML sample with number of viable cells and markers of apoptosis (AML3)

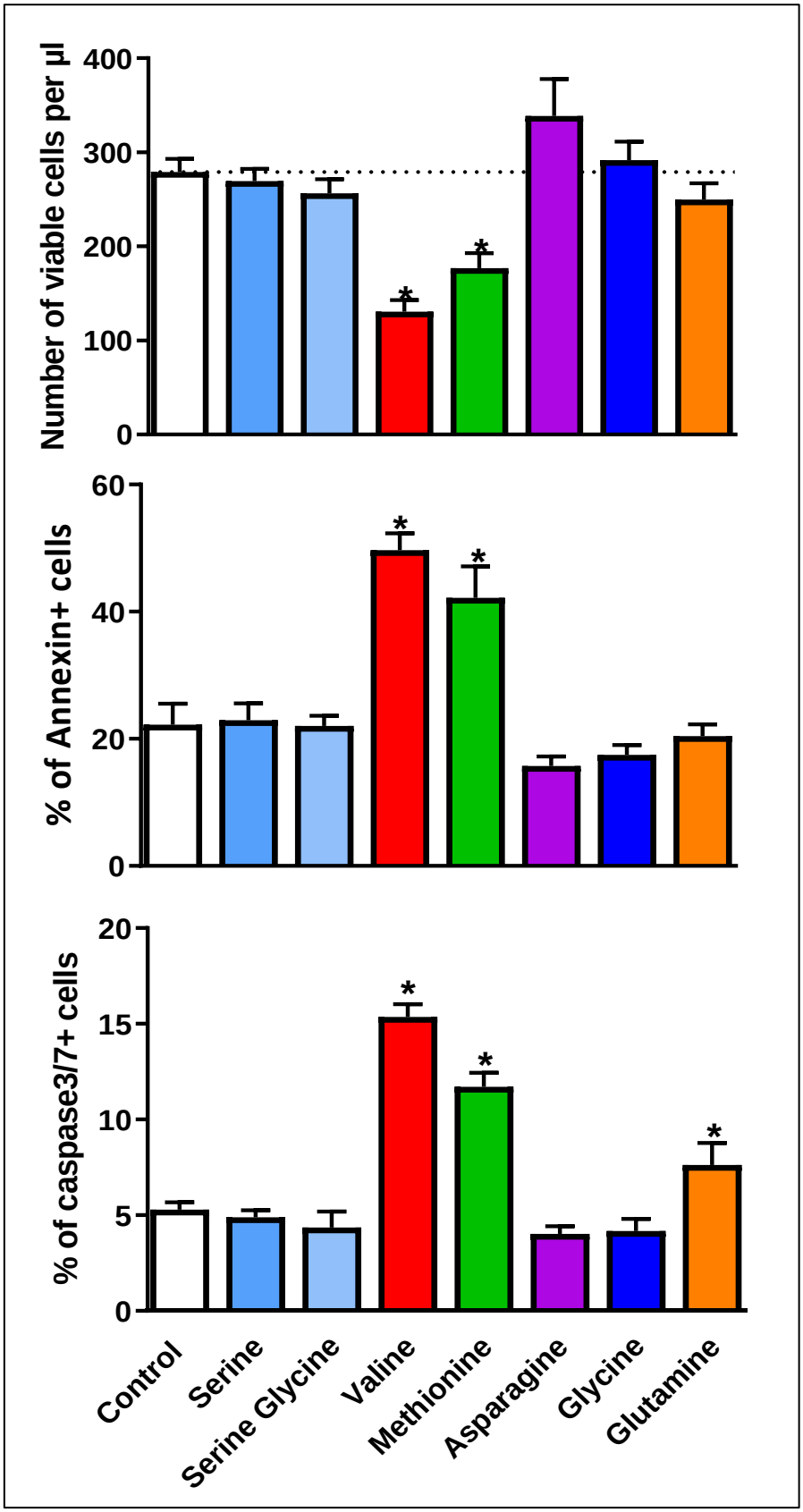

Figure 3.6: Bar chart for AML3 showing number of viable cells, and % of annexin and caspase 3/7 positive cells. Control = all AAs, Serine=serine deplete etc.

AML3 shows a clear significant difference in viable cell number in the valine and methionine deprived group. This is mirrored by a significant rise in the percentage of annexin and caspase 3/7 positive cells.

I went on to analyse a total of 30 primary AML samples. Annexin and caspase 3/7 results were comparable so annexin only was used in the majority of samples, in addition to viable cell number.

3.4.4 AML cells show specific amino acid dependencies

Figure 3.7 shows the specific amino acid dependencies of AML cells in co-culture. To a varying degree valine, methionine and glutamine deprivation induce cell death (all p values given in the figure). The apoptotic markers annexin and caspase 3/7 show a corresponding rise. A combination of serine and glycine deprivation has the same effect although only annexin is significantly increased. Paradoxically, asparagine withdrawal leads to a significant rise in the number of viable cells, with a significant fall in both annexin and caspase.

Next I gated the lymphocyte population to assess how they were effected.

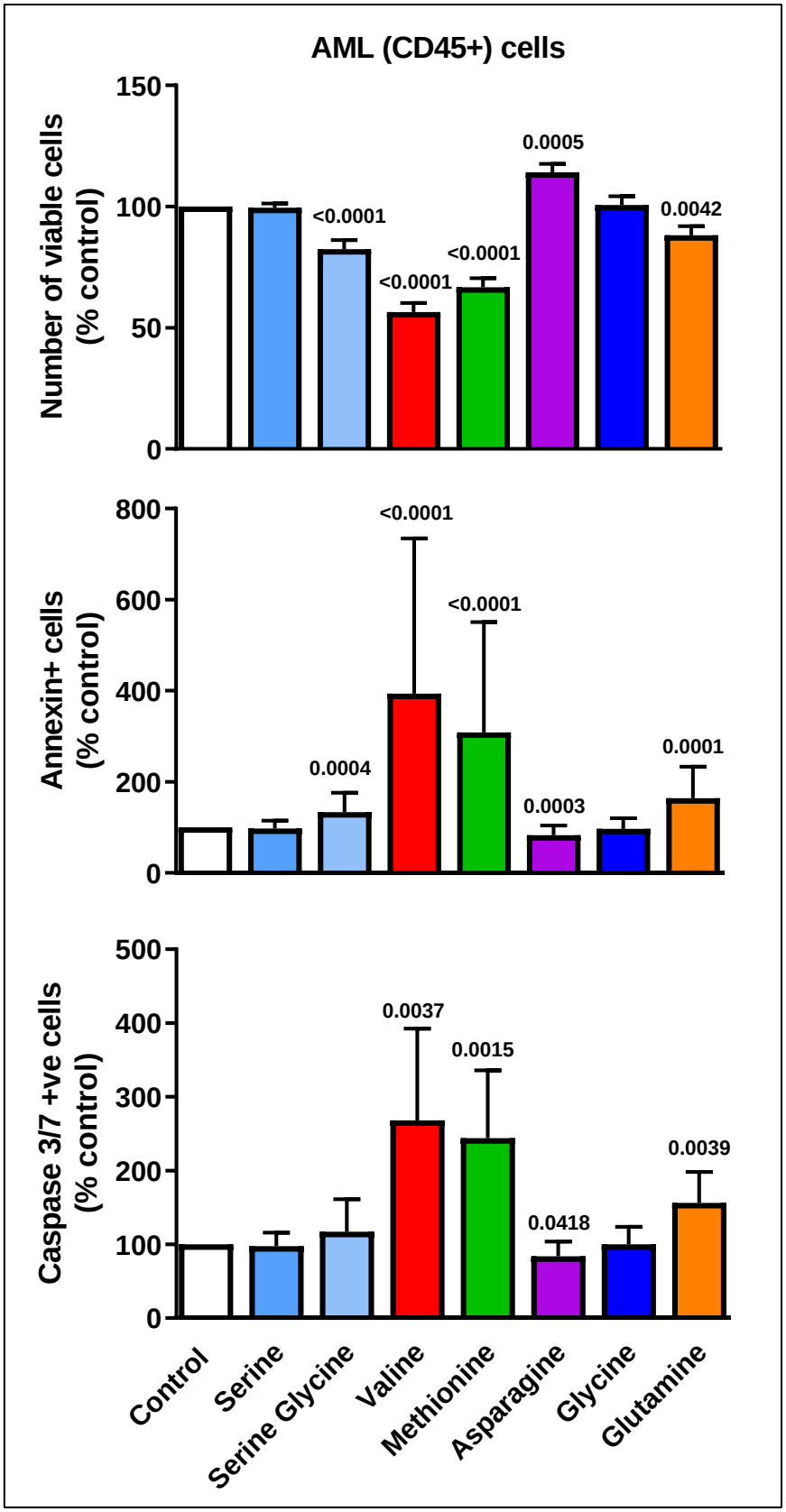

Figure 3.7: Bar chart for all (n=30) AML samples showing number of viable cells, and % of annexin and caspase 3/7 positive cells. Numbers represent the p value compared to control where p<0.05 using student t test.

3.4.5 Amino acid deprivation had no effect on lymphocyte population

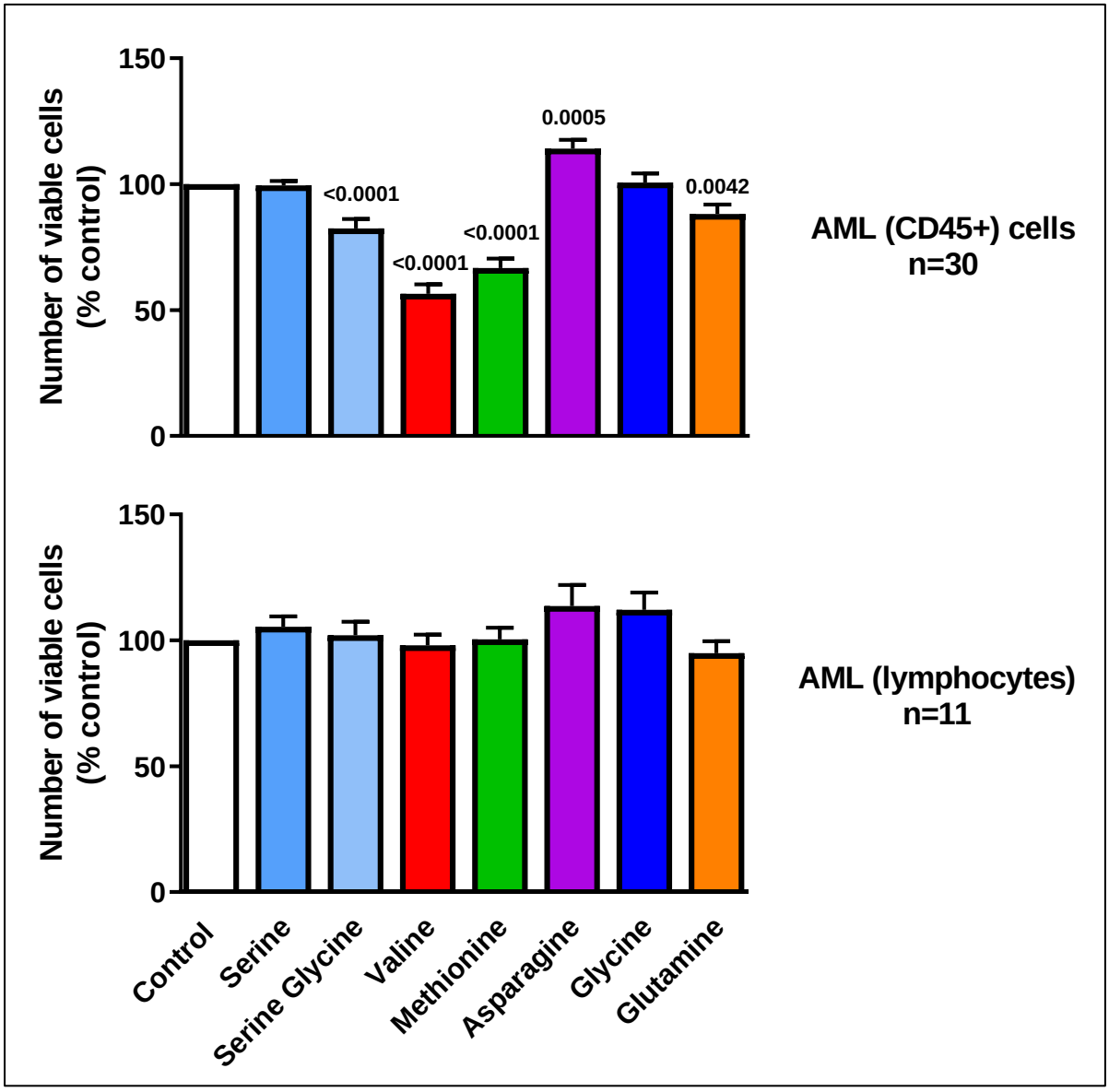

Figure 3.8 Bar chart showing number of viable cells (as a % of control) in both the CD45+ blast and lymphocyte populations.

Figure 3.8 shows that there was no significant change in viable cell number in the lymphocyte population in 11 of the AML samples, indicating that AML cells are affected by AA deprivation while lymphocytes are not.

I next looked at normal BM controls.

3.4.6 Normal BM cells are less affected by AA depletion

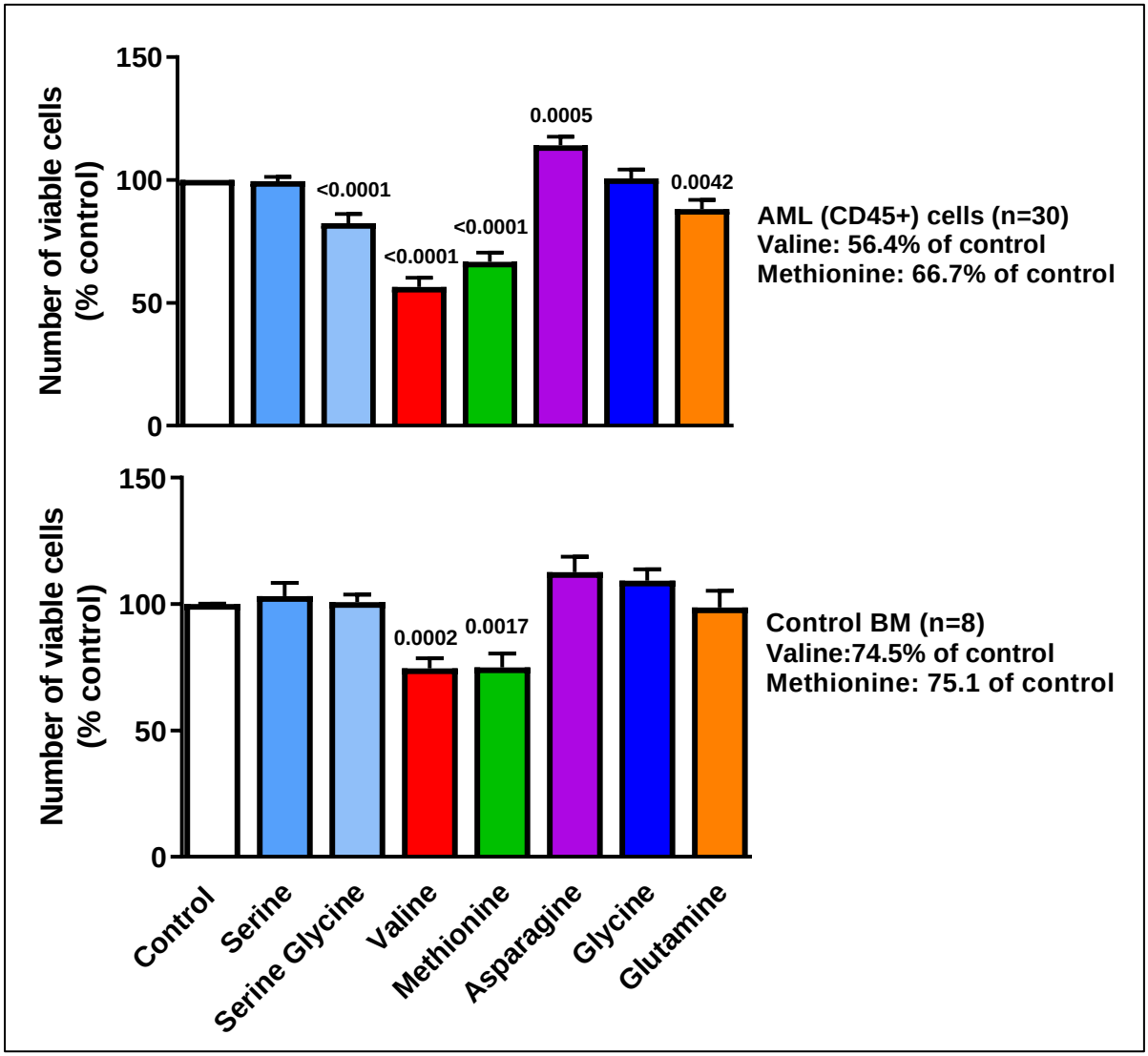

Figure 3.9: Bar chart showing number of viable cells (as a % of control) in both the AML and BM control groups.

In contrast to the AML samples, depletion of glutamine, asparagine or the serine/glycine combination had no effect on the BM control samples. Although the effect of valine and methionine depletion persisted it was less marked with values at 75% of control versus 66% for methionine in normal BM and AML, respectively.

Figure 3.10 shows the corresponding annexin data. Again, changes are less pronounced in the BM controls.

I then looked in more detail at the individual amino acids and the impact of risk classification.

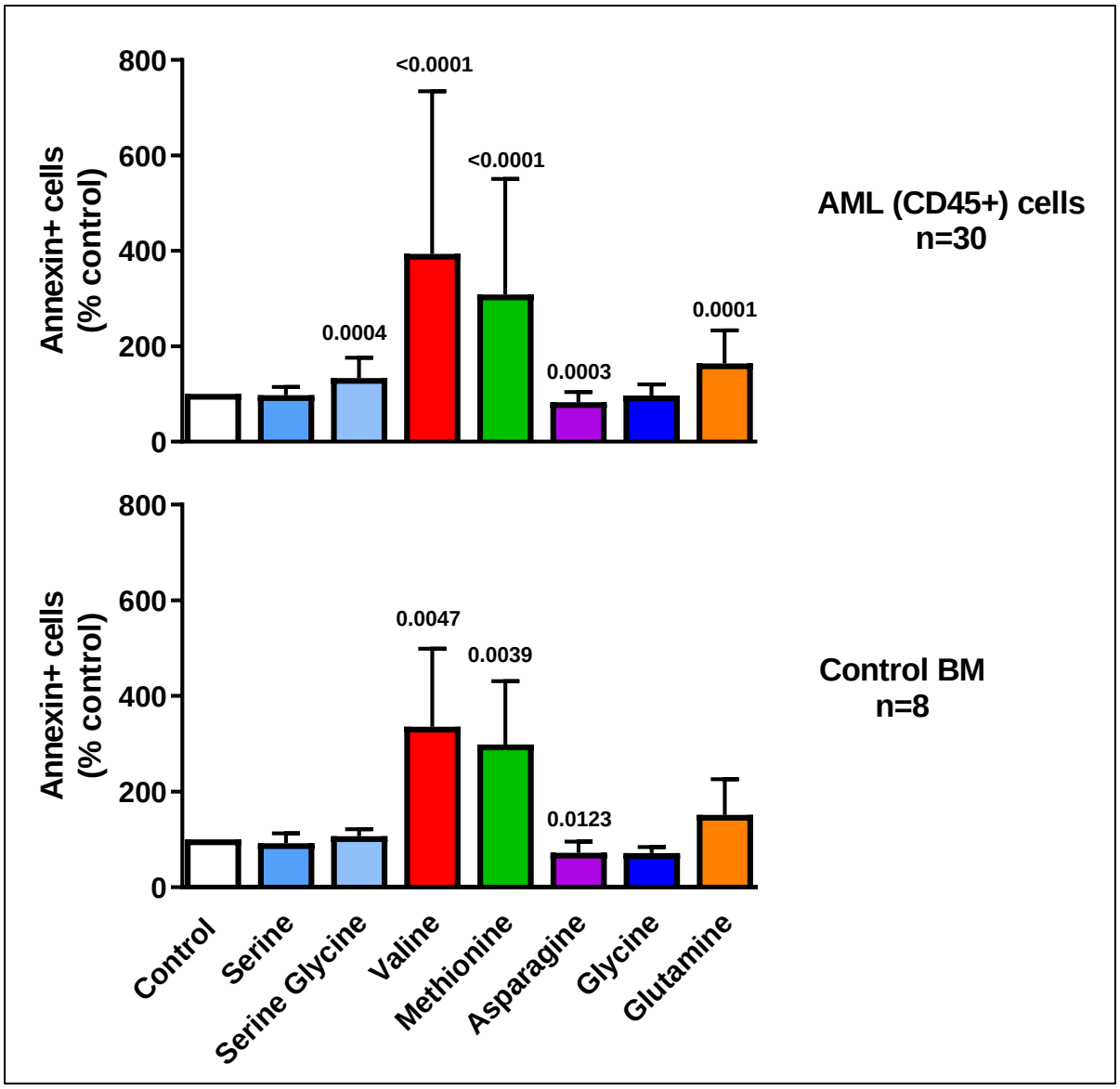

Figure 3.10: Bar chart showing number of annexin positive cells (as a % of control) in both the AML and normal BM control groups.

3.4.7 Valine depletion induces AML cell death in all risk groups

Figure 3.11 shows that valine depletion has a significant effect on viable cell number irrespective of risk classification compare to normal BM controls. There is no significant difference in number of annexin positive cells (figure 3.12).

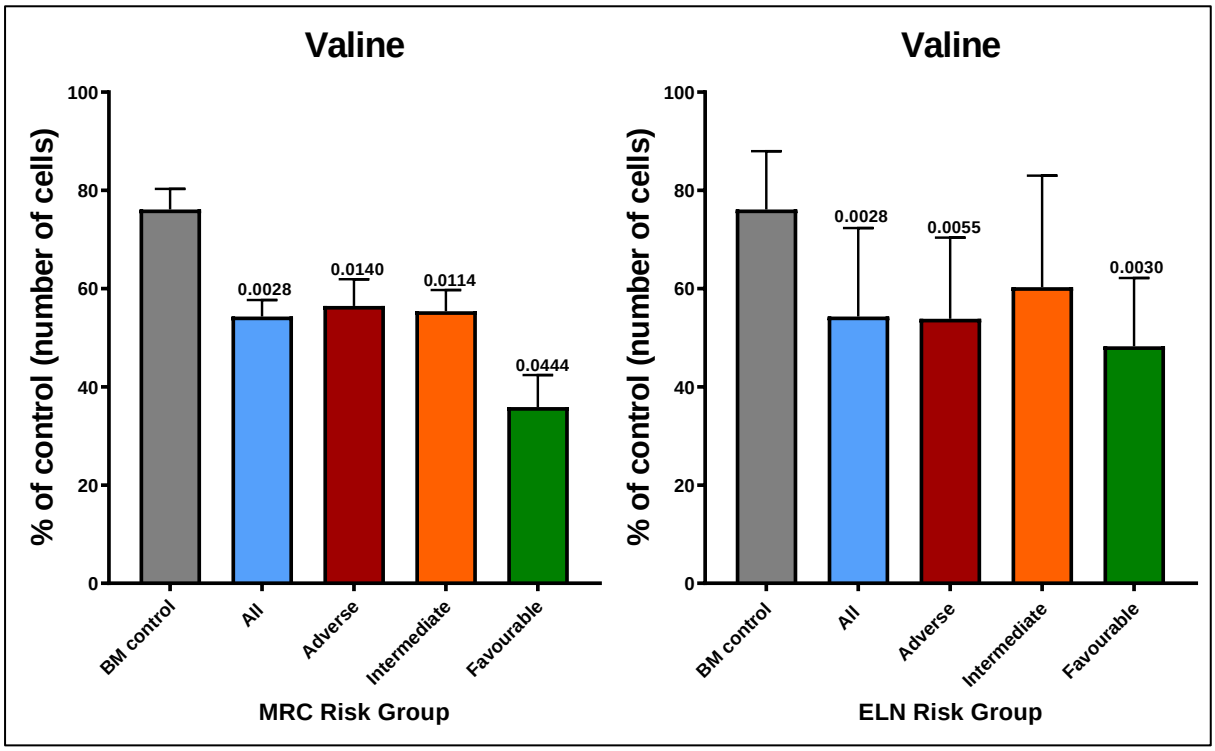

Figure 3.11: Bar charts showing the effect of valine depletion on viable cell number compared to normal controls. N=30. For MRC groups adverse n=8, intermediate n=20, favourable n=2. For ELN adverse n=13, intermediate n=9, favourable n=8. ($p<0.05$)

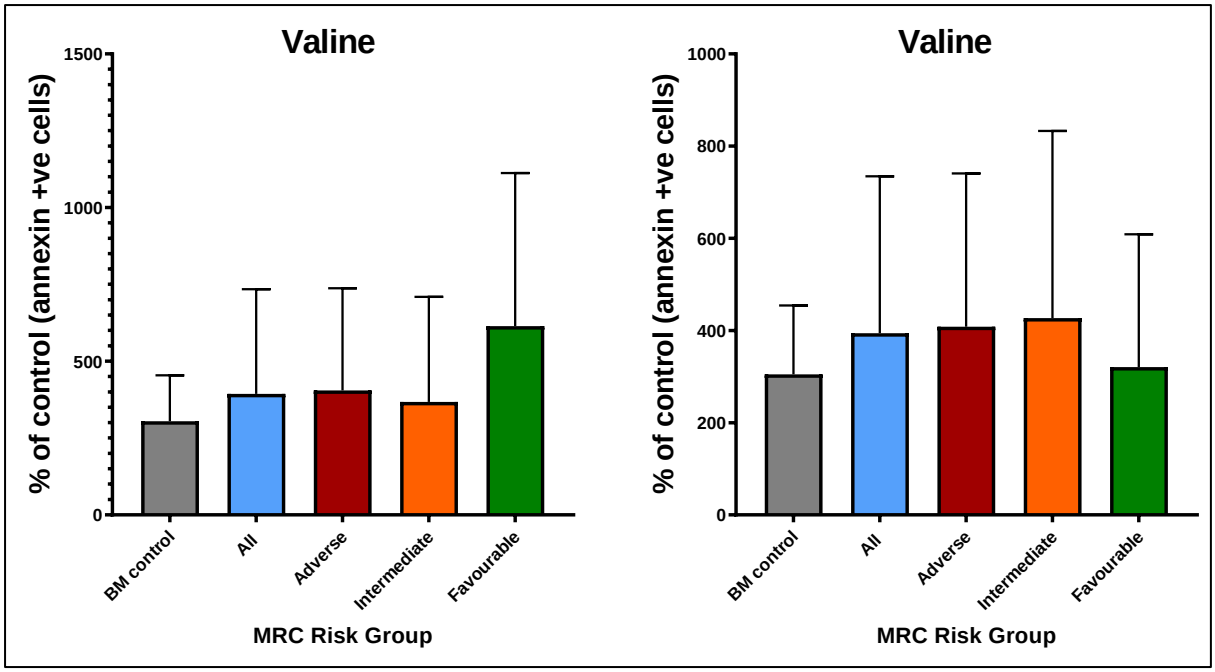

Figure 3.12: Bar charts showing the effect of valine depletion on annexin compared to normal controls. N=30. For MRC groups adverse n=8, intermediate n=20, favourable n=2. For ELN adverse n=13, intermediate n=9, favourable n=8.

3.4.8 Methionine depletion induces cell death in favourable risk AML

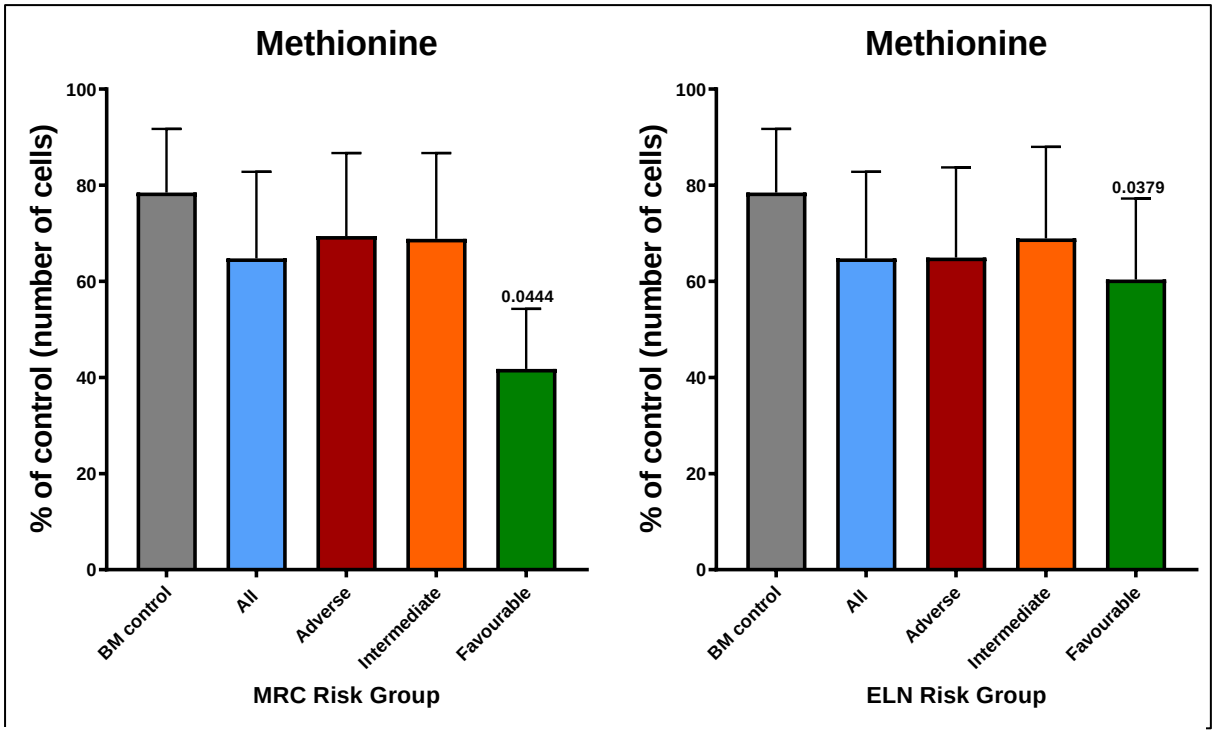

Figure 3.13: Bar charts showing the effect of methionine depletion on viable cell number compared to normal controls. N=30. For MRC groups adverse n=8, intermediate n=20, favourable n=2. For ELN adverse n=13, intermediate n=9, favourable n=8.

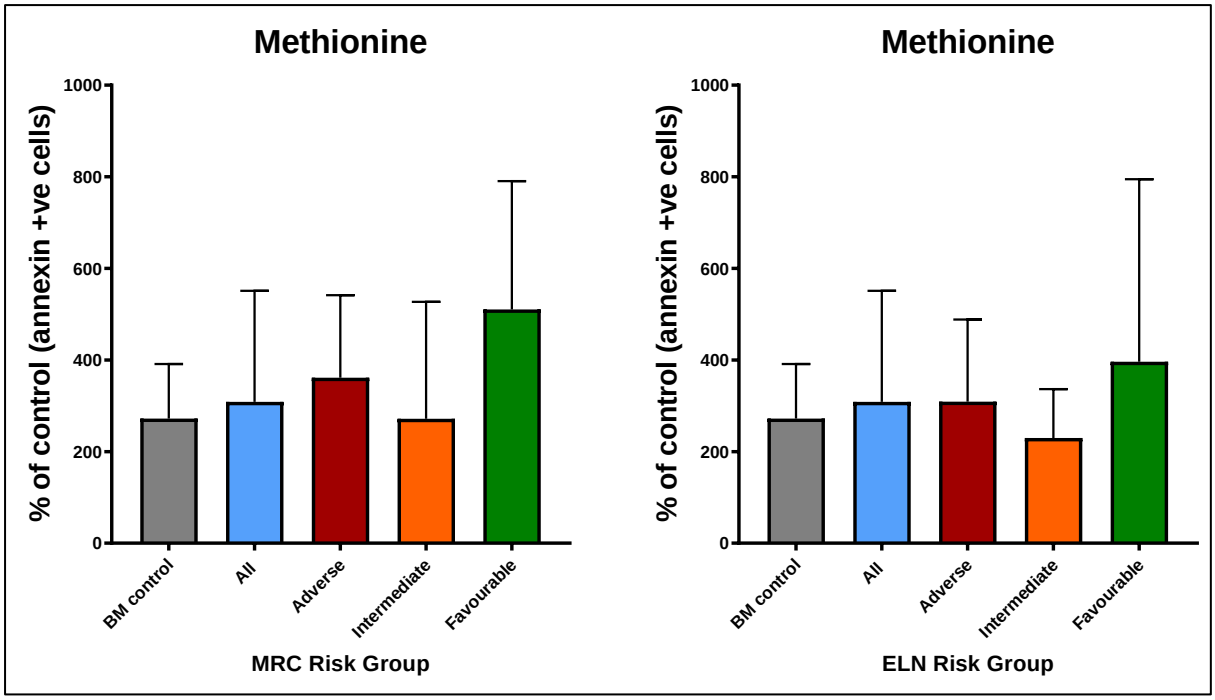

Figure 3.14: Bar charts showing the effect of methionine depletion on annexin compared to normal controls. N=30. For MRC groups adverse n=8, intermediate n=20, favourable n=2. For ELN adverse n=13, intermediate n=9, favourable n=8.

Figure 3.13 shows that methionine depletion only causes a significant reduction in viable cell numbers in favourable risk AML. There is no significant increase in number of annexin positive cells with methionine depletion compared to control (figure 3.14).

3.4.9 Serine and glycine deprivation induces cell death in higher risk AML

A statistically significant reduction in viable AML cell number was seen with a combination of serine and glycine depletion in all but the favourable risk groups (figure 3.15). Serine depletion alone had no significant effect on viable cell number. Glycine depletion alone led to a significant reduction in viable cell number in AML compared to control in the MRC intermediate risk group only (figure 3.17).

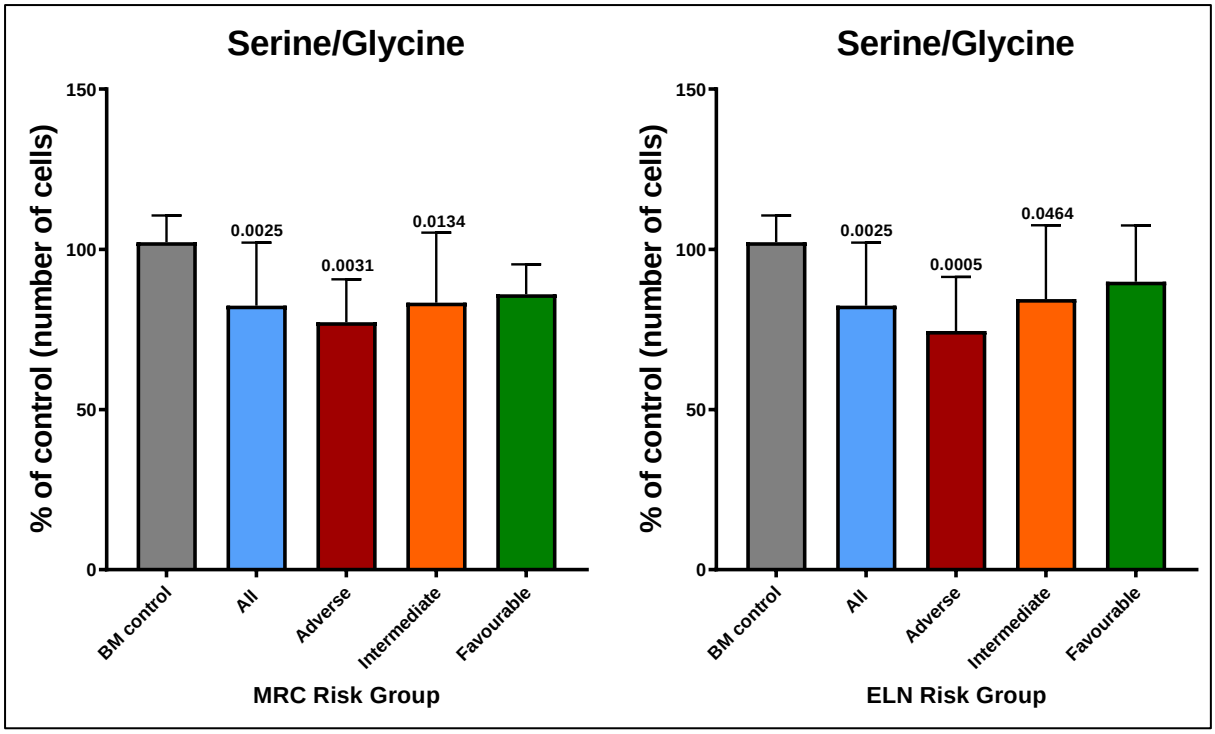

Figure 3.15: Bar charts showing the effect of serine & glycine depletion on viable cell number compare to normal controls. N=27. For MRC groups adverse n=5, intermediate n=20, favourable n=2. For ELN adverse n=10, intermediate n=9, favourable n=8. Mann-Whitney used.

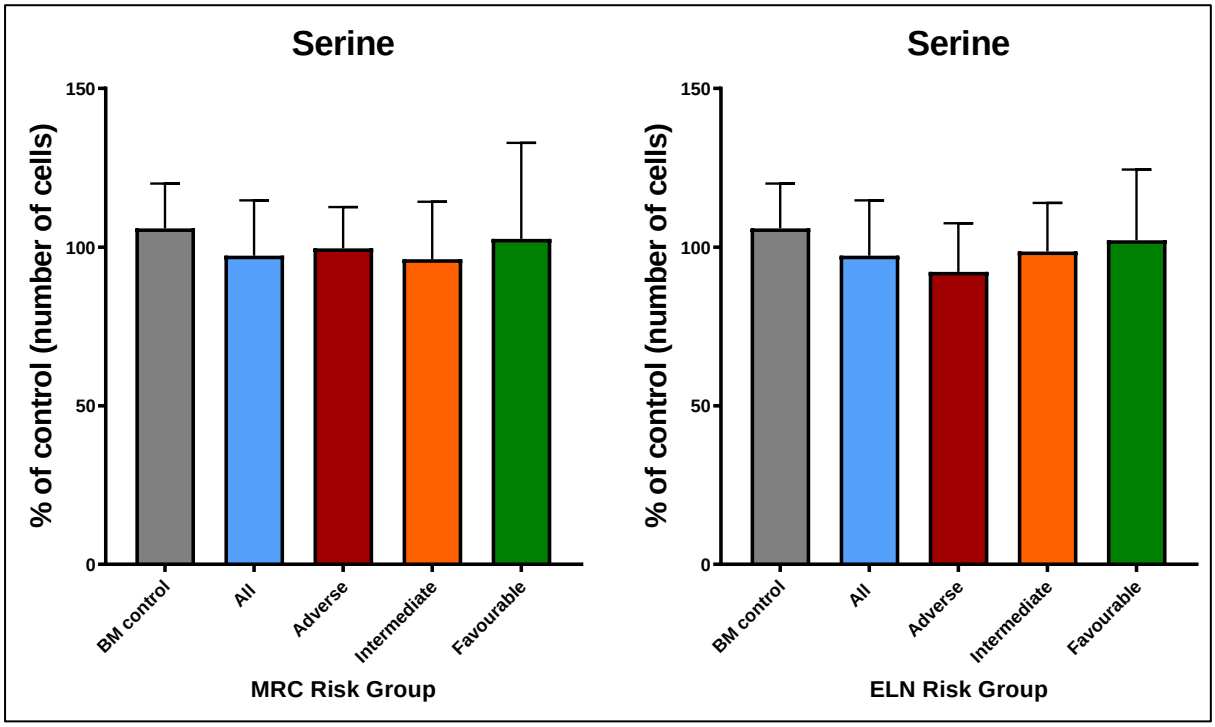

Figure 3.16: Bar charts showing the effect of serine depletion on viable cell number compare to normal controls. N=27. For MRC groups adverse n=5, intermediate n=20, favourable n=2. For ELN adverse n=10, intermediate n=9, favourable n=8. Mann-Whitney used.

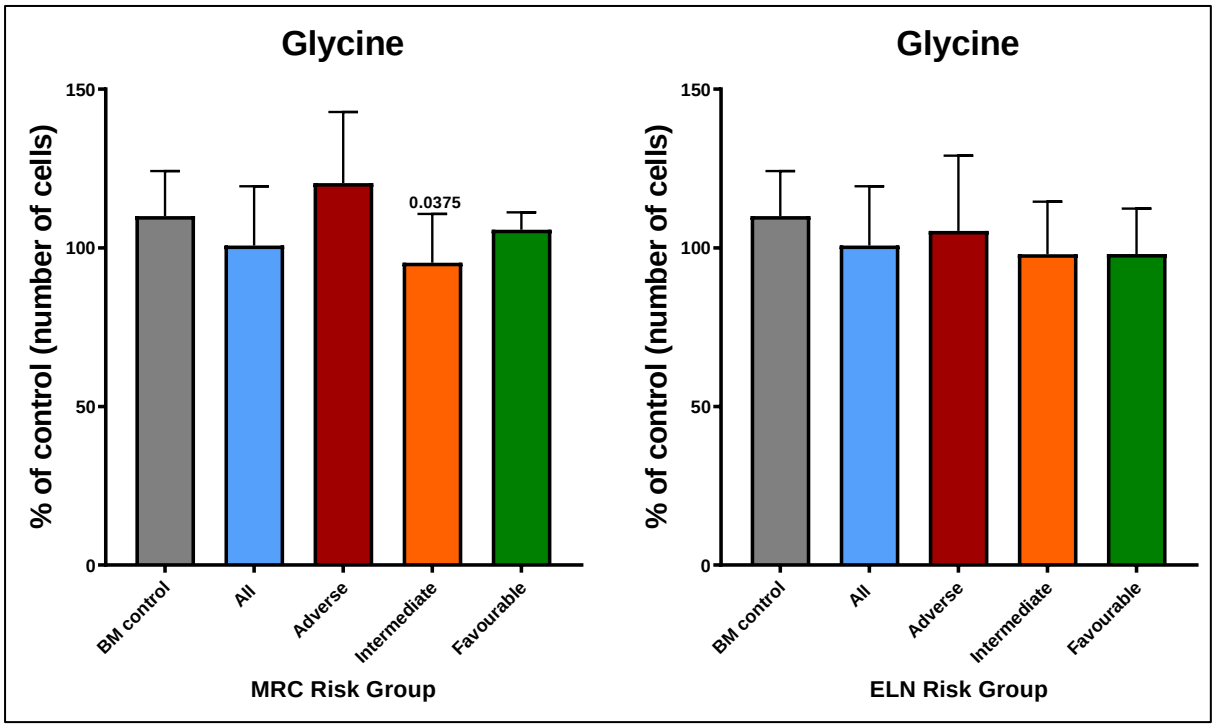

Figure 3.17: Bar charts showing the effect of glycine depletion on viable cell number compare to normal controls. N=27. For MRC groups adverse n=5, intermediate n=20, favourable n=2. For ELN adverse n=10, intermediate n=9, favourable n=8.

3.4.10 Glutamine deprivation does not lead to significant AML cell death compared to normal BM cells

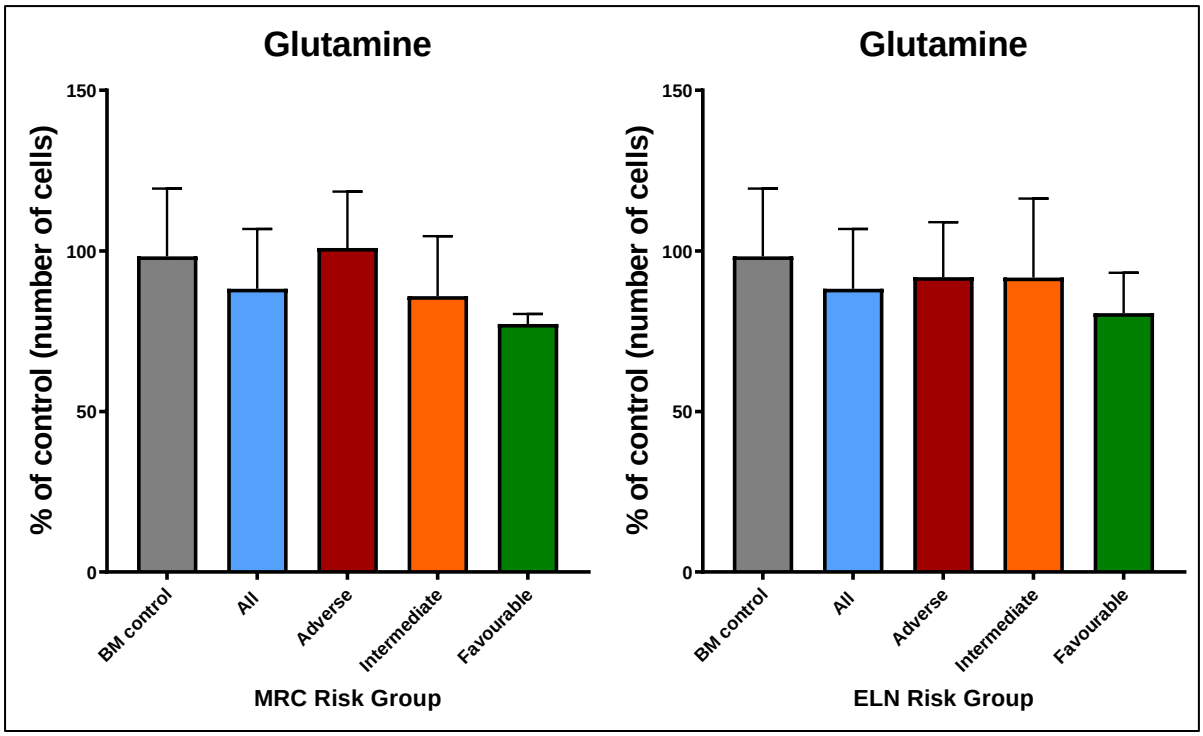

Figure 3.18: Bar charts showing the effect of glutamine depletion on viable cell number compare to normal controls. N=27. For MRC groups adverse n=5, intermediate n=20, favourable n=2. For ELN adverse n=10, intermediate n=9, favourable n=8.

3.4.11 Asparagine deprivation does not lead to significant AML cell death compared to normal BM cells

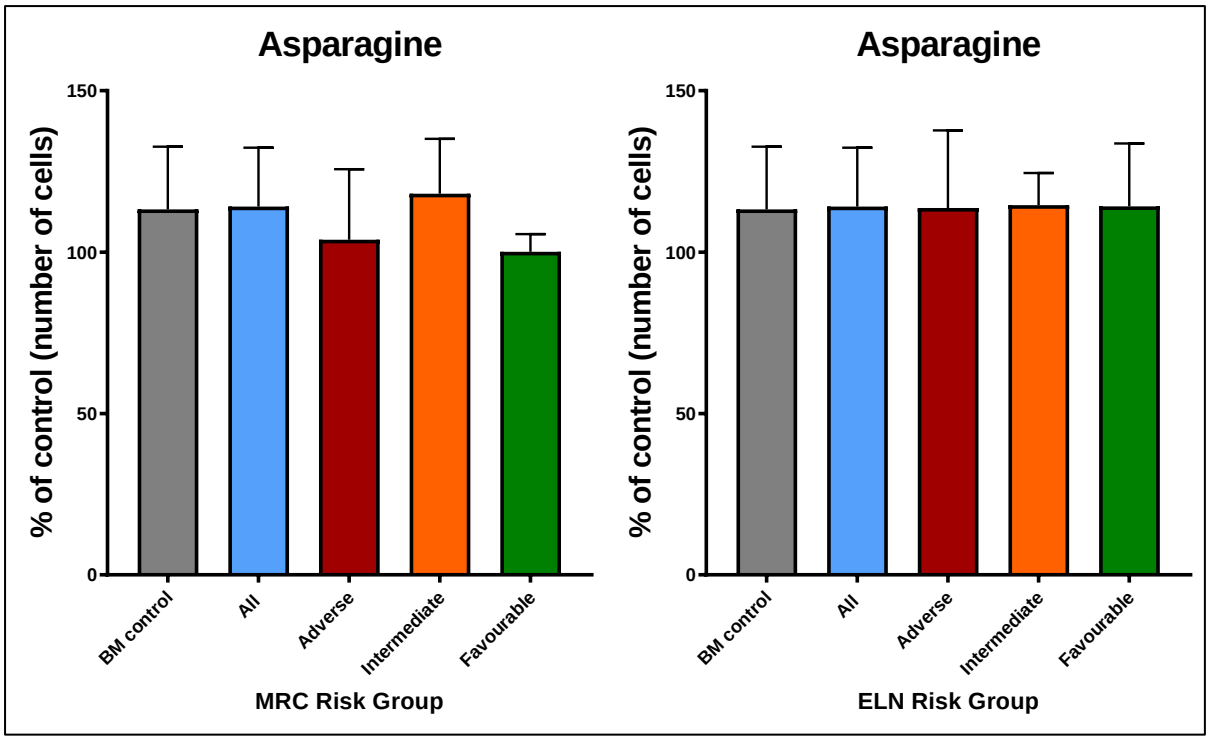

Figure 3.19: Bar charts showing the effect of asparagine depletion on viable cell number compare to normal controls. N=27. For MRC groups adverse n=5, intermediate n=20, favourable n=2. For ELN adverse n=10, intermediate n=9, favourable n=8.

3.4.12 Dose effect of methionine and valine restriction.

Given the effect of Val and Met depletion I next looked at dose concentration responses for both AAs.

Figures 3.20 and 3.21 show the response to sequential reductions of both valine and methionine concentrations from the control (i.e. normal media) concentration. All results are a % change from control. Gating was done for both the CD45+ blasts and lymphocytes.

For valine, there was a significant drop in the number of viable cells in the CD45+ group below 10nM (p=0.02). This was mirrored with a rise in annexin positive cells at

the same concentration (p=0.03). There was no significant change in the lymphocyte population to any level of valine restriction.

For methionine, only an absolute restriction showed a significant effect in the number of viable cells in the CD45+ population (0nM, p=0.004). There were no corresponding significant changes in annexin or in the lymphocyte population.

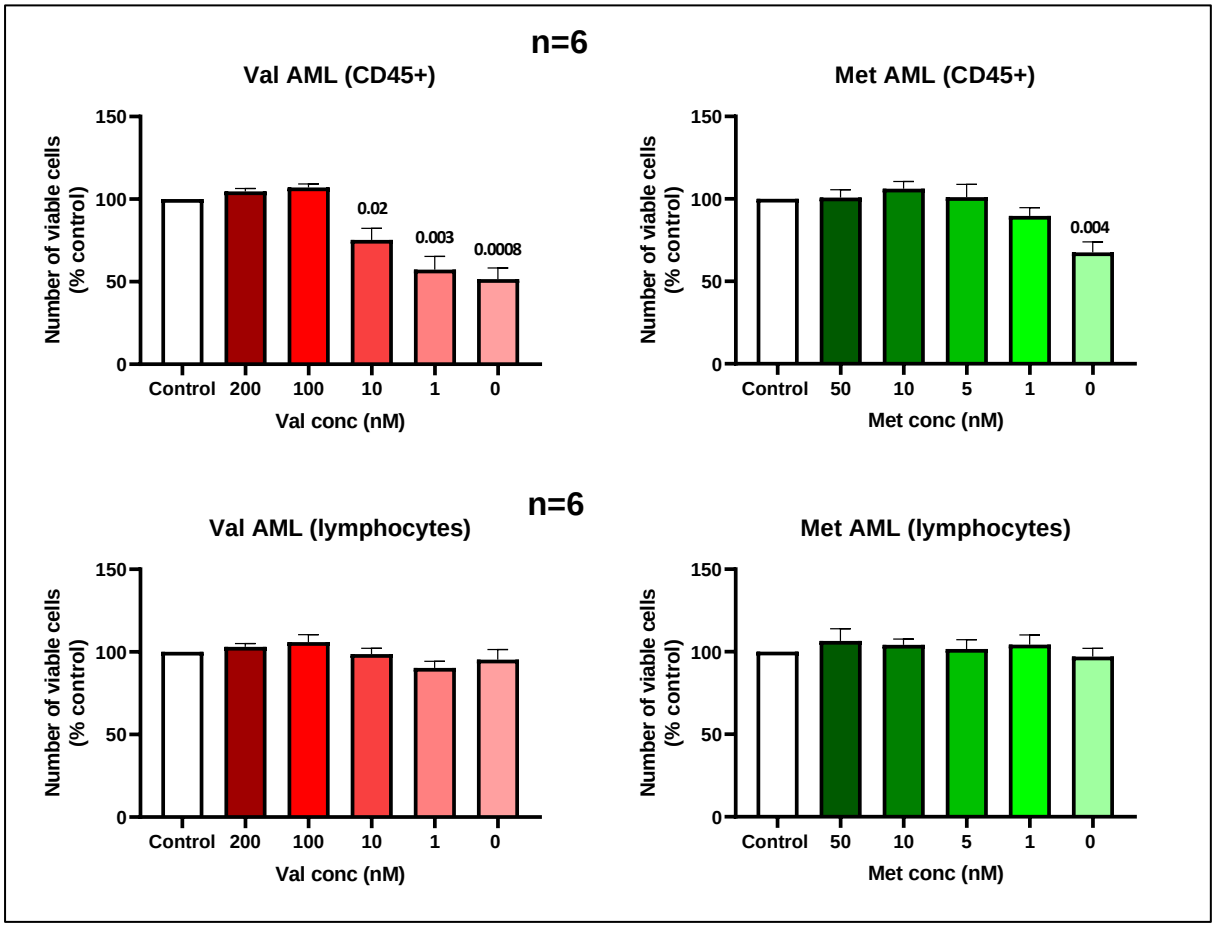

Figure 3.20: Number of viable cells as % of control (ie media with all AAs). Results shown are gated for both CD45+ cells and lymphocyte population. P values shown where significant.

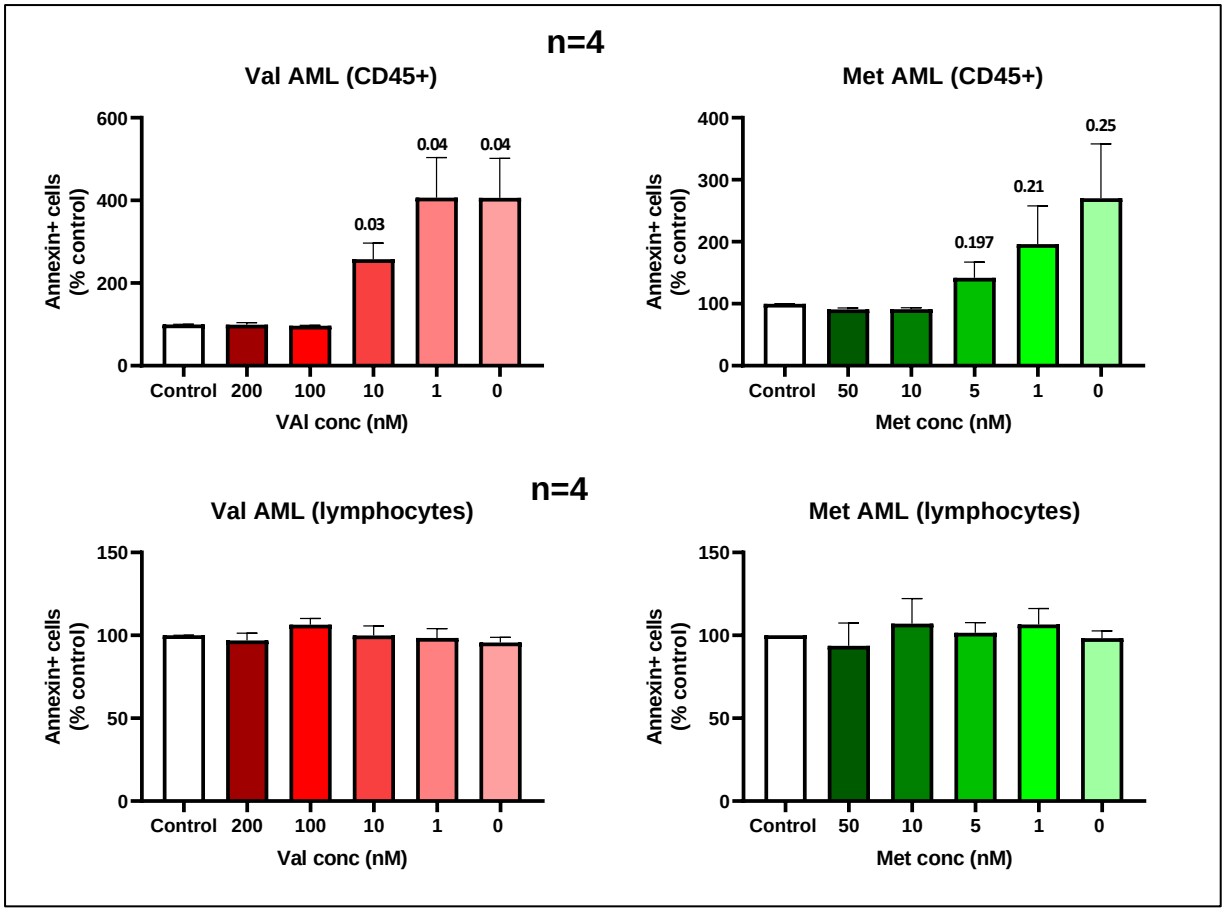

Figure 3.21: Number of annexin +ve cells as % of control (ie media with all AAs). Results shown are gated for both CD45+ cells and lymphocyte population. P values shown where significant.

Chapter 4: Combining AA deprivation with chemotherapy

4.1 Introduction

A single agent or strategy approach for treating AML is often unsuccessful for a number of reasons including cellular adaptation and resistance. The results from chapter 3 demonstrate the significant effect on AML cells of valine and methionine deprivation. The next step was to determine if the addition of chemotherapy had a synergistic effect when combined with AA depletion. Cytarabine (ARAC) was chosen as it has been a key drug in AML induction therapy for decades.

4.2 Summary of specific methods

4.2.1 AML samples

6 AML subjects in which there was *not* a significant response to valine and/or methionine depletion (as demonstrated in chapter 3) were selected. The sample characteristics are summarised in table 4.1.

ID	1˚/2˚	Sex	Age	Timing	Cytogenetics	MRC Risk	ELN Risk	NPM1	FLT3-ITD	Ratio	TP53
AML37	Primary	M	47	Relapse	7q-	Adverse	Adverse	No	No	n/a	NK
AML24	Primary	F	69	Diagnosis	-16, -18	Intermediate	Adverse	No	Yes	0.28	Yes
AML35	Secondary	F	64	Relapse	1q-	Intermediate	Intermediate	No	No	n/a	No
AML5	Primary	F	81	Relapse	Normal	Intermediate	Intermediate	No	No	n/a	NK
AML31	Primary	M	59	Diagnosis	Normal	Intermediate	Adverse	Yes	Yes	2.17	No
AML30	Primary	F	69	Diagnosis	Normal	Intermediate	Intermediate	Yes	Yes	0.87	No

Table 4.1: Primary AML sample characteristics.

4.2.2 Synopsis of co-culture method

Effective cyatrabine doses were established by our team in relation to other experimental work. The reconstitution is described in chapter 2. A schematic of the protocol is shown in figure 4.1.

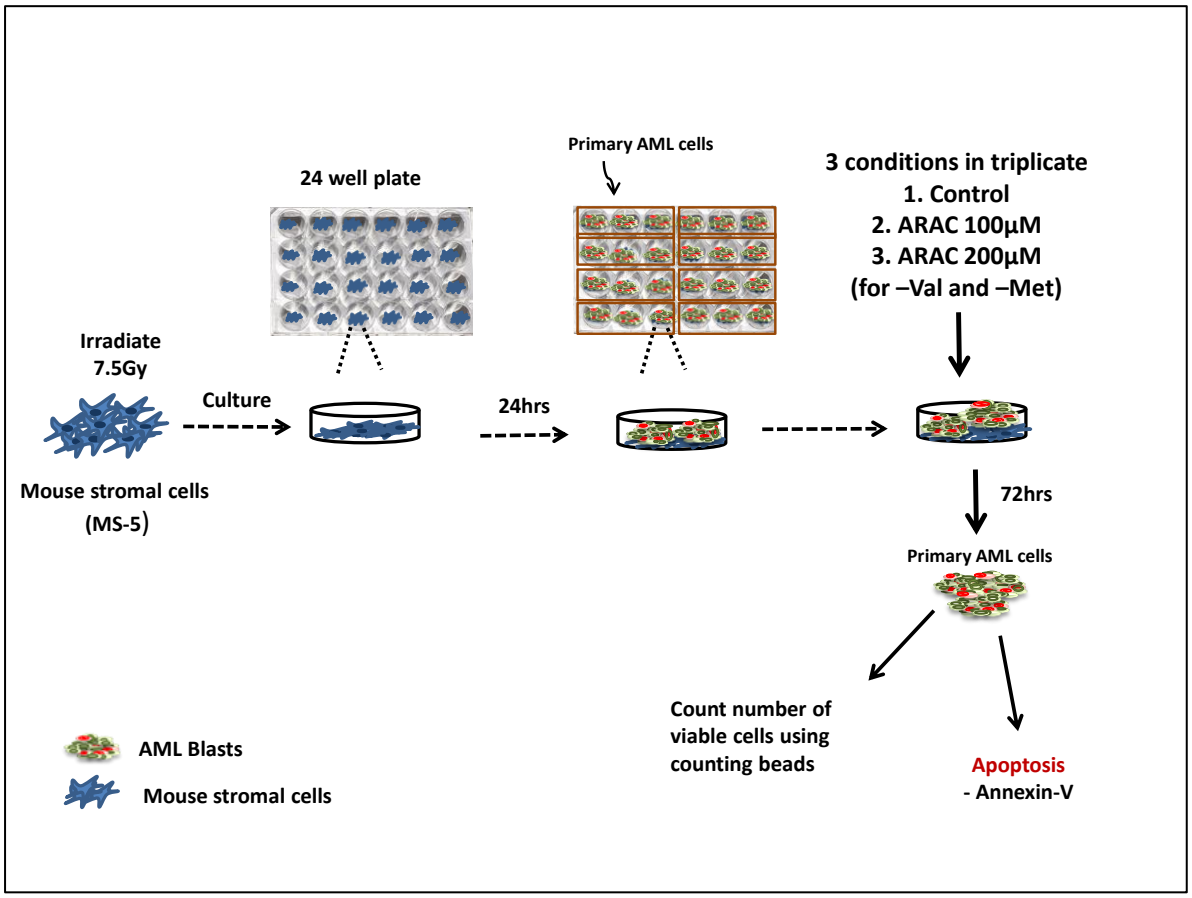

Figure 4.1: Schematic of the co-culture protocol.

4.2.3 Analysis

Statistical analysis was performed using Graphpad Prism. Significance was determined using a paired t-test ($p < 0.05$). Error bars shown are standard error of the mean (SEM).

4.3. Results

4.3.1 Sample characteristics

6 primary AML samples were investigated. 2/6 were male and the mean age 65 years. Half were taken at relapse and half at presentation. By MRC cytogenetic classification 1/6 (17%) was adverse risk and the remainder intermediate risk. By ELN classification 3/6 (50%) were adverse and 50% intermediate risk.

4.3.2 There is no synergism with cytarabine and AA depletion

Figures 4.2 and 4.3 follow. Figure 4.2 shows the effect on viable cell numbers of cytarabine in combination with either valine or methionine restriction. In 4 of the 6 control samples a significant fall in the number of viable cells was seen with either dose of cytarabine.

In half the samples, methionine restriction alone led to a significant fall in viable cell numbers and this was 5/6 samples with valine restriction. However, in no samples did the combination of cytarabine and AA restriction lead to a significant reduction in viable cell numbers. In 1 sample (AML30) there was significant paradoxical rise in viable cells when cytarabine 100μM was added to methionine restriction.

Figure 4.3 shows the corresponding results for annexin for the same 6 samples. Consistent with cell viability, all controls showed a significant rise in the number of annexin positive cells compared to control. Valine and methionine deprivation alone led to a significant rise in all 6 samples. In 1 sample (AML5) the combination of valine restriction and 200μM of cytarabine led to a significant rise in annexin positive cells.

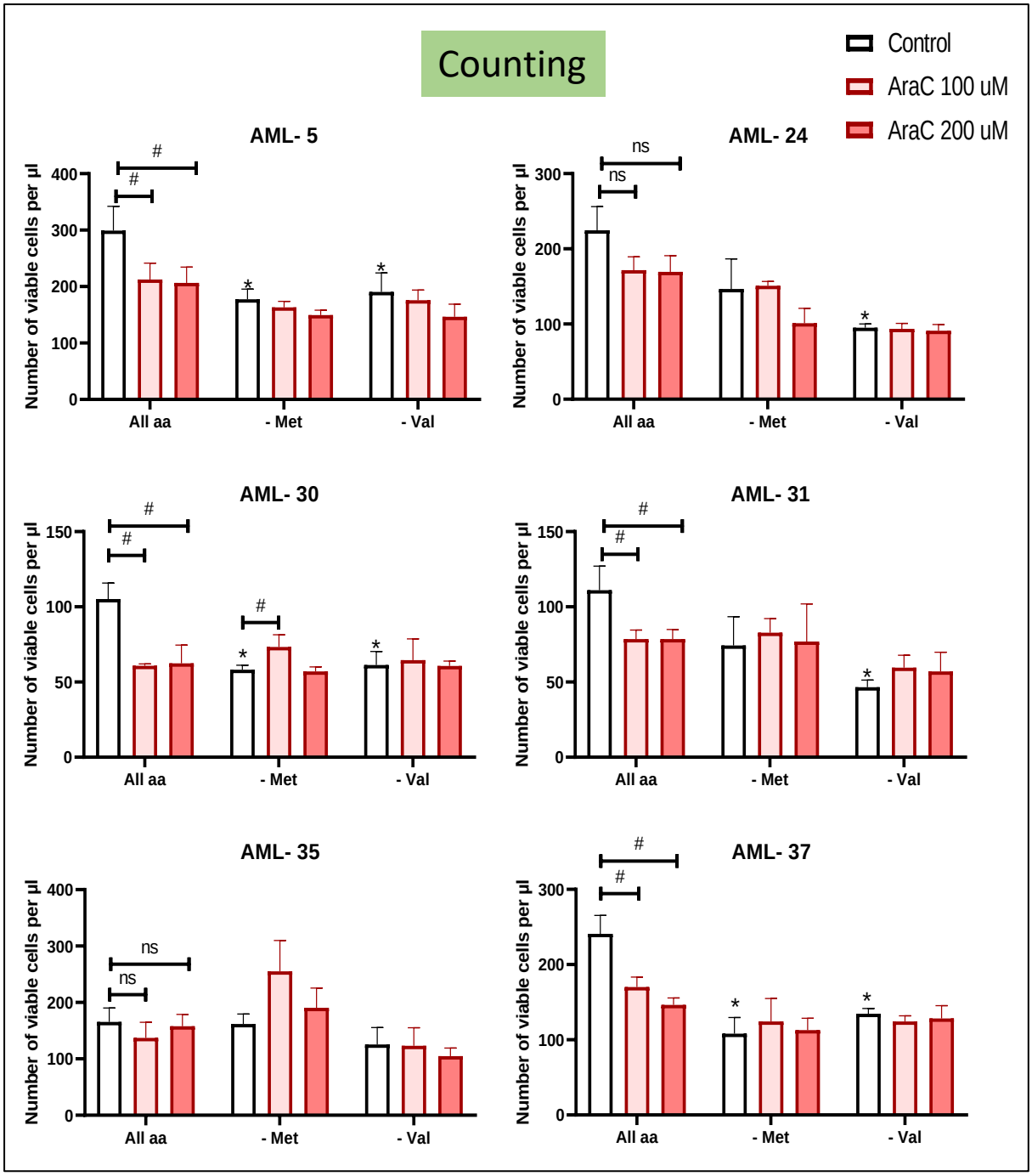

Figure 4.2: Number of viable cells following treatment with cytarabine in 6 AML samples. 3 conditions for each AML sample: All AAs, -Met and –Val.
*** indicates a statistically significant difference from the 'All AA' in the control samples.**
 # indicates a statistically significant difference within media conditions compared to control (untreated). P<0.05.

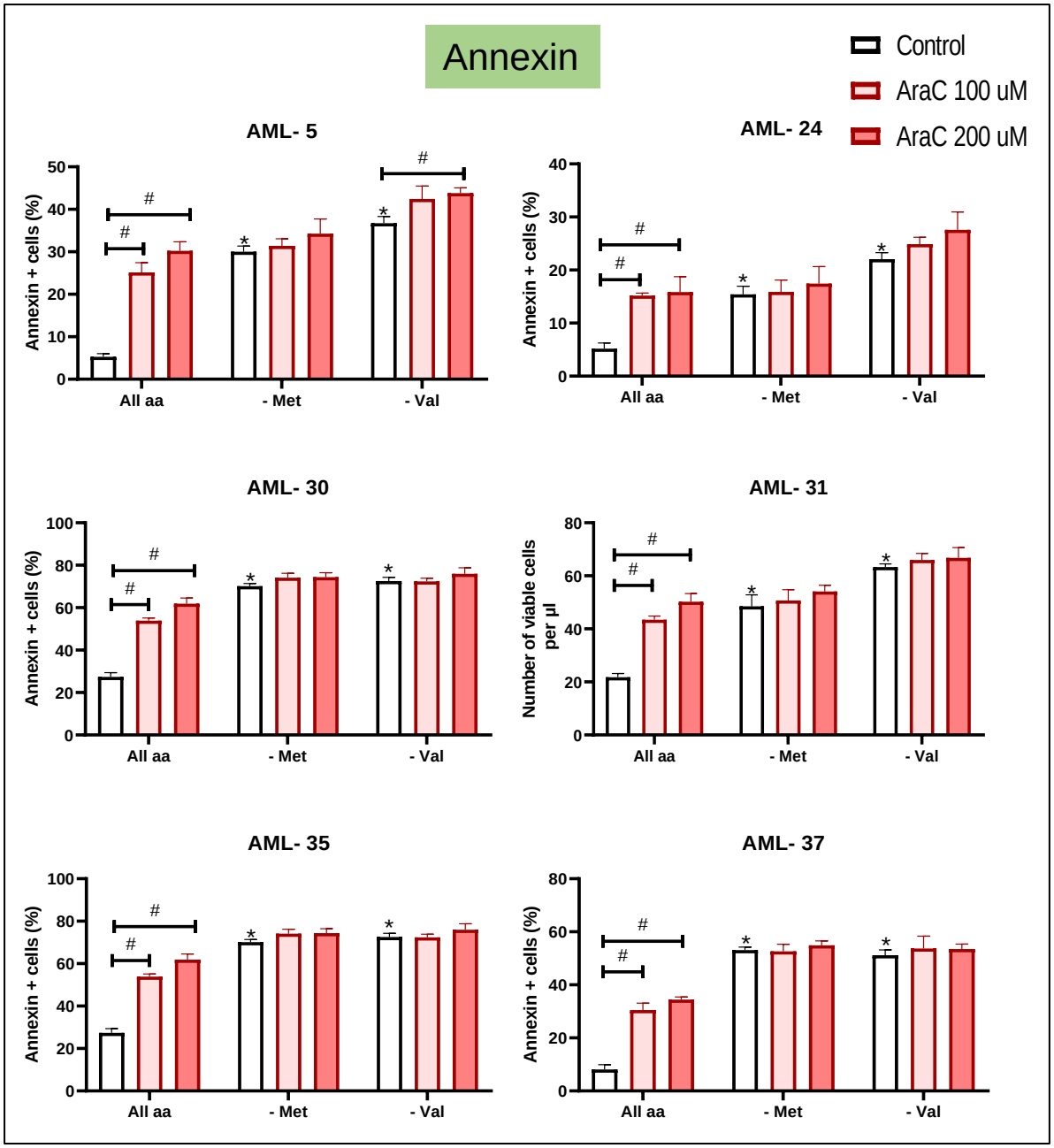

Figure 4.3: % annexin positive cells following treatment with cytarabine in 6 AML samples. 3 conditions for each AML sample: All AAs, -Met and –Val.
*** indicates a statistically significant difference from the 'All AA' in the control samples.**
 # indicates a statistically significant difference within media conditions compared to control (untreated). P<0.05.

Chapter 5: Measuring AA uptake by Liquid Chromatography Mass Spectrometry

5.1 Introduction

Results derived from the work in chapter 3 show the need of AML cells for selected amino acids. MS has been used to measure AA profiles in AML. The aim of this chapter was to measure intracellular AA uptake following co-culture to establish which AAs AML consumes most avidly. A secondary aim was to establish if changes in media/supernatant reflect cellular uptake. This was investigated across AML risk groups.

5.2 Summary of specific methods

5.2.1 AML samples

A summary of the characteristics of the primary AML samples used in this chapter is provided in table 5.1. Due to the number of cells required for co-culture, PB samples were used consistently. It was not possible to obtain data from control samples. Initial cell numbers were too low or cell viability fell dramatically with BM and GMPB control samples respectively.

5.2.2 Initial optimisation experiments

As detailed elsewhere, the project switched from an investigation of arginine deprivation to a broader study of AA dependence in the course of the first year. Initial optimisation work was performed during this time to assess the impact of processing factors on LC-MS results. This was performed on both AML cell lines and primary

AML samples. Methods established and relevant to this thesis include the minimum cell pellet size required, the optimum number of PBS washes required and the need for an MS-5 feeder layer for co-culture (stromal media derived from MS-5 did not sustain AML cells for the required culture period). Selected results are found in appendix 1.

5.2.3 Synopsis of the co-culture method

A schematic summarising the co-culture method detailed in chapter 2 is shown in figure 5.1.

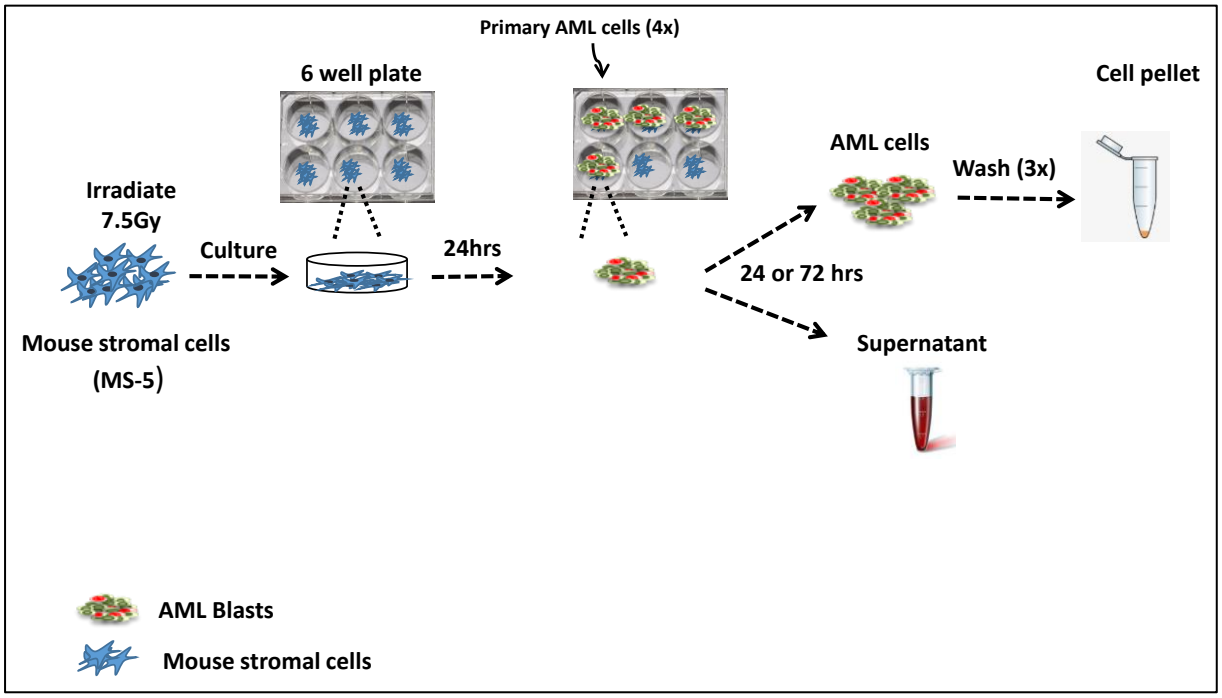

Figure 5.1: Schematic of the co-culture protocol used for primary AML samples.

5.2.4 AbsoluteIDQ® p180 kits

AbsoluteIDQ® p180 kits (Biocrates Life Sciences) were chosen for their relative simplicity, accuracy and reproducibility [142-145]. The 96-well plates quantify all AAs, contain validated internal standards and have been validated in clinical trials [146]. The LC-MS methods are detailed in chapter 2.

5.2.5 Statistical analysis

Initial analysis was performed on Graphpad Prism. Following testing for normality (D'Agostino-Pearson test), non-parametric testing was used (Wilcoxin Signed Rank test) ($p<0.05$).

The multivariate analysis was performed on SIMCA (Umetrics/Sartorius). SIMCA (Soft Independent Modelling of Independent Variables) uses an Orthogonal Partial Least Squares (OPLS) method for regression analysis. In brief, the horizontal component of the OPLS-DA (discriminant analysis) score scatter plot captures variation *between* groups and the vertical dimension captures variation *within* groups. This is a supervised modelling approach that provides information of separation of known groups (intermediate and adverse risk AML in this case).

The S-plot is a visualisation method that combines the modelled covariance (X axis) and modelled correlation (Y axis) of the OPLS-DA data. It allows the identification of the variables that are responsible for the separation between the groups with their relative importance, termed a VIP score (Variable of Importance).

5.3 Results

5.3.1 Sample characteristics

The 16 primary AML PB samples used in this chapter are shown in table 5.1. 5/16 (31%) were male and the mean age was 66 years (range 34-83). By MRC classification 2 (13%) were adverse risk, 74% intermediate risk and 13% favourable risk. By ELN classification 31% were adverse risk and 44% and 25% intermediate and favourable risk respectively.

ID	1˚/2˚	Sex	Age	Timing	Cytogenetics	MRC Risk	ELN Risk	NPM1	FLT3-ITD	Ratio	TP53
AML39	Primary	M	59	Diagnosis	Complex	Adverse	Adverse	No	No	n/a	Yes
AML58	Primary	M	73	Diagnosis	Complex	Adverse	Adverse	No	No	n/a	No
AML23	Primary	F	43	Diagnosis	Normal	Intermediate	Adverse	No	Yes	0.75	NK
AML20	Primary	M	72	Diagnosis	Normal	Intermediate	Adverse	No	Yes	0.36	No
AML24	Primary	F	69	Diagnosis	-16, -18	Intermediate	Adverse	No	Yes	0.28	Yes
AML5	Primary	F	81	Relapse	Normal	Intermediate	Intermediate	No	No	n/a	NK
AML25	Secondary	F	82	Diagnosis	i(22q)	Intermediate	Intermediate	No	No	n/a	NK
AML32	Secondary	M	78	Diagnosis	Failed	Intermediate	Intermediate	No	No	n/a	NK
AML16	Primary	F	72	Diagnosis	Normal	Intermediate	Intermediate	Yes	NK	n/a	NK
AML50	Primary	M	83	Diagnosis	8 gain	Intermediate	Intermediate	Yes	Yes	0.08	NK
AML2	Primary	F	69	Relapse	11 gain	Intermediate	Intermediate	Yes	No	n/a	No
AML30	Primary	F	69	Diagnosis	Normal	Intermediate	Intermediate	Yes	Yes	0.87	No
AML7	Primary	F	57	Diagnosis	Normal	Intermediate	Favourable	Yes	Yes	0.04	NK
AML47	Primary	F	55	Diagnosis	Normal	Intermediate	Favourable	Yes	No	n/a	No
AML21	Primary	F	34	Diagnosis	inv(16)	Favourable	Favourable	No	No	n/a	No
AML1	Primary	F	60	Diagnosis	t(8;21)	Favourable	Favourable	n/a	n/a	n/a	NK

Table 5.1: Characteristics of primary AML samples used in this chapter

5.3.2 Results following co-culture for 72 hours

Samples were first co-cultured for 72 hours consistent with the AA deprivation work described in chapter 3. 5 samples were analysed on a single Biocrates plate.

Figure 5.2 shows the results for cell pellets (indicating intracellular AA concentrations). AAs are listed on the X axis and on the Y axis the percentage change from the mean of baseline (i.e (72hr value – baseline value)/baseline value x100).

Figure 5.3 shows the results for media change in the same samples (i.e. the supernatant in which the AML cells were cultured). The scatter plot layout is the same.

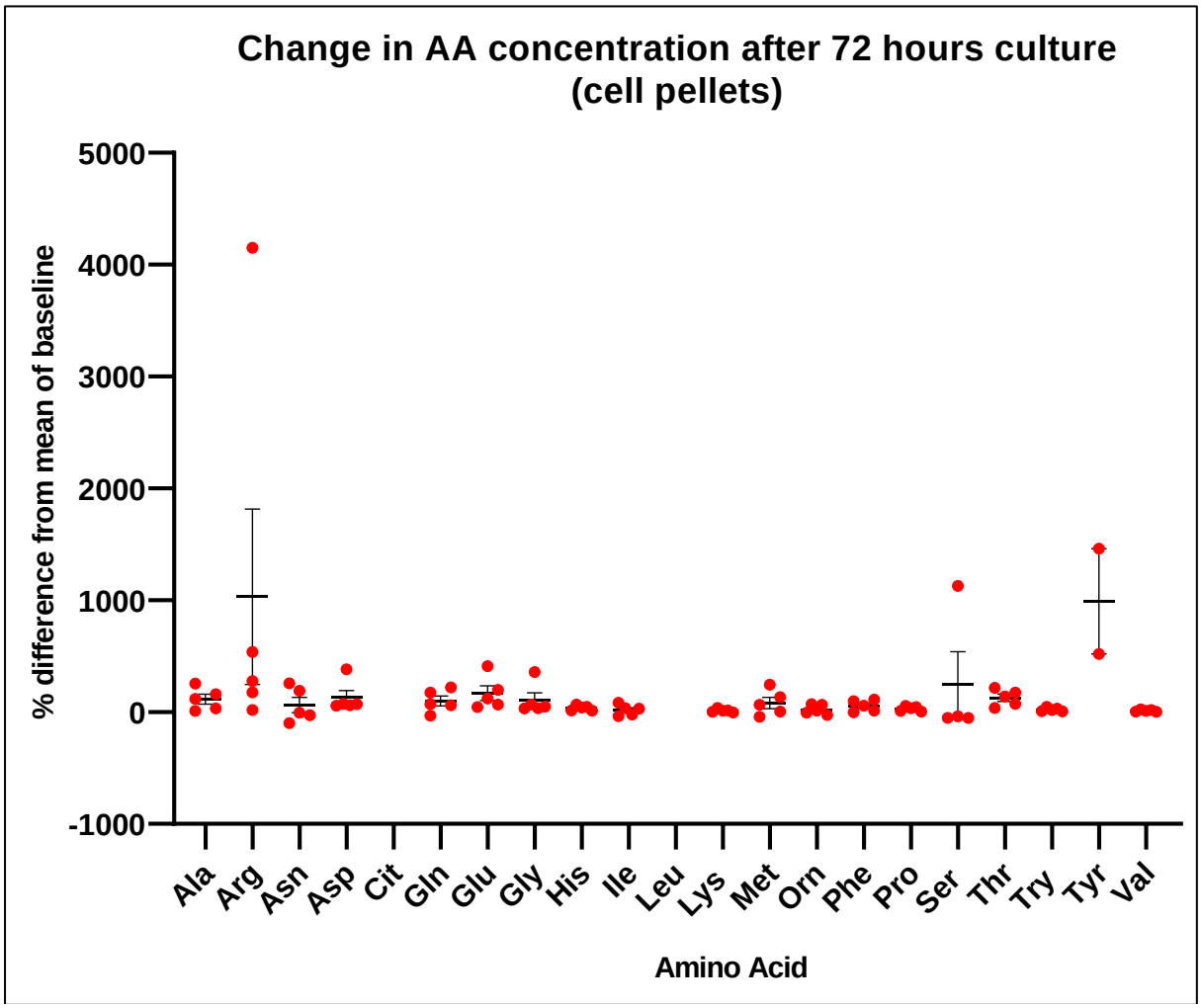

Figure 5.2: Scatter plot showing % change in cell pellet AA concentrations following co-culture for 72 hours. Each dot represents an AML sample (n=5). Each sample was run on LC-MS in quadruplicate and each dot represents the mean of the 4 wells. Error bars are SEM.

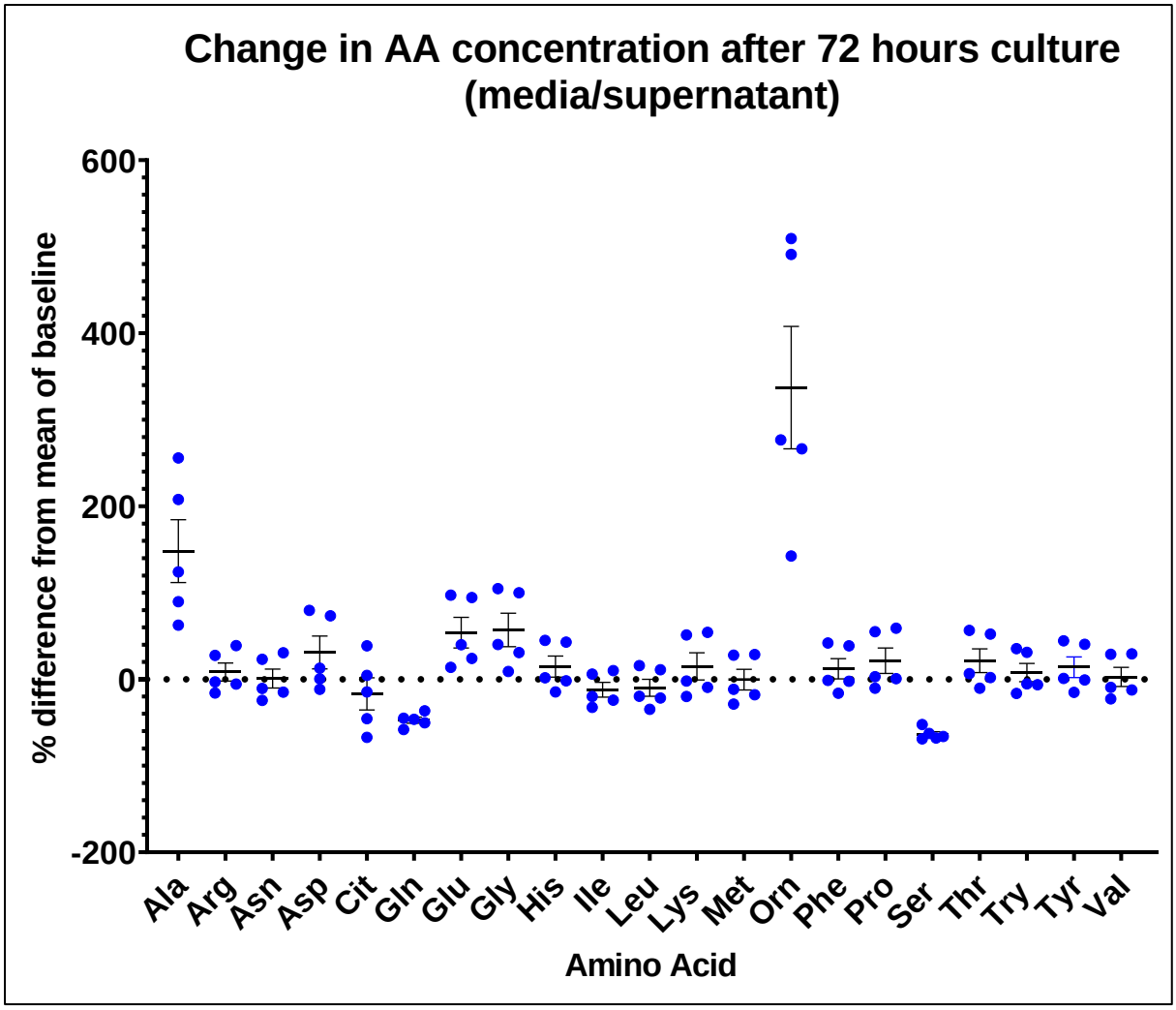

Figure 5.3: Scatter plot showing % change in media/supernatant AA concentrations following co-culture for 72 hours. Each dot represents an AML sample (n=5). Each sample was run on LC-MS in quadruplicate and each dot represents the mean of the 4 wells. Error bars are SEM.

Table 5.2 shows the mean percentage change in AA concentration. There was no signal in the cell pellets for either citrulline or leucine. There was an increase in cell pellet concentration in all other AAs (indicating an increase in in intracellular AAs), although none was significant.

There was a fall in the media concentration for 5 AAs (citrulline, glutamine, isoleucine, methionine and serine), although none was significant. The concentrations of all other AAs rose (none significant).

	Change (%) in AA concentration from baseline Mean value (p value)	
Amino Acid	**Cell pellet**	**Media**
Alanine	114.3 (0.06)	148.1 (0.06)
Arginine	1030.7(0.06)	8.4 (0.81)
Asparagine	61.8 (0.81)	0.8 (>0.99)
Aspartate	127.8 (0.06)	30.9 (0.19)
Citrulline	-	-16.8 (0.44)
Glutamine	98.4 (0.13)	-47.3 (0.06)
Glutamic Acid	167.6 (0.06)	53.9 (0.06)
Glycine	107.7 (0.06)	57.0 (0.06)
Histidine	35.6 (0.06)	14.6 (0.63)
Isoleucine	17.3 (0.81)	-12.1 (0.31)
Leucine	-	-9.8 (0.31)
Lysine	11.4 (0.19)	14.8 (0.81)
Methionine	80.3 (0.19)	-0.4 (>0.99)
Ornithine	22.3 (0.44)	337.2 (0.06)
Phenylalanine	54.8 (0.13)	12.1 (0.81)
Proline	29.0 (0.06)	21.4 (0.31)
Serine	245.2 (0.81)	-63.6 (0.06)
Threonine	127.3 (0.06)	21.4 (0.31)
Tryptophan	21.0 (0.06)	7.7 (0.81)
Tyrosine	989.1 (0.06)	13.9 (0.63)
Valine	10.8 (0.06)	2.7 (0.81)

Table 5.2: Percentage change in AA concentration compared to baseline (ie before 24 hour culture). P values in brackets (significant results in bold, p<0.05). Red shading denotes AA increase, blue shading denotes AA decrease. Blank values denote no signal/result.

No statistically significant results were seen following 72 hour culture. Cell losses in culture (given that we cannot replicate the in vivo conditions for optimal cell survival in vitro) caused problems given that a large numbers of cells were required. Although a minimum of $4x10^6$ cells were established per well in culture, frequently I was unable to obtain a pellet of $1x10^6$ cells at the end of the culture. Repeated ice-cold PBS washes were a contributing factor but these washes were essential to remove the

culture media from the pellets so that results were not a simply a reflection of the culture media.

The co-culture results in chapter 3 demonstrated significant cell death and apoptosis for selected AAs following co-culture for 24 hours.

For these reasons further analysis was done following 24 hour co-culture.

5.3.3 Results following 24 hour culture

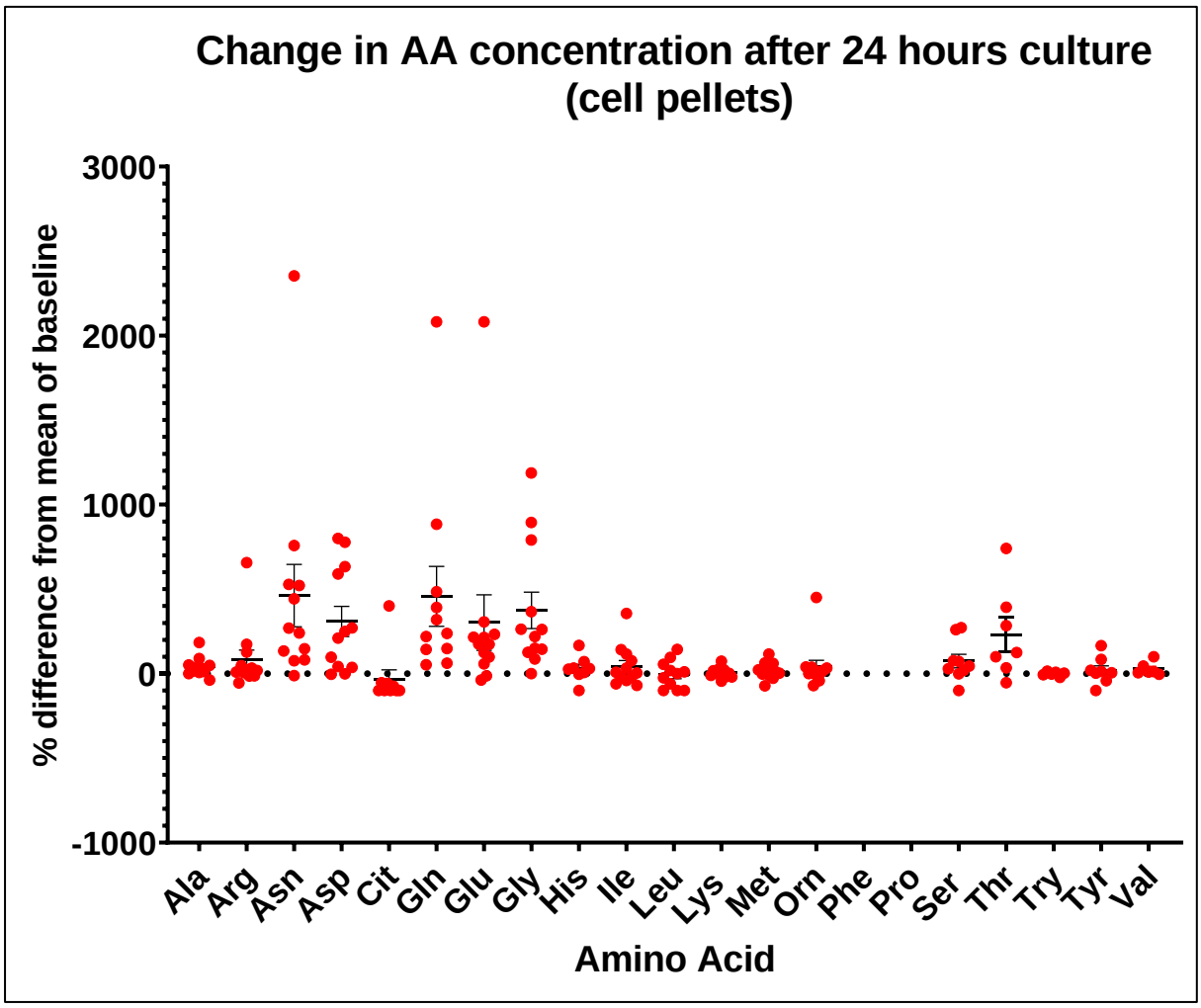

Figure 5.4: Scatter plot showing % change in cell pellet AA concentrations following co-culture for 24 hours. Each dot represents an AML sample (n=12). Each sample was run on LC-MS in quadruplicate and each dot represents the mean of the 4 wells. Error bars are SEM.

Figures 5.4 and 5.5 show the percentage change in AA concentration following 24 hour culture in cell pellets and media/supernatant, respectively.

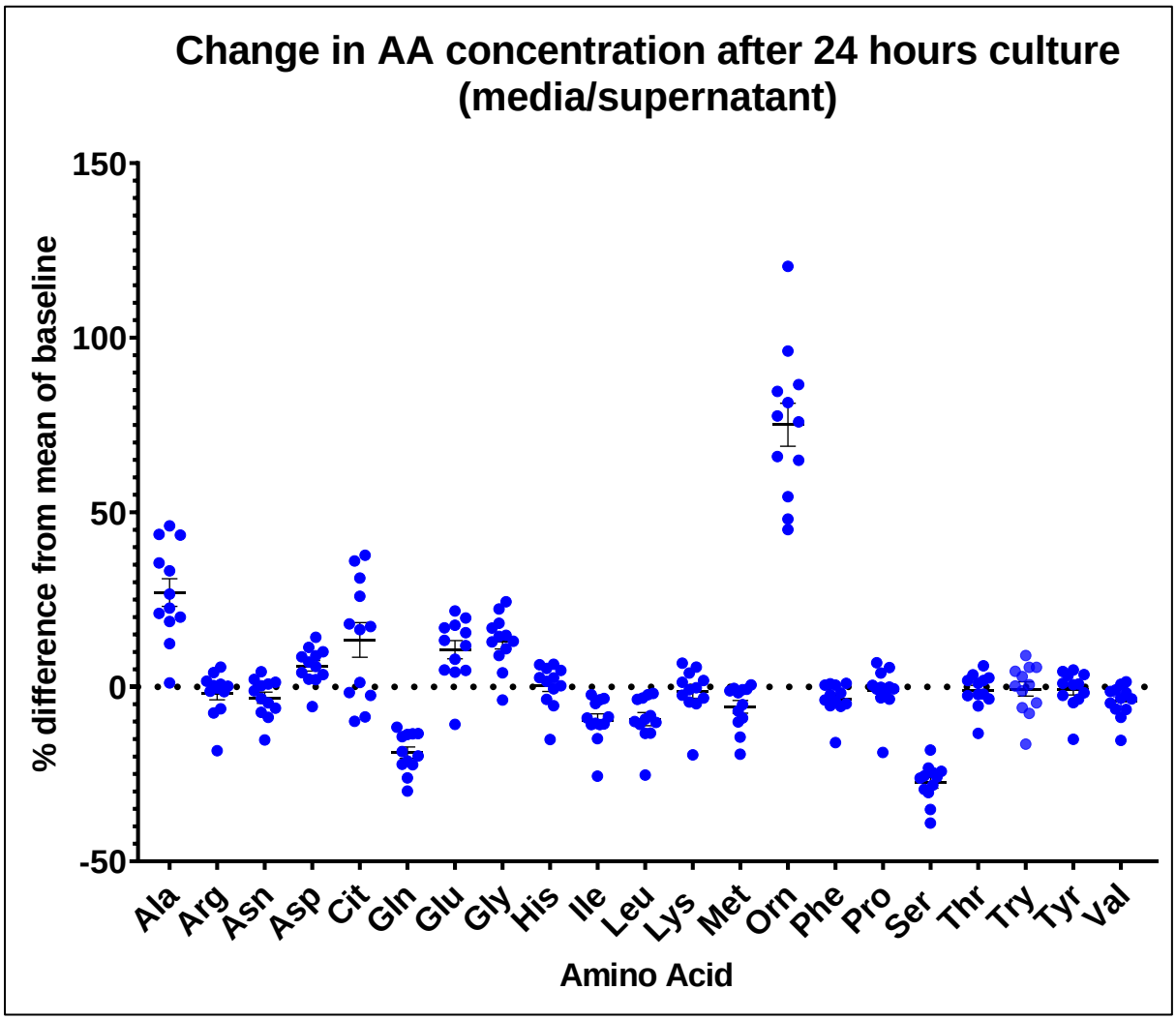

Figure 5.5: Scatter plot showing % change in media/supernatant AA concentrations following co-culture for 24 hours. Each dot represents an AML sample (n=12). Each sample was run on LC-MS in quadruplicate and each dot represents the mean of the 4 wells. Error bars are SEM.

	% change from baseline (before culture) Value (SEM)	
Amino Acid	**Cell pellet**	**Media**
Alanine	**39 (0.0269)**	**27 (0.001)**
Arginine	84 (0.106)	-2 (0.582)
Asparagine	**461 (0.001)**	-3 (0.1099)
Aspartate	**308 (0.0024)**	**6 (0.005)**
Citrulline	54 (0.1719)	**13 (0.0049)**
Glutamine	**457 (0.0005)**	**-19 (0.005)**
Glutamic Acid	**302 (0.0049)**	**11 (0.0063)**
Glycine	**374 (0.001)**	**13 (0.001)**
Histidine	47 (0.0527)	0 (0.4824)
Isoleucine	43 (0.5557)	**-10 (0.005)**
Leucine	30 (0.3223)	**-9 (0.005)**
Lysine	6 (0.6216)	-1 (0.791)
Methionine	15 (0.4111)	**-6 (0.0015)**
Ornithine	40 (0.2686)	**75 (0.005)**
Phenylalanine	-	-3 (0.021)
Proline	-	-1 (0.5186)
Serine	96 (0.0566)	-**27 (0.0005)**
Threonine	**234 (0.0068)**	-1 (0.8638)
Tryptophan	-1 (0.8594)	-1 (0.9697)
Tyrosine	36 (0.3398)	-1 (0.9697)
Valine	11 (0.0938)	**-4 (0.0034)**

Table 5.3: % change in AA concentration compared to baseline (ie before 24 hour culture). P values in brackets (significant results in bold, p<0.05). Red shading denotes AA increase, blue shading denotes AA decrease. Blank values denote no signal/result. Figures are % change with SEM in brackets.

Table 5.3 shows the mean percentage change from baseline following culture for the shorter period, 24 hours. There is a significant increase in the intracellular concentrations of alanine, asparagine, aspartate, glutamine, glutamic acid, glycine and threonine. Of those measurable, tryptophan was the only AA in which there was a fall in the intracellular concentration.

There is a more consistent fall in media/supernatant AA concentrations with the 24 hour culture, compared to 72 hours. Glutamine, leucine, isoleucine, methionine, serine and valine all fell significantly suggesting uptake from the media into cells.

These media/supernatant data are fully consistent with the date from figure 3.5 in which we showed that depriving AML of valine, methionine, glutamine and serine/glycine was associated with reduced numbers of viable cells and increased apoptosis. This provides strong confirmatory evidence for the dependence of AML on these AAs.

5.3.4 Results of 24 hour culture according to AML risk classification

Next we looked at these results to determine if different AML risk groups demonstrated different AA uptake indicating higher requirements. Figure 5.6 shows the cell pellet and media/supernatant methionine (as an example) concentration change following 24 hour culture. Results are displayed for adverse, intermediate and favourable risk AML for both ELN and MRC cytogenetic risk classifications.

Initial analysis focused on univariate analysis – looking at the effect of each amino acid change alone in relation to risk group.

The ELN intermediate and adverse risk groups each contained 5 AML samples. There was no statistically significant difference for any individual AA concentration change in either cell pellet or media/supernatant between these 2 groups.

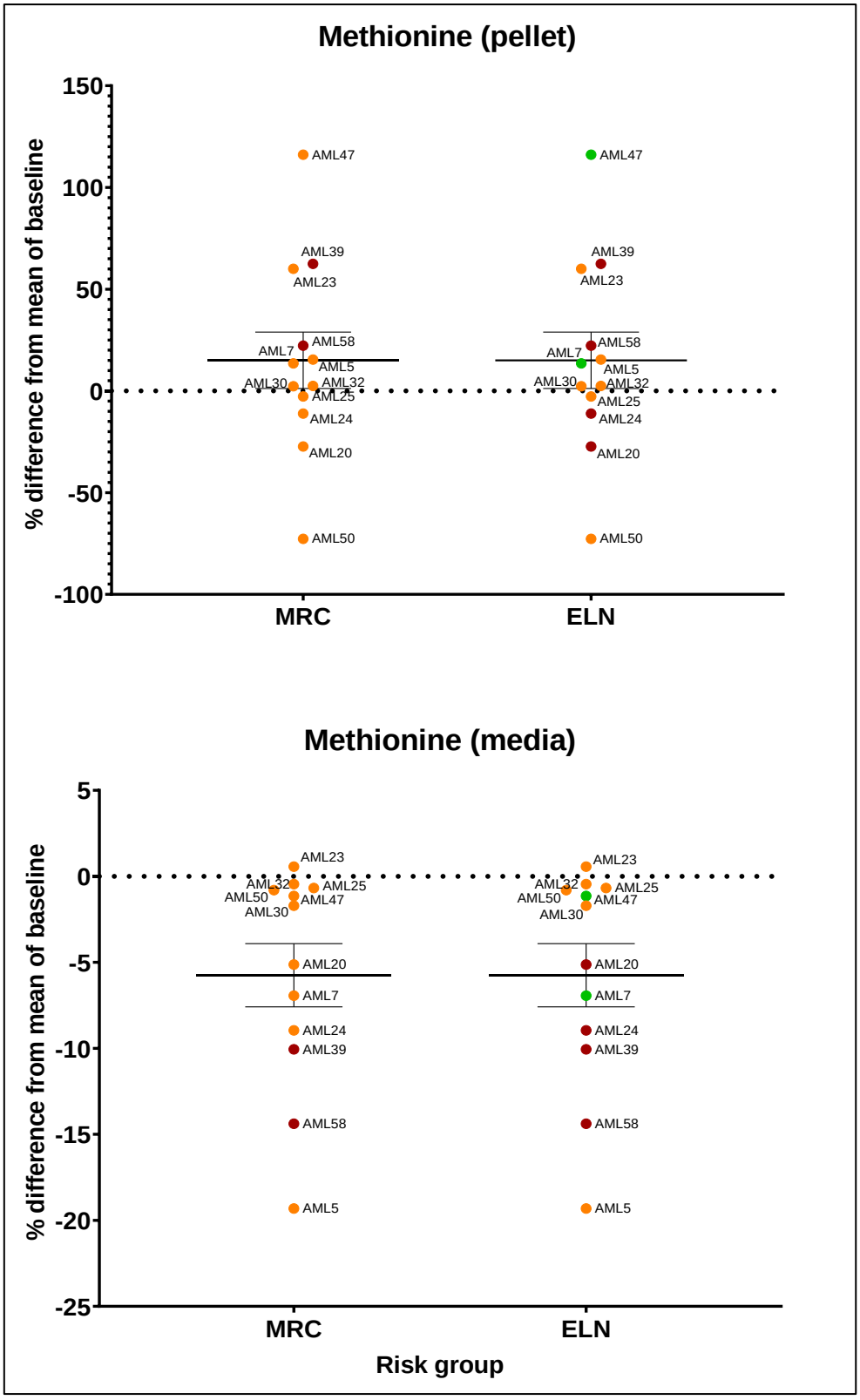

Figure 5.6: Scatter plot showing the % difference in methionine concentration in all AML samples compared to baseline by risk classification (MRC and ELN). Red = adverse, Orange = intermediate, green = favourable.

The ELN intermediate and adverse risk groups were then compared using multivariate analysis (looking at changes in all the amino acids together). Figure 5.7 shows the OPLS discriminant analysis score scatter plot for cell pellets. It shows separation of the the 2 groups, intermediate and adverse risk.

Figure 5.8 shows the S-plot (which combines the modelled covariance and modelled correlation from the OPLS-DA analysis) for the same data set. This suggests an increase in intracellular concentration for all AAs in the adverse group when compared to the intermediate risk group.

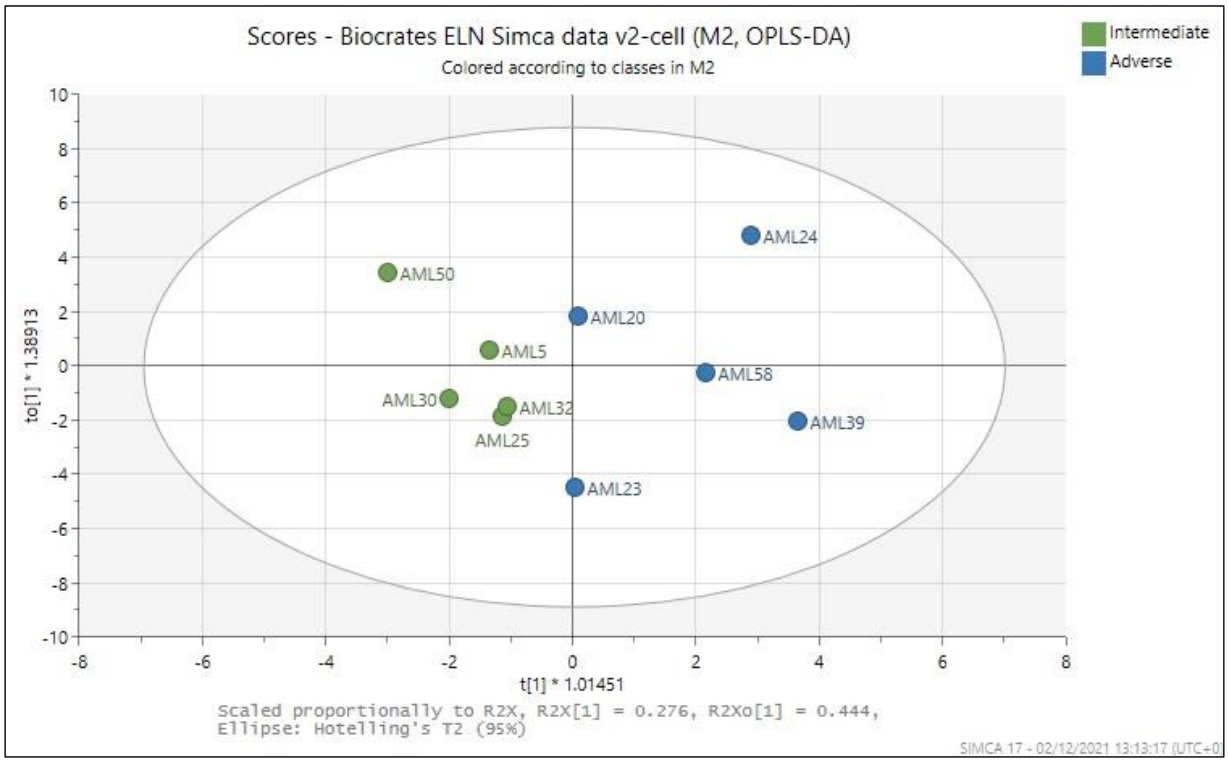

Figure 5.7: OPLS-DA multivariate analysis of changes in AA concentrations in cell pellets following culture for 24 hours. This shows discrimination between the Intermediate (green, n=5) and adverse (blue, n=5) ELN risk groups.

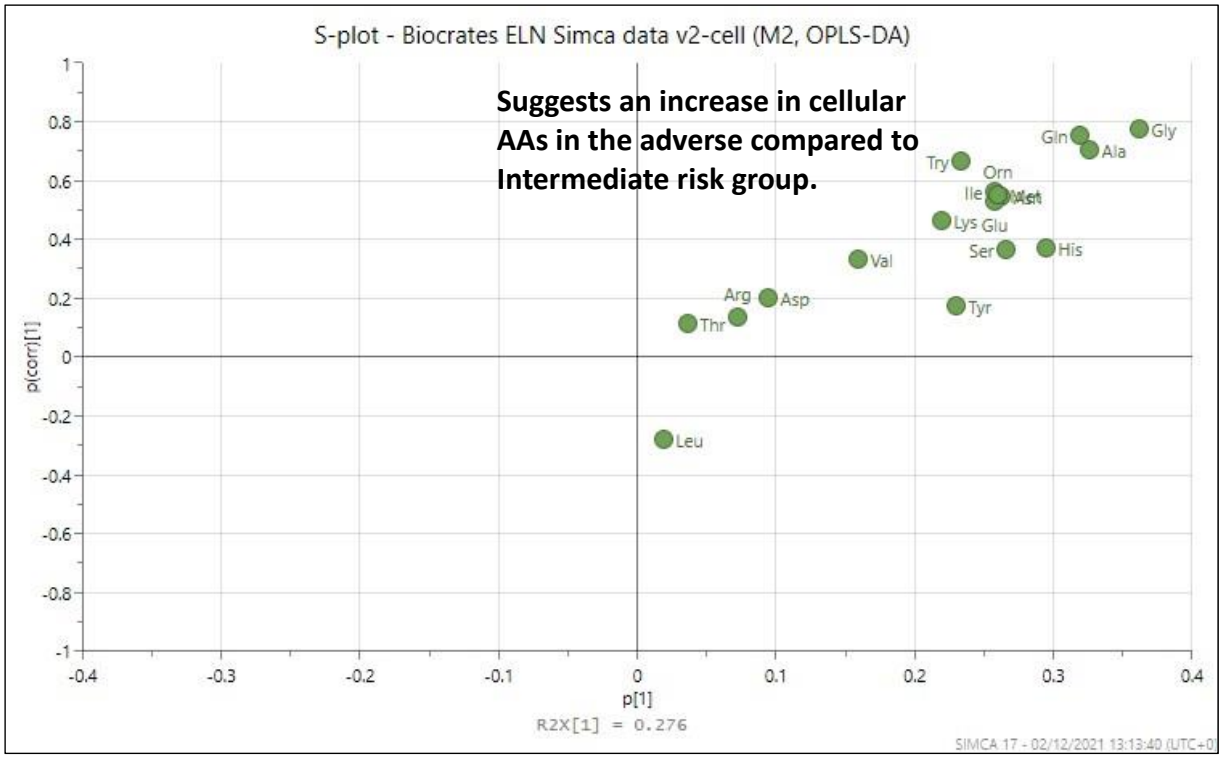

Figure 5.8: S-plot derived from OPLS-DA multivariate analysis showing change in cell pellet concentrations in AAs in ELN adverse risk (n=5) compared to intermediate risk (n=5) AML.

Figure 5.9 shows the OPLS-DA analysis for media changes in the same 10 AML samples. Although there is clustering of the intermediate and adverse risk groups there is an outlier sample (AML5).

Figure 5.10 shows the OPLS-DA analysis when the AML5 sample was removed and figure 5.11 the S-plot for the same data set.

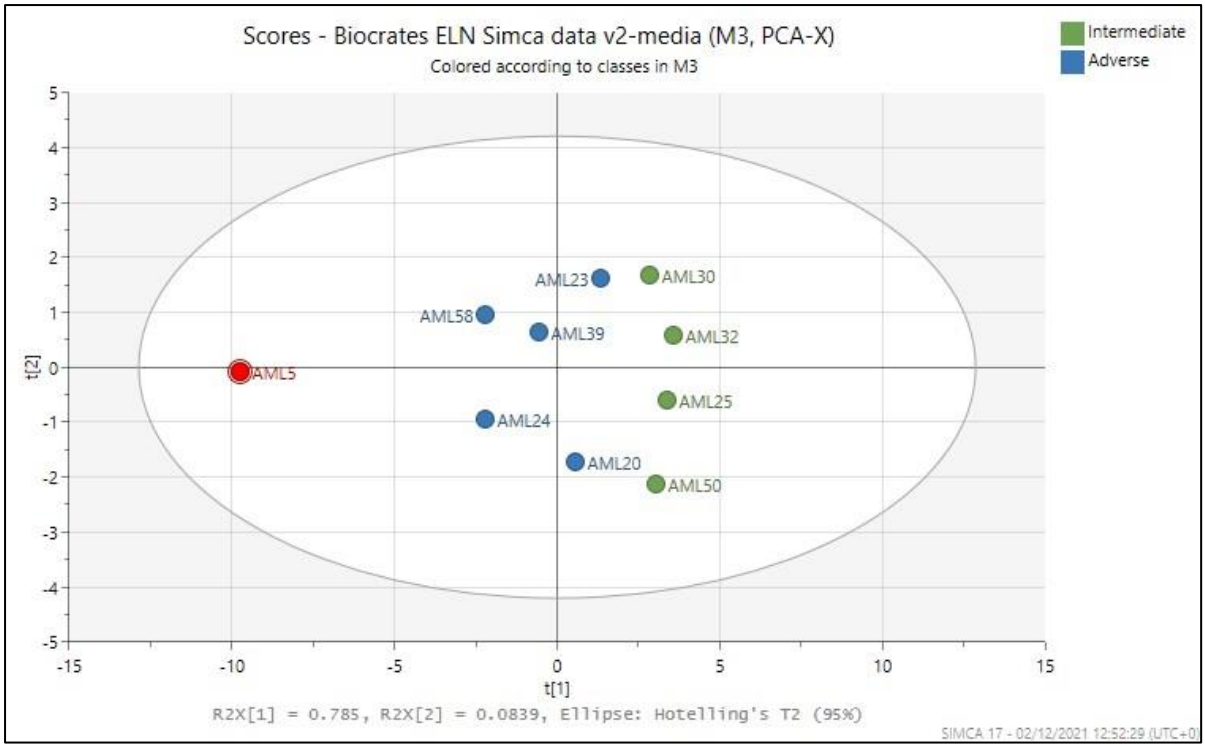

Figure 5.9: OPLS-DA multivariate of changes in AA concentrations in media following culture for 24 hours. This shows some clustering of the Intermediate (green, n=5) and adverse (blue, n=5) ELN risk groups.

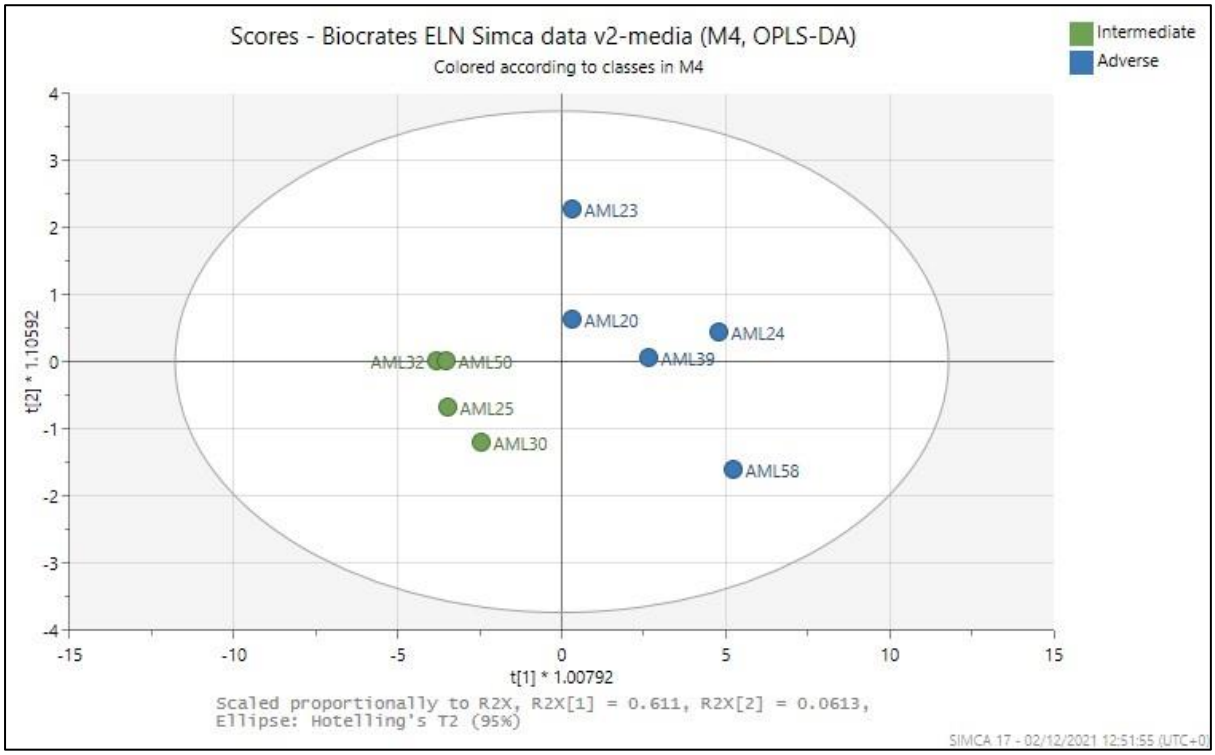

Figure 5.10: OPLS-DA multivariate of changes in AA concentrations in media following culture for 24 hours. This shows discrimination between the Intermediate (green, n=4) and adverse (blue, n=5) ELN risk groups when the outlying sample was excluded.

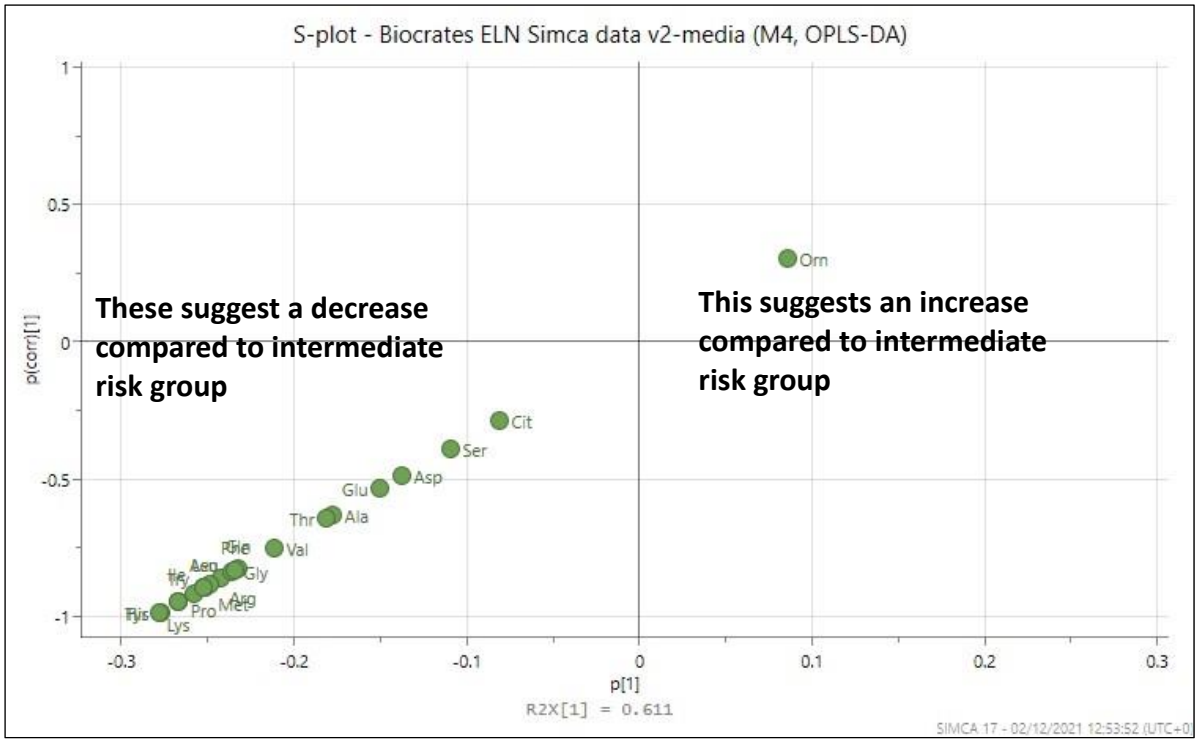

Figure 5.11: S-plot derived from OPLS-DA multivariate analysis showing change in media concentrations in AAs in ELN adverse risk (n=5) compared to intermediate risk (n=4) AML.

Figures 5.12 and 5.13 are bar charts showing the variables of importance in order for cell pellets and media respectively. These are the same data shown in figures 5.8 and 5.11, displayed in a different format. They show which AAs are most responsible for the discrimination between the 2 groups.

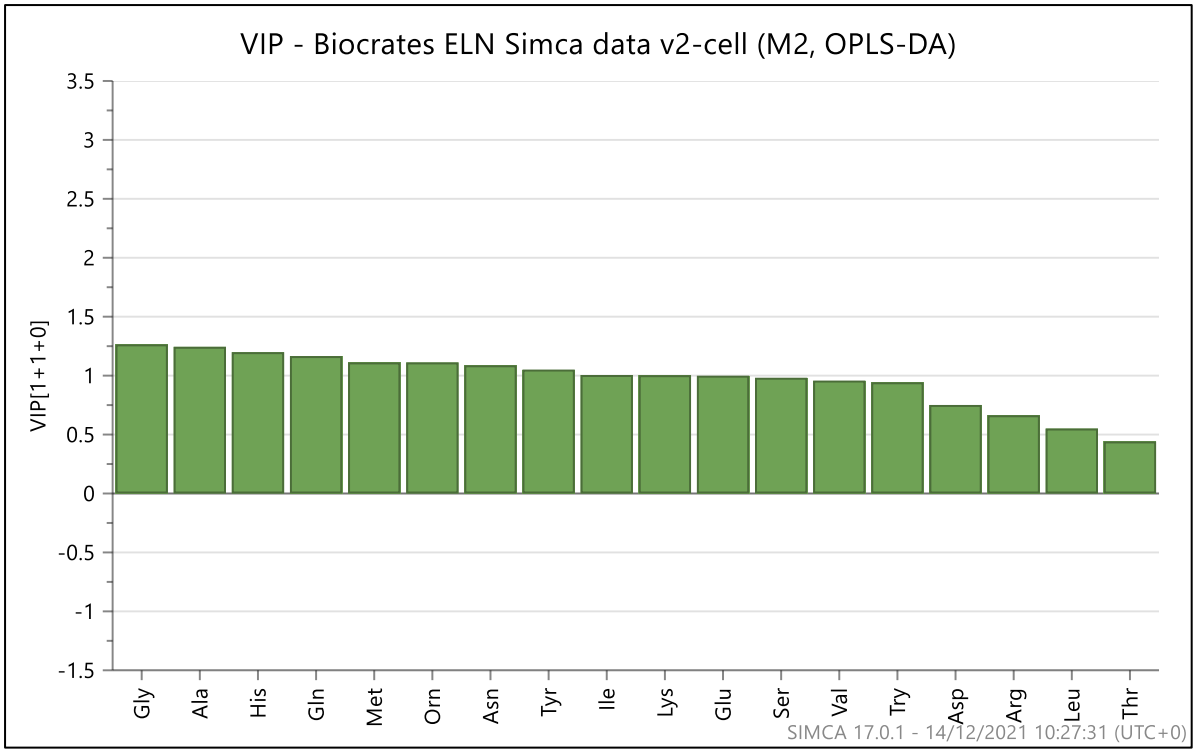

Figure 5.12: Bar chart showing Variable of Importance score for each AA in cell pellets. X axis shows AA and Y axis VIP score (glycine being the most important).

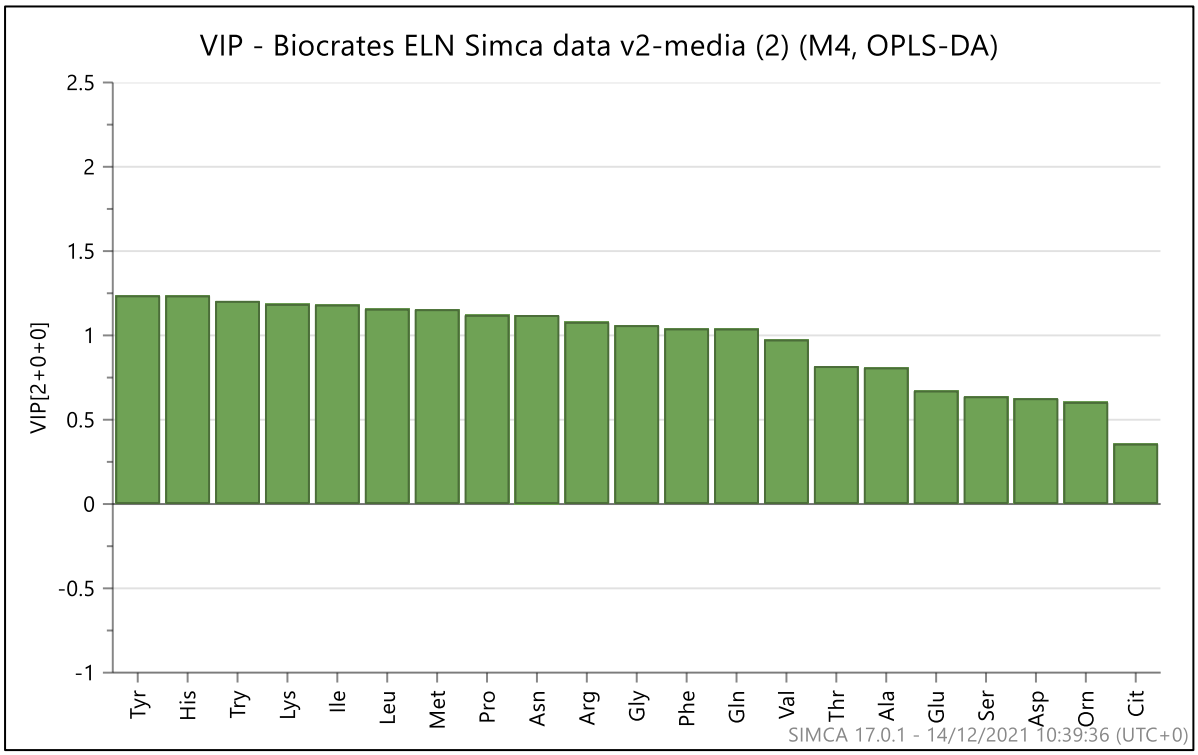

Figure 5.13: Bar chart showing Variable of Importance score for each AA in media/ supernatant. X axis shows AA and Y axis VIP score (tyrosine being the most important).

Chapter 6: Cellular control and compensation in amino acid deprivation

6.1 Introduction

I have focused on the integrated stress response pathway and the enzymes involved in methionine metabolism.

6.2 Summary of specific methods

6.2.1 Samples

A summary of the characteristics of the primary AML samples used in this chapter is found in table 6.1. Controls were obtained from both BM and GMPB.

6.2.2 Molecular techniques

The protocols for the molecular techniques are described in detail in chapter 2. For brevity, a list of the antibodies only is provided here.

6.2.2.1 Western blotting

The following antibodies were used: PHGDH, ATF4, GCN2, eIF2α (all Cell Signalling) MTAP and MAT2A (Sigma). GAPDH (Cell Signalling) and β-actin (Santa Cruz) were used as house-keeping genes.

6.2.2.2 PCR

Gene expression was assessed for the following: PHGDH, ATF4, GCN2 and eIF2α (all Life Technologies).

6.2.2.3 Immunofluoresence

MTAP (Sigma) and GAPDH (Cell Signalling) were used.

Sample ID	1˚/2˚	Sex	Age	Timing	Cytogenetics	MRC Risk	ELN Risk	NPM1	FLT3-ITD	Ratio	TP53
AML 39	Primary	M	59	Diagnosis	Complex	Adverse	Adverse	No	No	n/a	No
AML 37	Primary	M	47	Relapse	7q-	Adverse	Adverse	No	No	n/a	No
AML27	Primary	F	25	Relapse	Complex	Adverse	Adverse	Yes	No	n/a	No
AML 6	Primary	M	35	Diagnosis	+8	Intermediate	Adverse	No	Yes	>0.5	No
AML24	Primary	F	69	Diagnosis	-16, -18	Intermediate	Adverse	No	Yes	0.28	Yes
AML 17	Primary	M	75	Diagnosis	Normal	Intermediate	Intermediate	Yes	Yes	0.49	No
AML 19	Secondary	M	78	Diagnosis	Normal	Intermediate	Intermediate	Yes	No	No	No
AML 13	Primary	M	43	Relapse	t(9;11)	Intermediate	Intermediate	Yes	No	n/a	No
AML35	Secondary	F	64	Relapse	1q-	Intermediate	Intermediate	No	No	n/a	No
AML 10	Secondary	F	81	Diagnosis	Normal	Intermediate	Intermediate	No	No	n/a	NK
AML5	Primary	F	81	Relapse	Normal	Intermediate	Intermediate	No	No	n/a	NK
AML31	Primary	M	59	Diagnosis	Normal	Intermediate	Adverse	Yes	Yes	2.17	No
AML 29	Primary	F	67	Diagnosis	3 way	Intermediate	Adverse	Yes	Yes	7.82	No
AML29	Primary	F	67	Diagnosis	3 way	Intermediate	Intermediate	Yes	Yes	NK	NK
AML30	Primary	F	69	Diagnosis	Normal	Intermediate	Intermediate	Yes	Yes	0.87	No
AML28	Secondary	M	65	Diagnosis	+8	Intermediate	Intermediate	Yes	No	n/a	No
AML 2	Primary	F	69	Relapsed	.+11	Intermediate	Favourable	Yes	No	n/a	NK
AML 12	Primary	F	75	Diagnosis	Normal	Intermediate	Favourable	Yes	Yes	0.48	NK
AML7	Primary	F	57	Diagnosis	Normal	Intermediate	Favourable	Yes	Yes	0.04	NK
AML 16	Primary	F	72	Diagnosis	Normal	Intermediate	Favourable	Yes	No	n/a	NK
AML 18	Primary	M	64	Diagnosis	Normal	Intermediate	Favourable	Yes	Yes	NK	NK
AML40	Primary	F	40	Diagnosis	Normal	Intermediate	Favourable	Yes	No	n/a	No
AML47	Primary	F	55	Diagnosis	Normal	Intermediate	Favourable	Yes	No	n/a	No
AML 22	Primary	M	60	Diagnosis	inv(16)	Favourable	Favourable	No	No	n/a	NK
AML21	Primary	F	34	Diagnosis	inv(16)	Favourable	Favourable	No	No	n/a	No
AML22	Primary	M	60	Diagnosis	inv(16)	Favourable	Favourable	n/a	n/a	n/a	NK

Table 6.1 Characteristics of AML samples used in this chapter.

6.3 Results

Given that Met deprivation resulted in AML apoptosis (chapter 3) I investigated two of the key enzymes in Met metabolism, MTAP and MAT2A. MTAP is involved in the Met salvage pathway and salvages Met from MTA which is made from SAM (a universal methyl donor) and the products of polyamine metabolism. MAT2A is required for SAM synthesis following methionine metabolism[7]. I have included a diagram of the pathway to aid the results discussion.

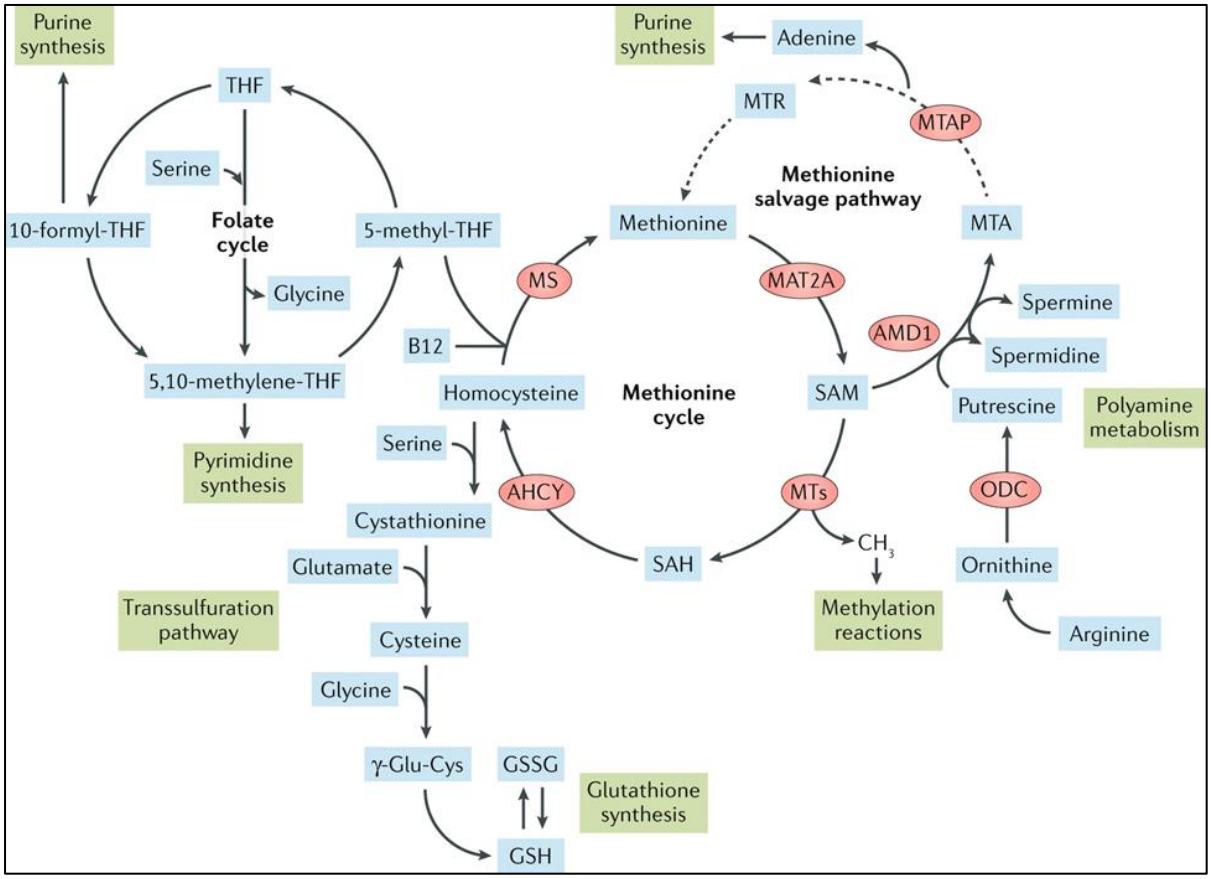

Figure 6.1: Methionine cycle showing the methionine salvage pathway [113].

[7] MTA: methylthioadenosine; MTAP: methylthioadenosine phosphorylase; MAT2A: methionine adenosyltransferase 2A; SAM:S-adenoysl methionine.

MTAP was expressed at higher levels in AML than GMPB (figure 6.1; p=0.002). These results are consistent with the demonstrated need for Met.

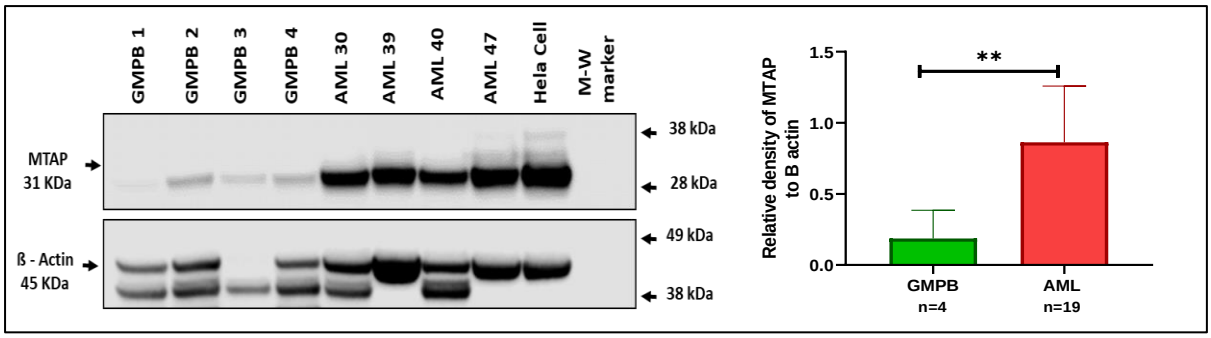

Figure 6.2: Western blots of AML and GMPB control lysates showing expression of MTAP (L). Hela cells used as positive control. Bar chart showing relative density of MTAP to B actin of the same samples (R).

This is visualised further with the immunofluorescence staining in figure 6.3

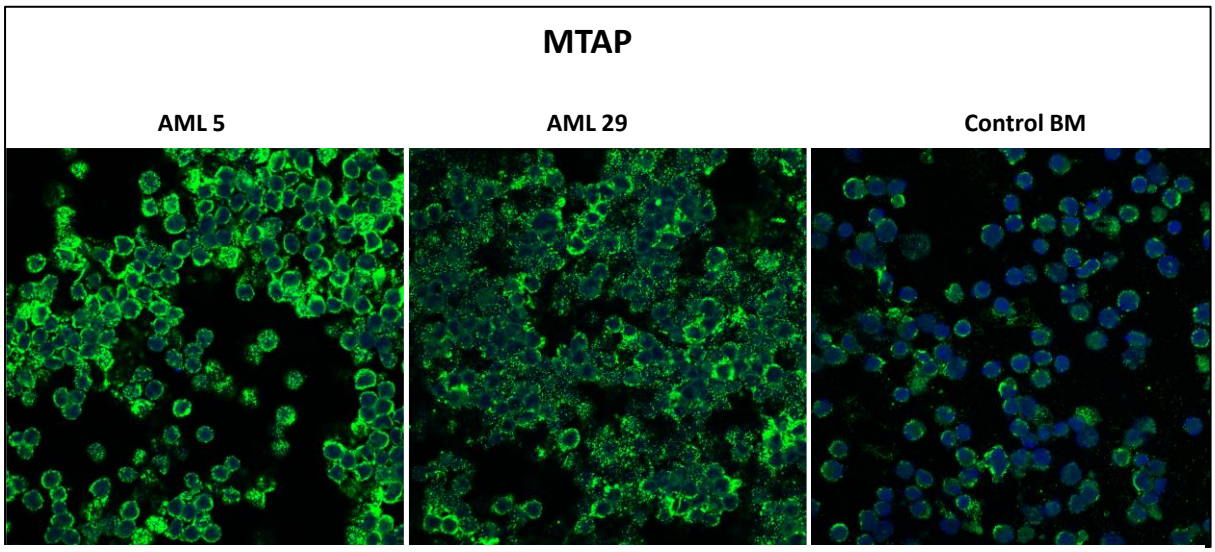

Figure 6.3: Immunofluorescence showing MTAP increased MTAP expression in 2 AML samples compared to normal BM control.

Figure 6.4 shows that there was no change in MTAP expression in response to Met deprivation (p=0.3829). Figure 6.4 shows that there was no change in MAT2A

expression in the same conditions (p=0.1649). In both, the control samples were cultured in AA replete media.

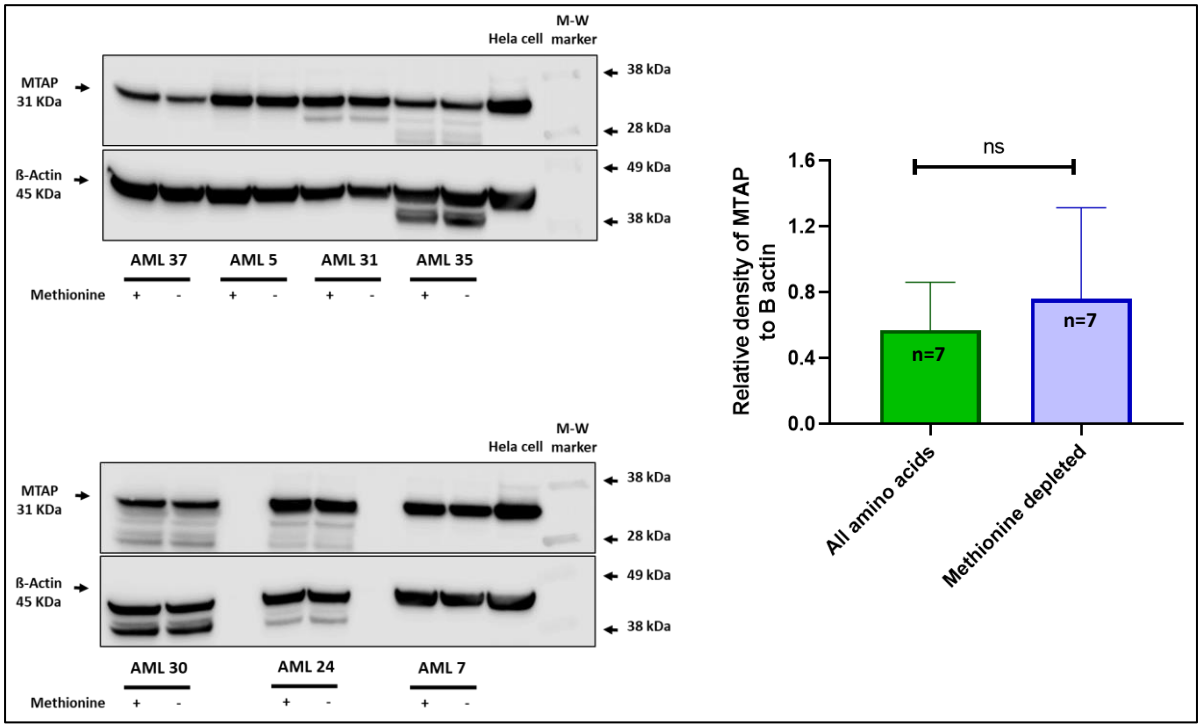

Figure 6.4: Western blots of 7 AML sample lysates showing expression of MTAP following culture for 24 hours. + indicates control media (all AAs), - indicates media without methionine (L). Bar chart showing relative density of MTAP in the control and methionine deplete groups (R).

The combined data suggest that the Met salvage pathway cannot keep up with Met needs in AML where there is Met deprivation. This may be because MTAP and MAT2A are not upregulated in response to Met deprivation.

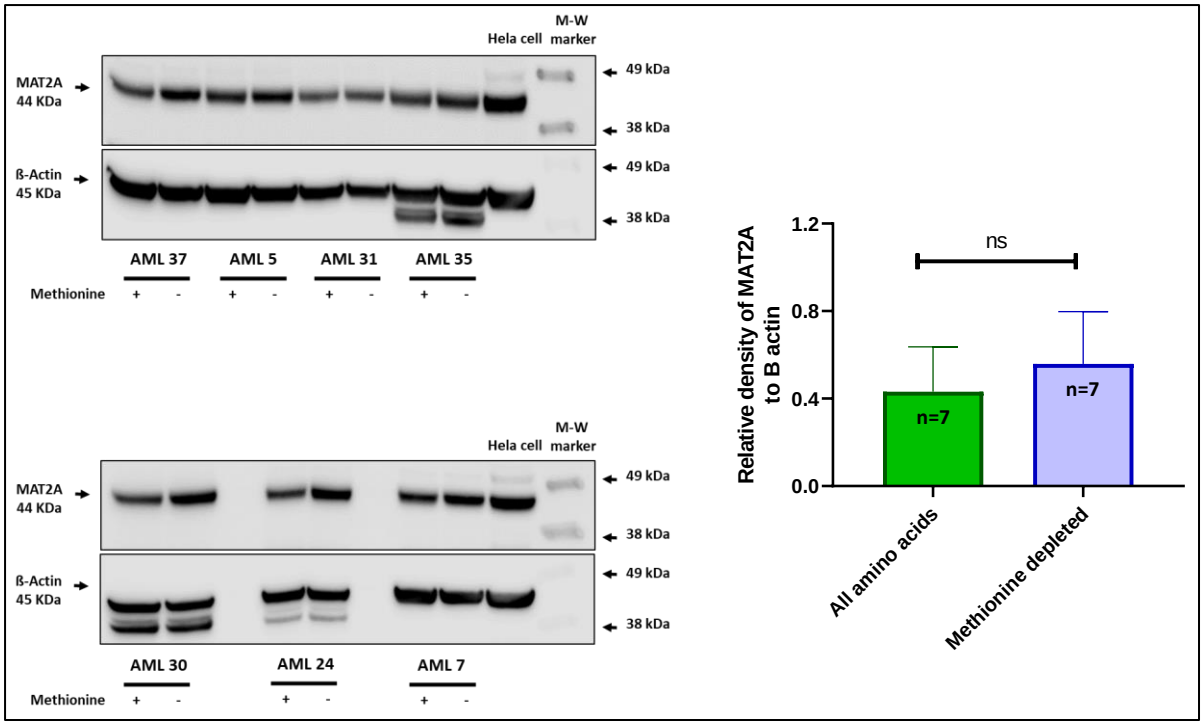

Figure 6.5: Western blots of 7 AML sample lysates showing expression of MAT2A following culture for 24 hours. + indicates control media (all AAs), - indicates media without methionine (L). Bar chart showing relative density of MTAP in the control and methionine deplete groups (R).

Components of the Integrated Stress Response (ISR) pathway (GCN2, eIF2α, ATF4 and PHGDH[8]) were quantified in AML cells to identify whether there is activity of the ISR in AML under normal conditions. The ISR pathway is described in chapter 1. Briefly, GCN2 is a molecular sensor of amino acid deprivation. In response to AA deficiency GCN2 phosphorylates eIF2α inhibiting protein synthesis generally, although it upregulates the master regulator, ATF4. One of the downstream targets of ATF4 is PHGDH. ATF4 upregulates PHGDH, one of the key enzymes in serine synthesis.

Western blotting and PCR were used to show eIF2α and GCN2 expression in AML. The PCR results in figure 6.6 shows that levels were significantly higher than in GMPB ($p=0.0017$ and $p=0.0004$ respectively).

[8] eIF2α: eukaryotic initiation factor 2 alpha; ATF4: activating transcription factor 4; GCN2: general control nonderepressible 2; PHGDH: phosphoglycerate dehydrogenase;

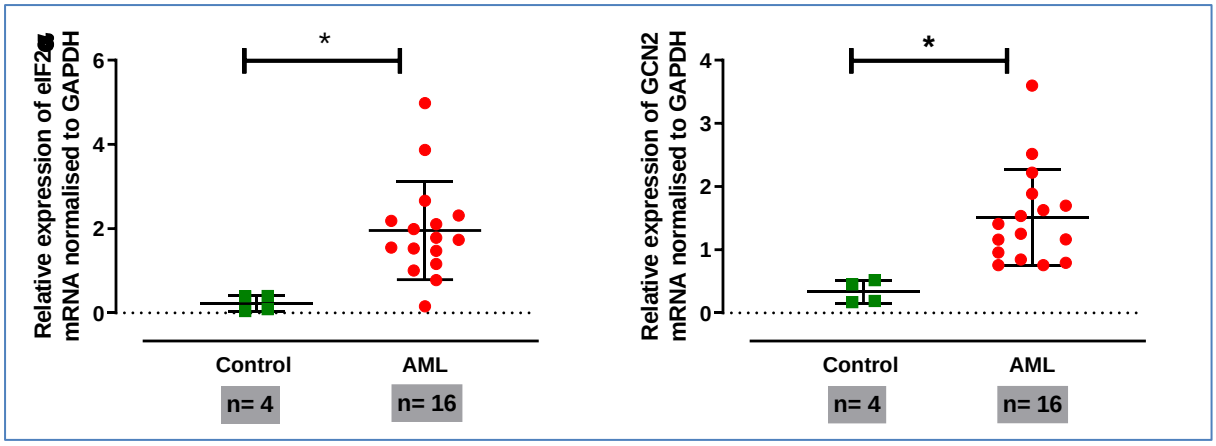

Figure 6.6: Scatter plots of qPCR results showing mRNA expression of AML and BM control samples normalised to GAPDH for eIF2α (L) and GCN2 (R).

Figure 6.7 shows that Western blotting results for eIF2α. Expression is significantly higher in the AML samples compare to GMPB (p=0.01).

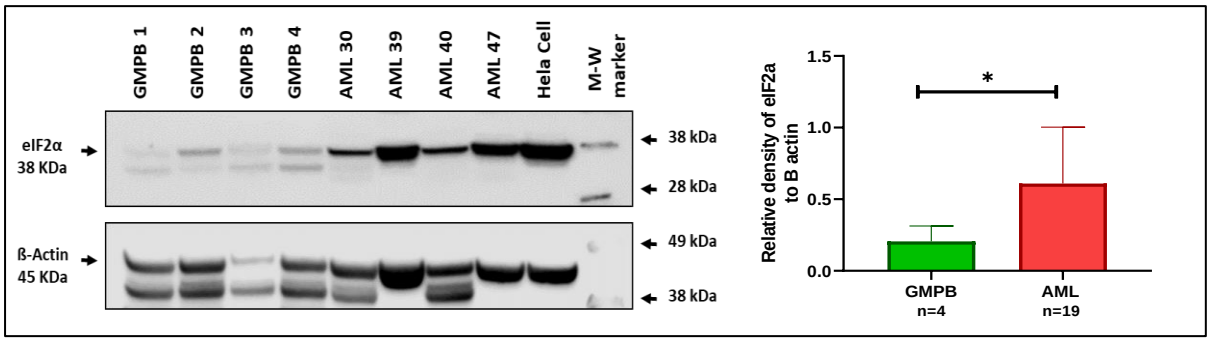

Figure 6.7: Western blots of AML and GMPB control lysates showing expression of eIF2α (L). Hela cells used as positive control. Bar chart showing relative density of eIF2α to B actin of the same samples (R).

Met deprivation did not increase the eIF2α expression (figure 6.8; p=0.3176). Of note the presence of protein alone does not signify activity - eIF2α is activated by phosphorylation by GCN2 in response to AA deprivation. Further studies using specific antibodies to phosphorylated eIF2α would be needed to address this.

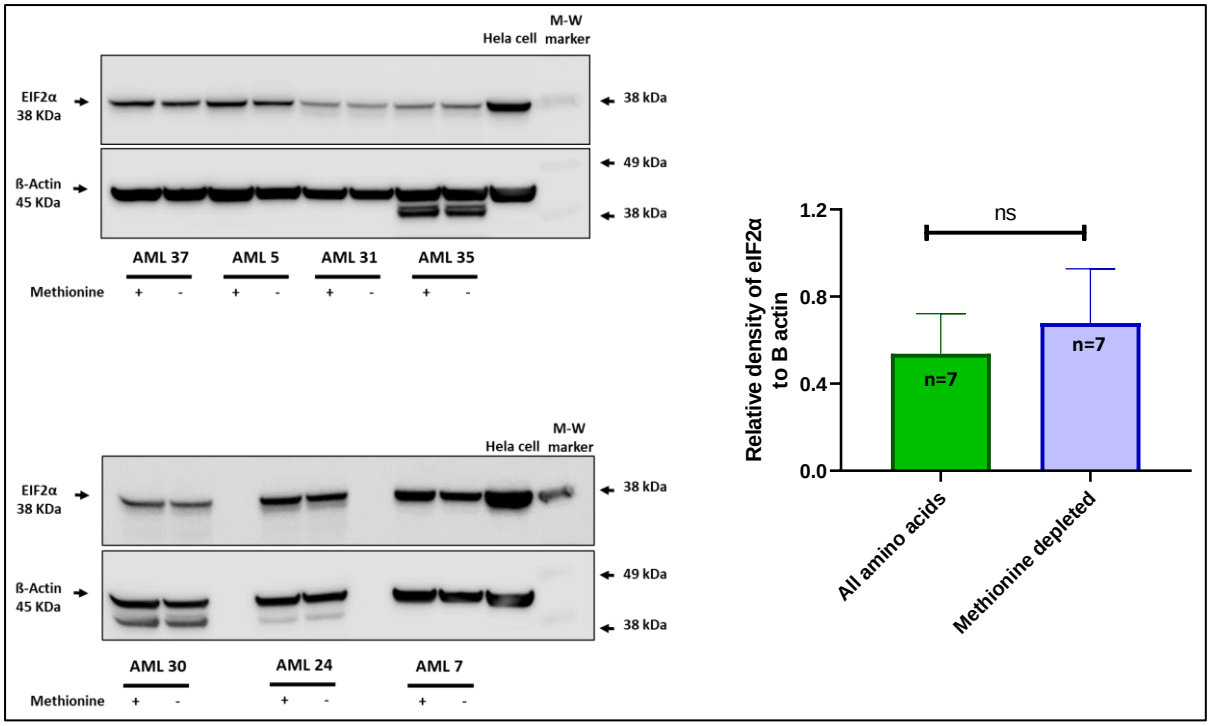

Figure 6.8: Western blots of 7 AML sample lysates showing expression of eIF2α following culture for 24 hours. + indicates control media (all AAs), - indicates media without methionine (L). Bar chart showing relative density of eIF2α in the control and methionine deplete groups (R).

ATF4 was not overtly expressed in either AML or GMPB when measured by Western blotting (figure 6.9; p=0.2) or PCR (figure 6.10; p=0.9635).

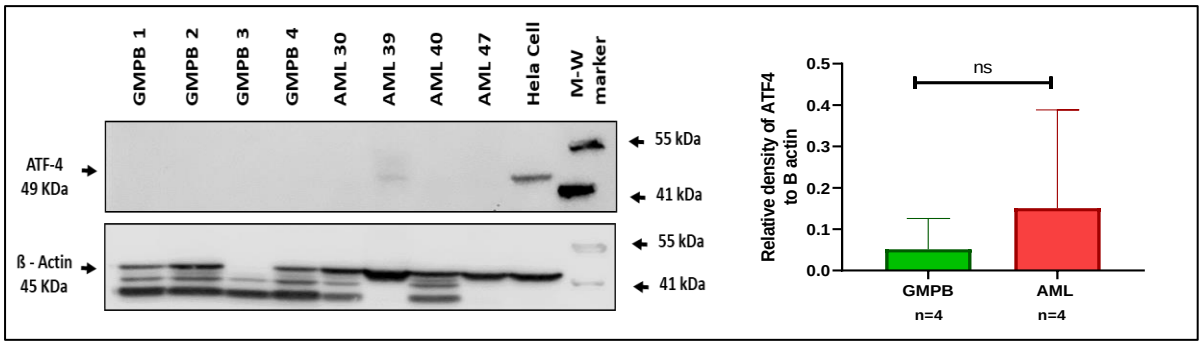

Figure 6.9: Western blots of AML and GMPB control lysates showing expression of ATF4 (L). Hela cells used as positive control. Bar chart showing relative density of ATF4 to B actin of the same samples (R).

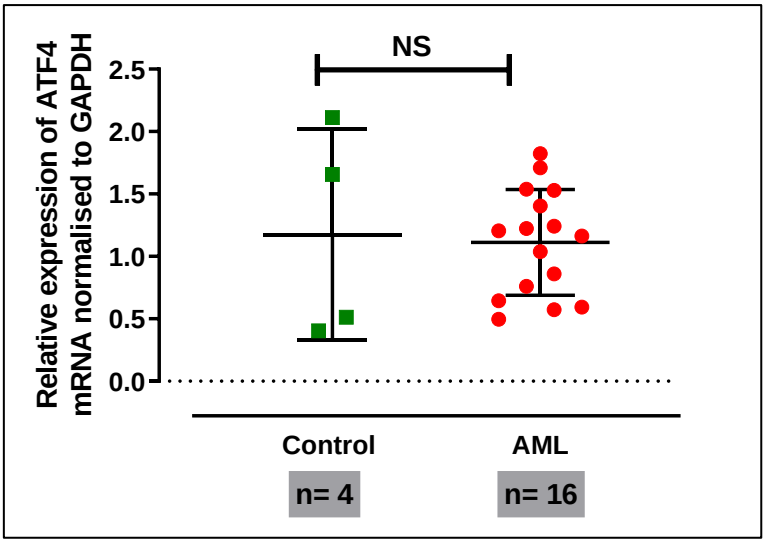

Figure 6.10: Scatter plot of qPCR results showing ATF4 mRNA expression of AML and BM control samples normalised to GAPDH.

PHGDH was not expressed in most AML samples (or GMPB) although two samples out of 12 AML samples had some expression on Western blotting (figure 6.11; p=0.8).

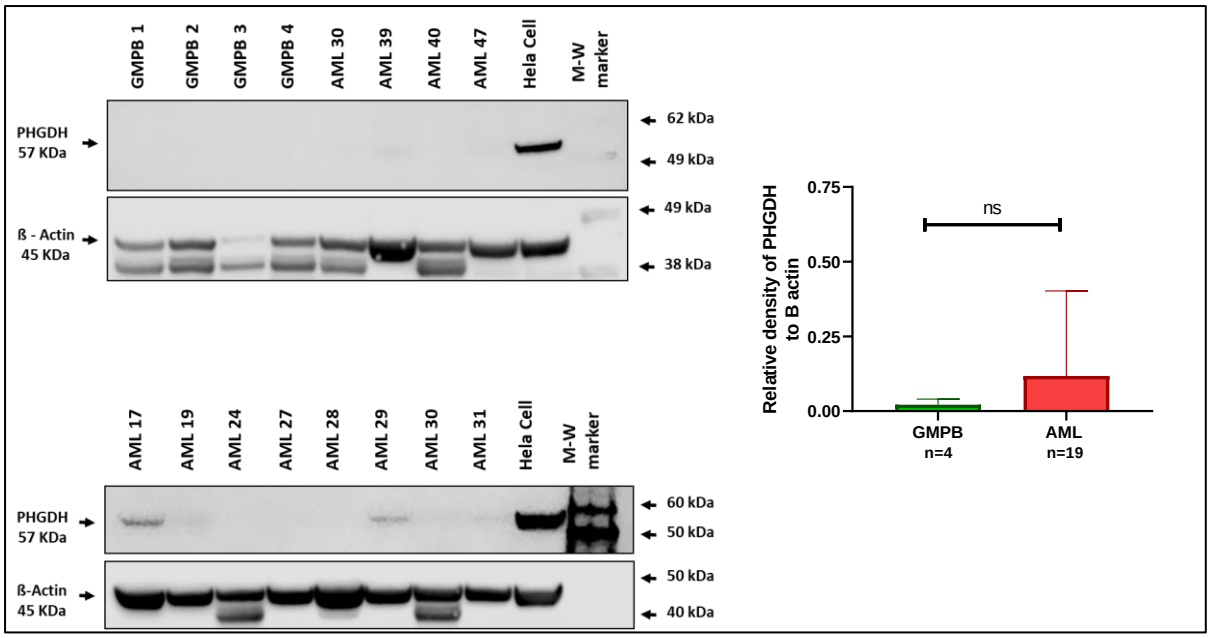

Figure 6.11: Western blots of AML and GMPB control lysates showing expression of PHGDH (L). Hela cells used as positive control. Bar chart showing relative density of PHGDH to B actin of the same samples (R).

The PCR results show that PHGDH expression is significantly higher in AML than in GMPB (p=0.366) although 2 out of the 15 AML samples show higher expression (figure 6.12).

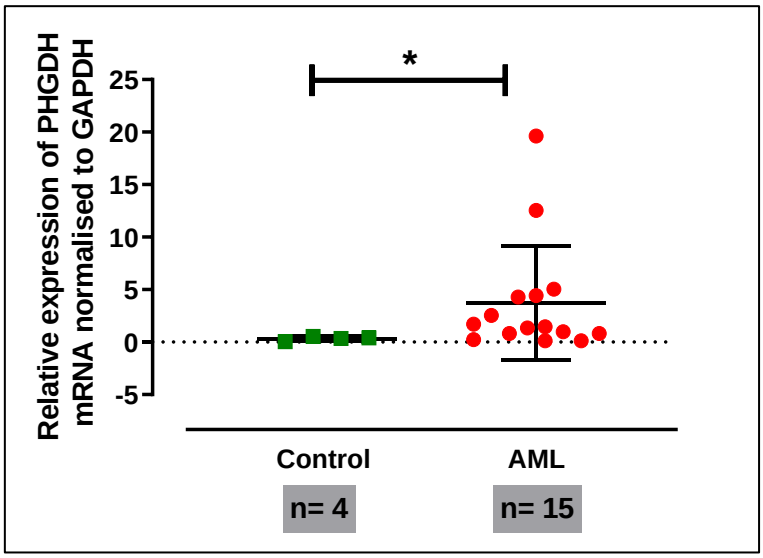

Figure 6.12: Scatter plot of qPCR results showing PHGDH mRNA expression of AML and BM control samples normalised to GAPDH.

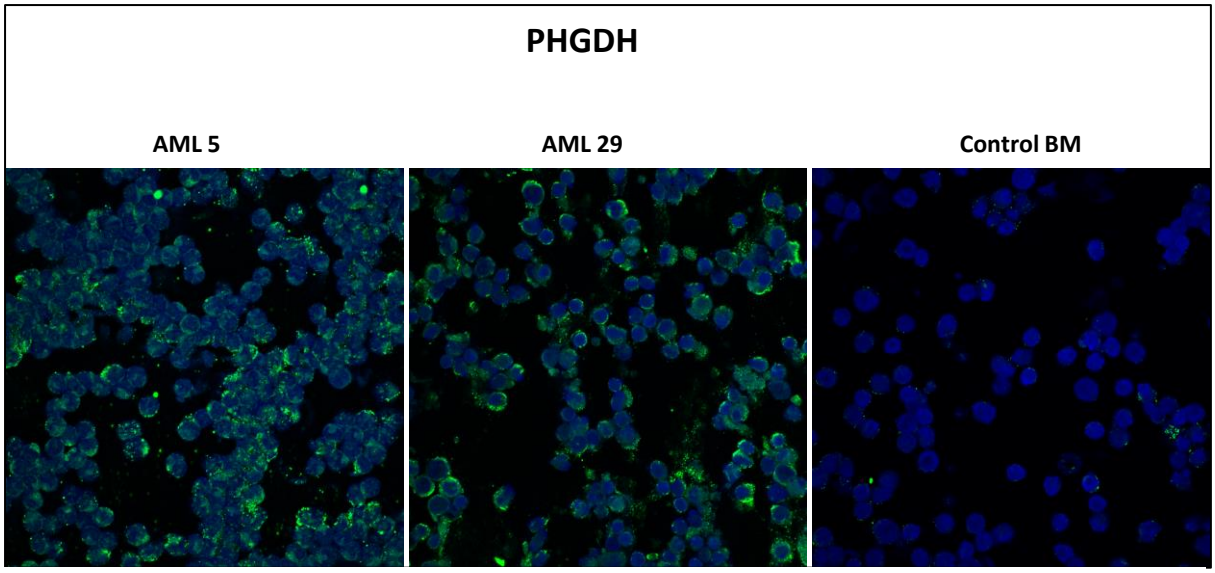

Figure 6.13: Immunofluorescence showing PHGDH expression in 2 AML samples compared to normal BM control.

Figure 6.13 shows the immunofluorescence results for 2 AML samples. Both show an increase in PHGDH expression compared to the BM control. The result for AML29 is consistent with the western blotting data in figure 6.11 (no blotting result available for AML5).

Chapter 7: Proteomic analysis of AML

7.1 Introduction

The results from previous chapters have demonstrated that valine and methionine are critical to AML cells. They may use valine and methionine either to make proteins or to make smaller metabolites.

To test whether AML is using these amino acids to make proteins we measured a wide range of proteins and peptides using proteomic analysis (of more than 8000 proteins) by mass spectrometry. We compared AML cells cultured in media deprived of methionine and valine with those cultured in normal media.

7.2 Summary of specific methods

The sample preparation methods are described in chapter 2. Briefly, the sample was T cell depleted using CD3 magnetic beads to remove lymphocytes. Cells were then co-cultured in duplicate in MS-5 in 3 media conditions (Control, -Met and –Val). Cell pellets were washed and snap frozen at 4 time point (baseline and 24, 48 and 72 hours).

The samples were then processed in a mass spectrometer using Isobaric Labelling through Tandem Mass Tags (TMTpro) [140].

Multivariate analysis was performed by Dr Theo Roumeliotis from the Functional Proteomics team at the ICR using ANOVA.

7.3 Results

7.3.1 AML sample

One sample was analysed successfully. The characteristics are summarised in table 7.1. This sample demonstrated a significant response to both valine and methionine deprivation.

ID	1°/2°	Sex	Age	Timing	Cytogene	MRC Risk	ELN Risk	NPM1	FLT3-ITD	Ratio	TP53
AML7	Primary	F	57	Diagnosis	Normal	Intermediate	Favourable	Yes	Yes	0.04	NK

Table 7.1: Patient characteristics.

7.3.2 Multivariate analysis

Figure 7.1 shows a heat map of the relative or scaled abundance of protein. In this, the row (protein) mean is centred at 100 and a linear regression model applied to each row to 'regress out' the control from the –Met and –Val. The regressed values ($p<0.01$) are the residuals following this regression (table 7.2).

I.e. the results are relative abundances across samples compare to the mean of the control and centred at zero. Blue (<0) means low relative abundance and red (>0) higher relative abundance. A figure of -20 equates to approximately 20% lower abundance compared to the mean of all.

Figure 7.2 shows the temporal pattern of protein change once the linear regression has been applied. There are some pattern differences, although the changes are minimal. More than 8000 proteins were analysed in this experiment. Once the regression analysis was applied and following multiple correction testing (for repeated comparisons) only 28/8000 were statistically significant ($p<0.05$). A list of these is shown in table 7.2. Of these, 13 were downregulated at 72 hours following Met depletion (17 upregulated) and 12 were downregulated following Val depletion (18 upregulated). One of the upregulated proteins, PHGDH, is downstream of the IRS

and this is a normal reaction to AA deprivation. There was no significant change in eIF2α. Neither GCN2 nor ATF4 were measured.

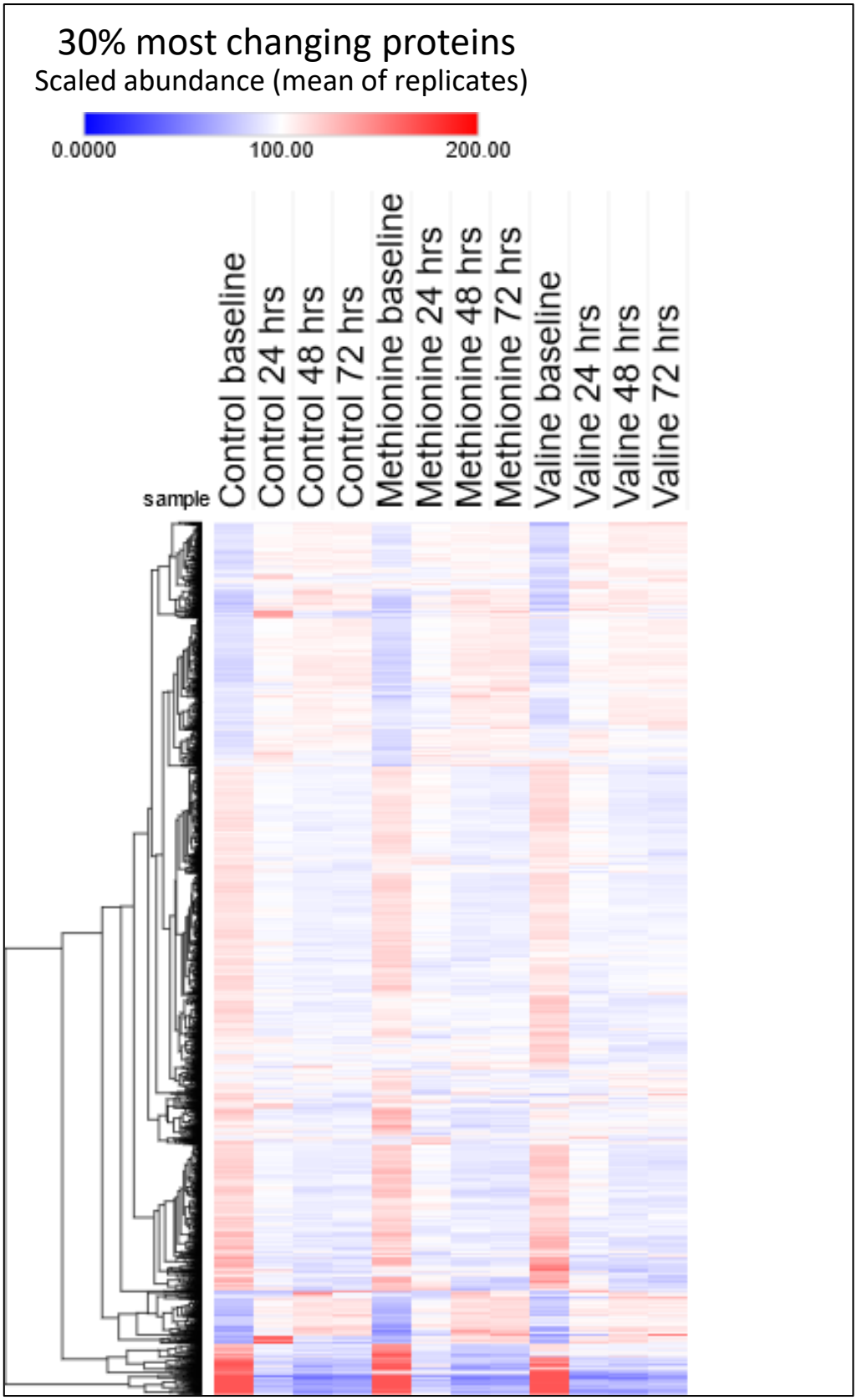

Figure 7.1: Heat map showing visual representation of the 30% most changing proteins and their abundance. Proteins listed on the left Y axis (text too small to visualise). Media conditions and 4 time points listed on top X axis (courtesy of Dr Theo Roumeliotis).

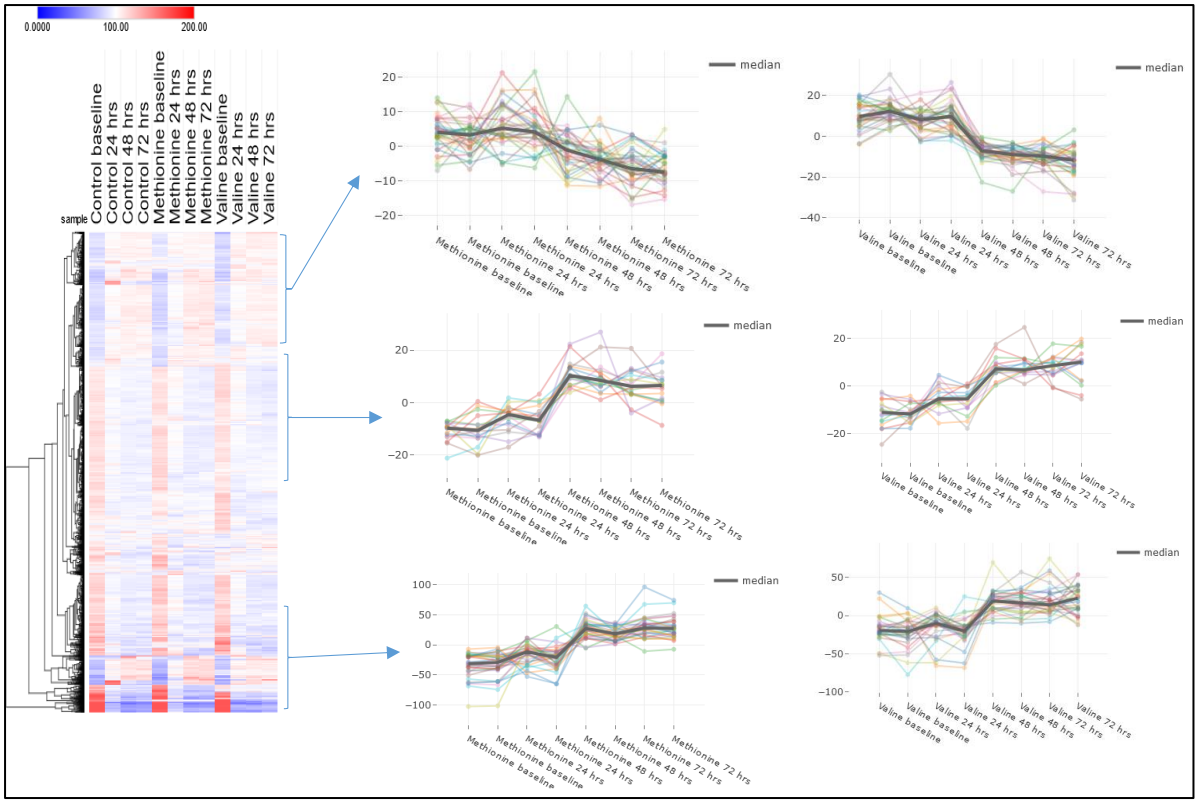

Figure 7.2: (L) Heat map from figure 7.1. (R) Temporal patterns at 3 points in the heat map showing the difference in proteins between the –Met (L) and –Val samples (R) once regression analysis has been applied.

Protein	Function	Regulation	
		Met	Val
AIF1	inflammatory response protein	Down	Down
LTA4H	pro-inflammatory mediator	Down	Down
TFG	endoplasmic reticulum function	Down	Down
HDGF	vascular enothelial protein	Down	Down
TBCA	tubulin binding protein	Down	Down
TCOF1	regulator of RNA polymerase	Down	Down
AIF1L	inflammatory response protein	Down	Down
EVI2B	myeloid differentiation (CEBPα target)	Down	Down
NPM2	histone chaperone	Down	Down
HSP90B1	molecular chaperone	Up	Up
RAB38	intracellular vesicular trafficking	Down	Down
RAB8B	intracellular transport	Down	Up
PNMA8B	protein coding	Down	Down
BN1P3L	mitochondrial protein	Up	Up
MAMDC2	putative secretory protein	Up	Up
PIGG	glycolipid biosynthesis	Up	Up
DCAF5	protein modification	Down	Down
PHGDH	Serine synthesis	Up	Up
PRDX4	protein folding pathway	Up	Up
UGDH	NADH production	Up	Up
MYDF	myeloid differentiation	Up	Up
SLC39A7	zinc transportation	Up	Up
F5	coagulation	Up	Up
ATP7B	copper tranportation	Up	Up
ITIH2	plasma protease inhibition	Up	Up
CALD1	smooth muscle contraction	Up	Up
CAV1	oncogenic membrane protein	Up	Up
OGFRL1	growth factor	Up	Up

Table 7.2: List of the significant (p<0.05) proteins following regression analysis and multiple correction testing indicating whether they are up- or down-regulated by AA media condition. Functions also listed.

PHGDH is upregulated by the GCN2/eif2α/ATF4 pathway in response to a fall in AA concentration[9]. There was a significant increase in abundance of PHGDH in response to both methionine and valine depletion following ANOVA regression analysis. Figure 7.3 shows the temporal response to AA deprivation before regression was applied.

[9] PHGDH: phospoglycerate dehydrogenase

This still shows the relative increase in both the –Met and –Val samples. In the control there is an initial rise before the level falls again. With both Met and Val depletion there is a sequential rise of approximately 50% over 72 hours.

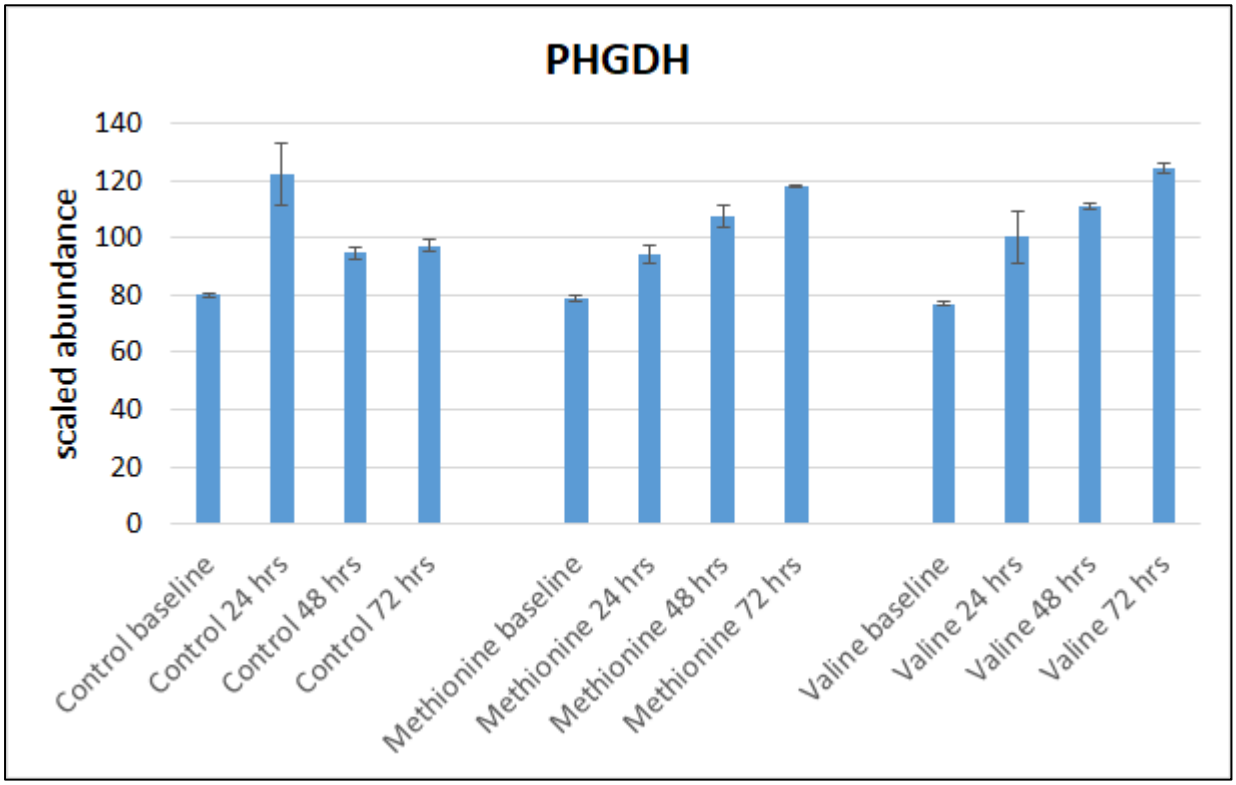

Figure 7.3: Bar chart showing linear rise in PHGDH protein level in response to Met and Val depletion.

Chapter 8: Discussion

In this thesis I have attempted to establish the amino acid dependence of AML and whether this differs across risk groups.

8.1 Measuring AA dependence using co-culture

8.1.1 General points

There are some more general themes that warrant noting from this work. Cell lines are frequently used in culture experiments but do have their limitations. The 3 'AML' cell lines used in this chapter are certainly not typical of the range of primary samples that were used. FKH-1 was derived from a patient with CML transformed to AML, HL60 from a patient with APML (albeit with differentiation) and Kasumi a 7 year old with refractory disease. In addition, the evolution of cell lines in culture over time can affect the reproducibility of the data derived from them [147]. Over 300 drug compounds have been tested against evolved MCF7 breast cancer cell lines, for example, with highly variable responses [148].

However, one challenge of AML co-culture experiments is the need for a stromal feeder layer to support the AML cells. This is not an inert system but does secrete a range of cytokines and growth factors and its AA demands and impact on metabolism are unknown [149].

There were challenges in obtaining control samples with sufficient cell numbers for culture experiments. BM controls have consistently been used by our team at the request of peer reviewers and are commonly used in co-culture work [149]. Mononuclear cells were used for both the AML and control samples. Another option would have been to sort the blast population in AML samples but this would have required higher cell numbers. Given the *in vitro* work our team has done with arginine deprivation this could have been used as a positive control.

In addition, measurement of cell viability by counting cell numbers does not exclude blast maturation and therefore may not be truly representative.

Finally, both risk classifications have been used throughout the thesis to distinguish the risk groups and, while they define subtypes of AML, there is an inevitable range of outcomes within these groups. Most samples obtained were intermediate risk. AML is a heterogeneous disease and this, combined with low sample numbers, can limit interpretation of statistical analysis.

8.1.2 AML has specific AA dependencies

There are some striking results in this large cohort of primary AML samples. Valine depletion led to significant reduction in viable AML cell numbers. Whilst one argument is that this should be expected with the absolute restriction of an essential AA, the result was significant compared to normal BM controls. In addition, it had no effect on the lymphocyte population. It has been shown that valine depletion affects HSCs meaning that long-term absolute restriction would not be viable (and is not feasible) but shorter periods of restriction may be sufficient. This could potentially be clinically exploitable (for example pre-allograft to enhance the AML killing effect of conditioning chemo-radiation).

Interestingly, the effect of methionine depletion was less marked with a significant effect only in those AMLs known to respond better to chemotherapy. The methionine salvage pathway may contribute to this and therefore a longer period of restriction may be required to overcome this. As discussed in the introduction there is growing evidence that methionine restriction could expose cellular vulnerabilities [114, 115, 117].

Exploitation of the serine synthesis pathway shows promise in a number of tumour groups. Results from this chapter demonstrate that both AAs are critical to AML survival for both adverse and intermediate risk AML. Depletion of one can generally be overcome by the other stressing that the enzymes in this synthetic pathway show promise as a drug target. Interestingly, favourable risk AML survival is not significantly impacted by their restriction.

Glutamine deprivation was found not to have a significant effect on AML cell viability. The role of glutamine in oxidative phosphorylation and altered cancer metabolism has been reviewed elsewhere in this thesis so this result is somewhat surprising. The use of BM controls, the MS-5 feeder layer or the duration of culture may all affect this result.

The paradoxical rise in viable cells seen with asparagine depletion is also unexpected. One explanation is that a synthetic pathway is triggered and glutamine, aspartate and asparagine synthetase compensate for it. Glutamine is the most abundant AA in culture media.

8.1.3 Potential further experimental work

There are many examples of the direct and novel clinical applications of amino acid depletion as a strategy for treatment. AA depletion is not envisioned as a viable sole strategy but it should be considered as a means of priming the metabolic vulnerabilities of diseases such as AML. Valine and methionine have received less attention than some other AAs but there is sufficient evidence to investigate them in more detail.

It would be helpful to compare the effect of essential AA depletion on HSCs, LSCs and AML cells and to determine what duration of depletion is required to disrupt leukaemogenesis. This was beyond the scope of this thesis.

Recently published work by Thandapani and colleagues in T-ALL highlights a potential avenue of exploration for valine deprivation in AML [150]. They identified that valine tRNA biogenesis is altered in T-ALL with upregulation of valine aminoacyl tRNA synthetase. This is regulated by NOTCH1. Using mouse and human xenograft models and valine restriction they demonstrated the dependency of T-ALL on valine. Valine restriction led to defective assembly of complex 1 and impaired oxidative phosphorylation. Of note, upregulation of BCL-2 in response to valine restriction identified this a possible mechanism of resistance. They demonstrated synergism when valine restriction was combined with the BCL-2 inhibitor venetoclax.

While NOTCH1 activating mutations are present in the majority of cases of T-ALL their role in AML is less well defined [151, 152]. Expression levels of NOTCH1 and activation of the pathway are associated with adverse outcome in AML [153, 154].

While T-ALL is a different entity, further exploration of the role of NOTCH1 signalling in valine restriction in AML and testing synergism with venetoclax warrants further attention.

8.2 Combining AA deprivation with chemotherapy

8.2.1 There is no synergistic effect with cytarabine

The samples used in this experiment were selected as they proved to be less responsive to AA depletion when compared to normal BM controls. In the control media arm, although only 4/6 showed a significant reduction in cell numbers all were annexin positive suggesting that, if cultured for longer, the counting would reflect this.

Despite the effect of chemotherapy in the controls I was unable to demonstrate synergism with cytarabine. These samples may simply be less responsive to depletion with the 2 AAs. Irrespective of risk classification, the patients from whom all 6 samples derive had refractory or relapsed disease and proved challenging to treat.

8.2.2 Potential further experimental work

There are a number of avenues that warrant further investigation. The first would be to test this strategy on AML samples in which valine or methionine depletion had a significant effect. This would allow for a better and simpler assessment of synergism. It is worth noting however that, although these 6 samples did demonstrate a response to valine or methionine depletion, it was less than with other samples.

Although using AML samples that are less susceptible to AA deprivation may be useful in investigating synthetic lethality this is a much larger experiment. I would consider testing synergism with drugs other than cytarabine. Both azacitidine and venetoclax

affect the metabolic and epigenetic regulation of AML and are now widely used in the relapsed or refractory setting [155, 156]. If effective, this would be tested against different concentrations of methionine and valine. The role of AA depletion in CAR-T therapy is also now being investigated [120].

8.3 Measuring AA uptake using LC-MS

8.3.1 General points

One of the main challenges was obtaining AML samples with adequate cell numbers to allow the collection of $1x10^6$ cell pellets in quadruplicate at both baseline and following co-culture. Some cellular samples had AA signal that was either undetectable or too low for quantification.

The analysis serves as a snap shot of a single time point in the metabolome. Although published elsewhere, absolute baseline intracellular AA concentrations are not presented here. For some AAs cellular concentrations were undetectable (eg proline) and for others concentrations were below the level of quantification (eg valine). Some data were therefore extrapolated using the internal standard concentrations. Baseline samples have the additional complication that other pre-analytical variables may strongly influence results. Time of sampling, circadian rhythm and fasting state can all effect steady state AA levels and impact on metabolism [157, 158]. Pre-processing factors such as collection tubes, delays and storage duration are also significant [159-161]. Delays in mononuclear cell isolation affect phosphorylation in AML cell lines [162]. Both EDTA and citrate tubes have been used in sample collection at the RMH. These effects were confirmed in some of my preliminary experiments.

For these reasons I concentrated on the relative change in AA concentrations in both cell pellets and media.

8.3.2 Duration of co-culture impacts results

The cell pellet AA concentration indicates the intracellular concentration. An increase can be caused by *de novo* AA synthesis (in non-essential AAs) or uptake from the surrounding media/supernatant. A fall in media AA concentration suggests the latter. Although a rise in intracellular AA concentration was seen in all (measurable) AAs this was associated with a corresponding fall in media concentration in only 5 AAs. No changes were significant. Given the fall in AML viability through apoptosis seen at 72 hours (chapter 3) and the cell losses sustained with this duration of co-culture, a shorter co-culture period should be used. Many of the cell pellet concentrations were below the level of quantification.

The shorter 24 hour co-culture period yielded results that are fully consistent with the data derived in chapter 3 and provides confirmatory evidence for the specific AA requirements of AML. Valine, methionine, glutamine and serine/glycine are critical for AML cell survival. Furthermore, the same effect is seen with the other branched-chain AAs (BCAAs), leucine and isoleucine.

Intracellular AA concentrations show less consistent results. This may reflect the challenges in obtaining adequate signal with LC-MS. Even a cell pellet of $1x10^6$ cells often led to results that were below the level of quantification or, in cases, undetectable. While using pellets of higher cell numbers is an option future studies should focus on supernatant/media values at 24 hours.

8.3.3 Multivariate analysis suggests adverse risk AML has higher AA requirements

Univariate analysis reveals no significant difference in AA demand between the intermediate and adverse risk groups (the 2 largest in this cohort). However, when the AAs were looked at together though a multivariate tool, there is separation of the two groups. This calculates a VIP score (variable of importance) which allows for the identification of the variables responsible for the separation. In the cell pellet analysis it is glycine, alanine and glutamine that are most responsible for this separation. In the media analysis there are more AAs responsible.

8.3.4 Potential further experimental work

The first step would be to extend the sample cohort. Ideally this would be with pellets of a larger cell number but, in reality, this may not be feasible given the number of samples with a sufficient number of mononuclear cells received at the RMH. Further, selecting out only high white count AML would not be representative [34, 163]. Using media/supernatant at 24 hours would be the best approach.

Our team has previously used flux experiments to demonstrate intracellular uptake using labelled $^{13}C_6$ arginine [64]. I have demonstrated that that 2 essential AAs are critical to AML cell growth and that media concentrations of both fall following 24 hour culture. Flux experiments using labelled Met and Val would provide further confirmatory evidence and indicate how rapidly the uptake occurs.

Whilst I have focused on valine, the media/supernatant data demonstrate a significant fall in the concentration of the other BCAAs indicating that they may be as critical. Leucine and isoleucine depleted co-culture experiments would further define this.

8.4 Cellular control and compensation in AA deprivation

8.4.1 MTAP expression demonstrates demand for methionine

In chapters 3 and 5 I have identified significant and critical AA requirements of AML cells. The hypothesis here was that the cellular response to AA deprivation was ATF4/eIF2α/GCN2 pathway mediated. MTAP was highly expressed in AML cells consistent with need for Met demonstrated in earlier chapters. The lack of significant response to Met depletion suggests that the Met salvage pathway cannot compensate in this scenario.

GCN2 and eIF2α expression is increased in AML patients suggesting that changes in AA levels are detected. Although the PHGDH is variable, there is no increase in ATF4 expression which would have provided evidence that changes are ISR mediated.

8.4.2 Potential further experimental work

I have not been able to demonstrate that the response to AA depletion is ISR mediated. The sample size is small. Given the combined data from chapters 3 and 5 I would measure ISR pathway enzymes following culture in Val deplete media.

The results from chapter 3 show that methionine deprivation is only effective in favourable risk AML. MTAP itself has been shown to aid prognostication in a number of tumour groups [164-166]. Quantifying MTAP expression across AML risk groups would be informative.

8.5: Proteomic analysis of AML

8.5.1 Proteomic changes are relatively small following AA depletion

Over 8000 proteins and peptides were measured in this analysis. The changes and patterns were change are considered relatively small in the Val and Met depleted cells compared to control. Overall this suggests that the effect of AA depletion in AML is at a metabolomic level rather a proteomic one. There is a significant increase in PHGDH which is expected. No change was observed in eIF2α which is consistent with the results in chapter 6 (eIF2α is highly expressed in AML cells but no increase in response to AA depletion was demonstrated). It is unfortunate that the other enzymes in the ISR pathway (ATF4, GCN2) or downstream (MTAP, MAT2A) are not measured in this panel.

8.5.2 Potential further experimental work

One sample was analysed in this experiment and the first step would be to repeat this with other AML samples. As mentioned in section 8.1.1, AML is heterogeneous and this must be emphasised in a single sample experiment. However, if similar results

were to be obtained then concentrating on changes in metabolites in response to AA depletion would be sensible.

8.6: Conclusions

8.6.1 Summary of key findings

AML cells have specific amino acid requirements on which they are dependent for survival. Depletion of glutamine, valine, methionine and serine/glycine caused apoptosis. In all but glutamine this was significantly increased compared to normal BM cells but this effect was not uniform across AML risk groups.

This was confirmed by significant media depletion of these AAs following co-culture for 24 hours. This effect was also seen with the other branched-chain leucine and isoleucine. Intracellular AA concentration was difficult to measure consistently due to low cell numbers. Multivariate analysis suggests that adverse risk AML consumes AAs more avidly than intermediate risk but further numbers are required.

There was no synergism when Val or Met depletion was combined with cytarabine but synergism should be tested in AML samples in which there was a significant response to AA depletion alone. It should also be tested with other drugs and in a greater number of AML samples.

The enzymes of the methionine salvage pathway are strongly expressed in AML consistent with the need for Met. Further work is needed to elucidate the role of the GCN2/eIF2α/ATF4 integrated stress response pathway.

Analysis of the AML proteome in response to Val and Met depletion reveals that only a small number of proteins change significantly suggesting that the effect is generally at a metabolomic level. A significant increase in PHGDH, a downstream enzyme in the ISR pathway, was however seen in response to AA depletion.

8.6.2 Potential clinical application

AA depletion is a proven treatment for haematological malignancies. Valine and methionine depletion seems likely to induce metabolic and epigenetic changes in AML cells that could potentially prime them and render them vulnerable to exploitation. 2 potential avenues are by drugs that target epigenetic changes or, in the case of valine, with short term depletion in combination with conditioning prior to haematopoietic stem cell transplantation.

Appendix 1: Results from LC-MS optimisation experiments

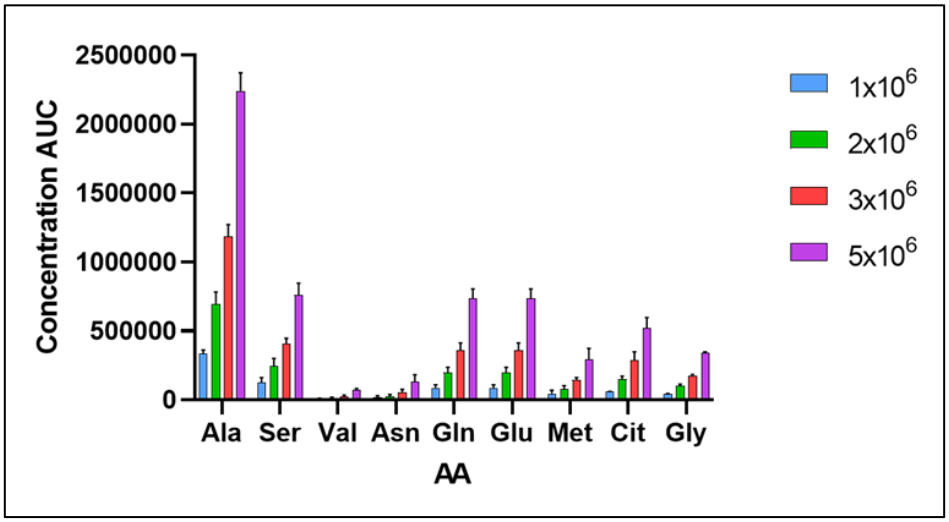

Appendix 1a: Bar chart showing AA signal from cell pellets of different cell number. This was to determine if results could be extrapolated when AA signal was low

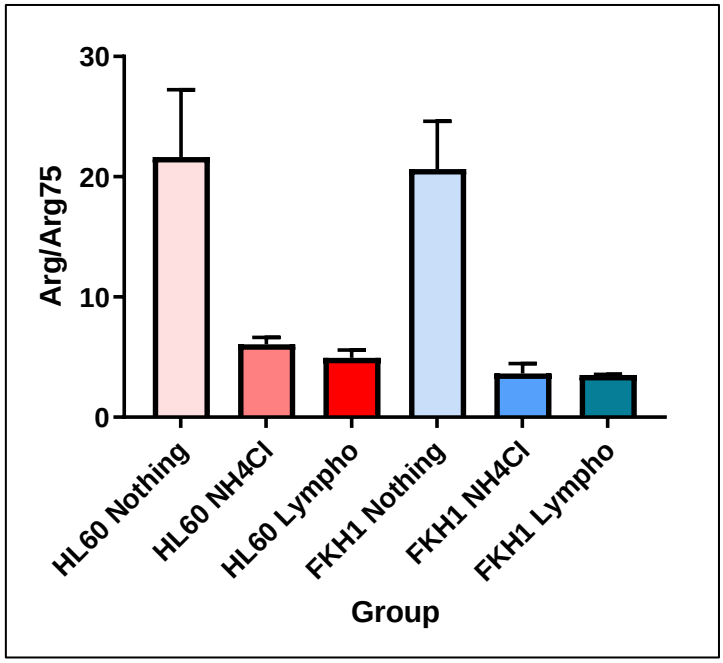

Appendix 1b: The effect of different methods of isolating mononuclear cells on AA signal (using arginine as an example). Nothing = slow separation on bench, Lympho = lymphoprep. Results indicate need for either NH4Cl or density centrifugation.

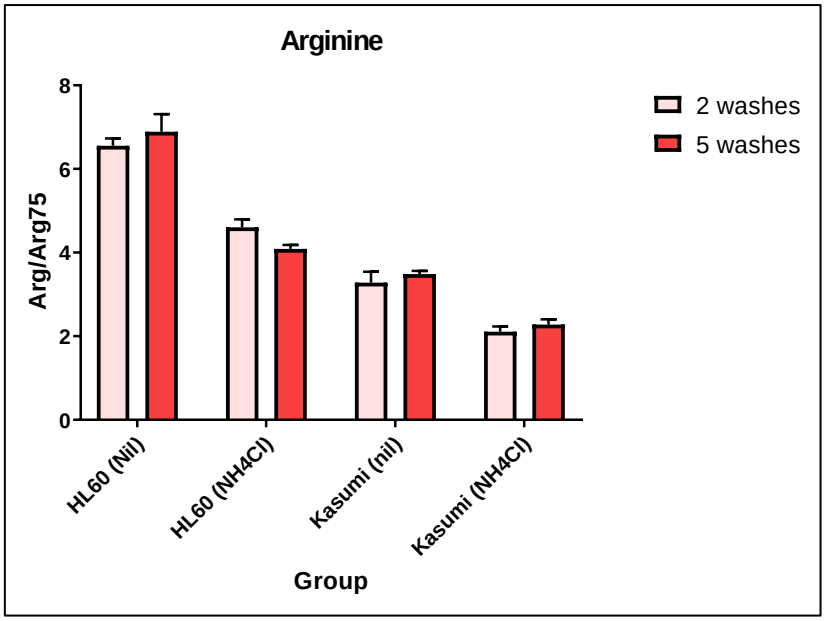

Appendix 1c: The addition of 3 extra washes does not change AA signal significantly

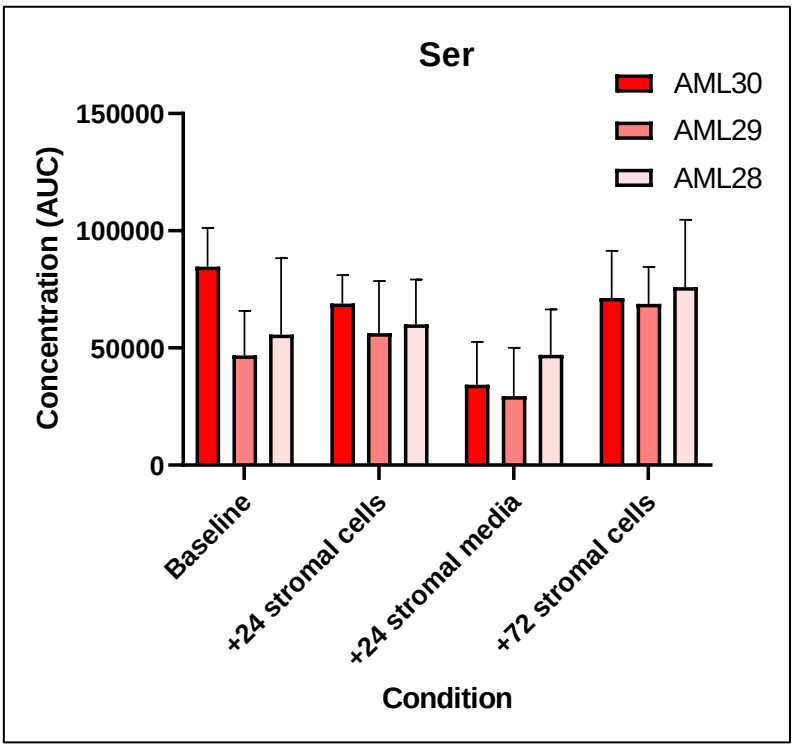

Appendix 1d: Media derived from MS-5 did not sustain cells in culture (insufficient cells at 72 hours to obtain LC-MS signal).

References

1. Khwaja, A., et al., *Acute myeloid leukaemia.* Nat Rev Dis Primers, 2016. **2**: p. 16010.
2. Döhner, H., D.J. Weisdorf, and C.D. Bloomfield, *Acute Myeloid Leukemia.* N Engl J Med, 2015. **373**(12): p. 1136-52.
3. Higgins, A. and M.V. Shah, *Genetic and Genomic Landscape of Secondary and Therapy-Related Acute Myeloid Leukemia.* Genes (Basel), 2020. **11**(7).
4. *Cancer Research UK*. https://www.cancerresearchuk.org/health-professional/cancer-statistics/statistics-by-cancer-type/leukaemia-aml/mortality, 2019.
5. Burnett, A.K., *Treatment of Older Patients With Newly Diagnosed AML Unfit for Traditional Therapy.* Clin Lymphoma Myeloma Leuk, 2018. **18**(9): p. 553-557.
6. Chen, W. and H.S. Luu, *Immunophenotyping by Multiparameter Flow Cytometry.* Methods Mol Biol, 2017. **1633**: p. 51-73.
7. Galera, P.K., C. Jiang, and R. Braylan, *Immunophenotyping of Acute Myeloid Leukemia.* Methods Mol Biol, 2019. **2032**: p. 281-296.
8. Schuurhuis, G.J., et al., *Minimal/measurable residual disease in AML: a consensus document from the European LeukemiaNet MRD Working Party.* Blood, 2018. **131**(12): p. 1275-1291.
9. Short, N.J., et al., *Association of Measurable Residual Disease With Survival Outcomes in Patients With Acute Myeloid Leukemia: A Systematic Review and Meta-analysis.* JAMA Oncol, 2020. **6**(12): p. 1890-1899.
10. Arber, D.A., et al., *The 2016 revision to the World Health Organization classification of myeloid neoplasms and acute leukemia.* Blood, 2016. **127**(20): p. 2391-2405.
11. Cancer Genome Atlas Research, N., et al., *Genomic and epigenomic landscapes of adult de novo acute myeloid leukemia.* N Engl J Med, 2013. **368**(22): p. 2059-74.
12. Kandoth, C., et al., *Mutational landscape and significance across 12 major cancer types.* Nature, 2013. **502**(7471): p. 333-339.
13. Li, S., et al., *Distinct evolution and dynamics of epigenetic and genetic heterogeneity in acute myeloid leukemia.* Nat Med, 2016. **22**(7): p. 792-9.
14. Dohner, H., et al., *Diagnosis and management of AML in adults: 2017 ELN recommendations from an international expert panel.* Blood, 2017. **129**(4): p. 424-447.
15. Grimwade, D., et al., *Refinement of cytogenetic classification in acute myeloid leukemia: determination of prognostic significance of rare recurring chromosomal abnormalities among 5876 younger adult patients treated in the United Kingdom Medical Research Council trials.* Blood, 2010. **116**(3): p. 354-65.
16. Grimwade, D., et al., *The importance of diagnostic cytogenetics on outcome in AML: analysis of 1,612 patients entered into the MRC AML 10 trial. The Medical Research Council Adult and Children's Leukaemia Working Parties.* Blood, 1998. **92**(7): p. 2322-33.

17. van der Lee, D.I., et al., *Mutated nucleophosmin 1 as immunotherapy target in acute myeloid leukemia.* J Clin Invest, 2019. **129**(2): p. 774-785.
18. Larrosa-Garcia, M. and M.R. Baer, *FLT3 Inhibitors in Acute Myeloid Leukemia: Current Status and Future Directions.* Mol Cancer Ther, 2017. **16**(6): p. 991-1001.
19. Gale, R.E., et al., *The impact of FLT3 internal tandem duplication mutant level, number, size, and interaction with NPM1 mutations in a large cohort of young adult patients with acute myeloid leukemia.* Blood, 2008. **111**(5): p. 2776-84.
20. Metzeler, K.H., et al., *ASXL1 mutations identify a high-risk subgroup of older patients with primary cytogenetically normal AML within the ELN Favorable genetic category.* Blood, 2011. **118**(26): p. 6920-9.
21. Rücker, F.G., et al., *TP53 alterations in acute myeloid leukemia with complex karyotype correlate with specific copy number alterations, monosomal karyotype, and dismal outcome.* Blood, 2012. **119**(9): p. 2114-21.
22. Padmakumar, D., et al., *A concise review on the molecular genetics of acute myeloid leukemia.* Leuk Res, 2021. **111**: p. 106727.
23. Federici, L. and B. Falini, *Nucleophosmin mutations in acute myeloid leukemia: a tale of protein unfolding and mislocalization.* Protein Sci, 2013. **22**(5): p. 545-56.
24. Medinger, M. and J.R. Passweg, *Acute myeloid leukaemia genomics.* British Journal of Haematology, 2017. **179**(4): p. 530-542.
25. Thiede, C., et al., *Prevalence and prognostic impact of NPM1 mutations in 1485 adult patients with acute myeloid leukemia (AML).* Blood, 2006. **107**(10): p. 4011-4020.
26. Zhao, J.C., et al., *A review of FLT3 inhibitors in acute myeloid leukemia.* Blood Rev, 2021: p. 100905.
27. Papaemmanuil, E., et al., *Genomic Classification and Prognosis in Acute Myeloid Leukemia.* N Engl J Med, 2016. **374**(23): p. 2209-2221.
28. Dombret, H. and R. Itzykson, *How and when to decide between epigenetic therapy and chemotherapy in patients with AML.* Hematology Am Soc Hematol Educ Program, 2017. **2017**(1): p. 45-53.
29. Haferlach, T. and I. Schmidts, *The power and potential of integrated diagnostics in acute myeloid leukaemia.* British Journal of Haematology, 2020. **188**(1): p. 36-48.
30. Moors, I., et al., *Clinical implications of measurable residual disease in AML: Review of current evidence.* Crit Rev Oncol Hematol, 2019. **133**: p. 142-148.
31. Bewersdorf, J.P., M. Stahl, and A.M. Zeidan, *Are we witnessing the start of a therapeutic revolution in acute myeloid leukemia?* Leuk Lymphoma, 2019. **60**(6): p. 1354-1369.
32. Mohamed, I., R.K. Hills, and A.K. Burnett, *Who is an "older" patient with acute myeloid leukaemia (AML)? An investigation of two NCRI/AML trials.* Br J Haematol, 2014. **165**(1): p. 147-51.
33. Daver, N., et al., *New directions for emerging therapies in acute myeloid leukemia: the next chapter.* Blood Cancer J, 2020. **10**(10): p. 107.
34. Burnett, A.K., et al., *A randomized comparison of daunorubicin 90 mg/m2 vs 60 mg/m2 in AML induction: results from the UK NCRI AML17 trial in 1206 patients.* Blood, 2015. **125**(25): p. 3878-85.

35. Loke, J., et al., *The role of allogeneic stem cell transplantation in the management of acute myeloid leukaemia: a triumph of hope and experience.* Br J Haematol, 2020. **188**(1): p. 129-146.
36. Ringdén, O., et al., *Outcome of Allogeneic Hematopoietic Stem Cell Transplantation in Patients Age >69 Years with Acute Myelogenous Leukemia: On Behalf of the Acute Leukemia Working Party of the European Society for Blood and Marrow Transplantation.* Biol Blood Marrow Transplant, 2019. **25**(10): p. 1975-1983.
37. Krug, U., et al., *The treatment of elderly patients with acute myeloid leukemia.* Dtsch Arztebl Int, 2011. **108**(51-52): p. 863-70.
38. Kantarjian, H., et al., *Intensive chemotherapy does not benefit most older patients (age 70 years or older) with acute myeloid leukemia.* Blood, 2010. **116**(22): p. 4422-9.
39. Dombret, H., et al., *International phase 3 study of azacitidine vs conventional care regimens in older patients with newly diagnosed AML with >30% blasts.* Blood, 2015. **126**(3): p. 291-9.
40. DiNardo, C.D. and A.H. Wei, *How I treat acute myeloid leukemia in the era of new drugs.* Blood, 2020. **135**(2): p. 85-96.
41. Burnett, A. and R. Stone, *AML: New Drugs but New Challenges.* Clin Lymphoma Myeloma Leuk, 2020. **20**(6): p. 341-350.
42. DiNardo, C.D., et al., *Venetoclax combined with decitabine or azacitidine in treatment-naive, elderly patients with acute myeloid leukemia.* Blood, 2019. **133**(1): p. 7-17.
43. Schmalbrock, L.K., et al., *Clonal evolution of acute myeloid leukemia with FLT3-ITD mutation under treatment with midostaurin.* Blood, 2021. **137**(22): p. 3093-3104.
44. Yao, K., et al., *Resistance to mutant IDH inhibitors in acute myeloid leukemia: Molecular mechanisms and therapeutic strategies.* Cancer Lett, 2022. **533**: p. 215603.
45. Katoh, M., *Genomic testing, tumor microenvironment and targeted therapy of Hedgehog-related human cancers.* Clin Sci (Lond), 2019. **133**(8): p. 953-970.
46. Konopleva, M.Y., *Mechanisms for resistance in AML insights into molecular pathways mediating resistance to venetoclax.* Best Pract Res Clin Haematol, 2021. **34**(1): p. 101251.
47. Gu, X., et al., *Decitabine- and 5-azacytidine resistance emerges from adaptive responses of the pyrimidine metabolism network.* Leukemia, 2021. **35**(4): p. 1023-1036.
48. DiNardo, C.D., et al., *Molecular patterns of response and treatment failure after frontline venetoclax combinations in older patients with AML.* Blood, 2020. **135**(11): p. 791-803.
49. Huang, A., et al., *Synthetic lethality as an engine for cancer drug target discovery.* Nat Rev Drug Discov, 2020. **19**(1): p. 23-38.
50. Bajpai, R., et al., *Targeting glutamine metabolism in multiple myeloma enhances BIM binding to BCL-2 eliciting synthetic lethality to venetoclax.* Oncogene, 2016. **35**(30): p. 3955-64.
51. Pan, R., et al., *Synthetic Lethality of Combined Bcl-2 Inhibition and p53 Activation in AML: Mechanisms and Superior Antileukemic Efficacy.* Cancer Cell, 2017. **32**(6): p. 748-760.e6.

52. Maifrede, S., et al., *Tyrosine kinase inhibitor-induced defects in DNA repair sensitize FLT3(ITD)-positive leukemia cells to PARP1 inhibitors.* Blood, 2018. **132**(1): p. 67-77.
53. Gale, R.E., et al., *No evidence that CD33 splicing SNP impacts the response to GO in younger adults with AML treated on UK MRC/NCRI trials.* Blood, 2018. **131**(4): p. 468-471.
54. Cicconi, L., et al., *Long-term results of all-trans retinoic acid and arsenic trioxide in non-high-risk acute promyelocytic leukemia: update of the APL0406 Italian-German randomized trial.* Leukemia, 2020. **34**(3): p. 914-918.
55. Ferguson, P., et al., *An operational definition of primary refractory acute myeloid leukemia allowing early identification of patients who may benefit from allogeneic stem cell transplantation.* Haematologica, 2016. **101**(11): p. 1351-1358.
56. Moser, C., et al., *A clinically applicable gene expression–based score predicts resistance to induction treatment in acute myeloid leukemia.* Blood Advances, 2021. **5**(22): p. 4752-4761.
57. Alwash, Y., et al., *Development of TP53 mutations over the course of therapy for acute myeloid leukemia.* Am J Hematol, 2021. **96**(11): p. 1420-1428.
58. DeWolf, S. and M.S. Tallman, *How I treat relapsed or refractory AML.* Blood, 2020. **136**(9): p. 1023-1032.
59. Zuanelli Brambilla, C., et al., *Relapse after Allogeneic Stem Cell Transplantation of Acute Myelogenous Leukemia and Myelodysplastic Syndrome and the Importance of Second Cellular Therapy.* Transplant Cell Ther, 2021. **27**(9): p. 771.e1-771.e10.
60. Endicott, M., M. Jones, and J. Hull, *Amino acid metabolism as a therapeutic target in cancer: a review.* Amino Acids, 2021. **53**(8): p. 1169-1179.
61. Warburg, O., *On the origin of cancer cells.* Science, 1956. **123**(3191): p. 309-14.
62. Matre, P., et al., *Inhibiting glutaminase in acute myeloid leukemia: metabolic dependency of selected AML subtypes.* Oncotarget, 2016. **7**(48): p. 79722-79735.
63. Liberti, M.V. and J.W. Locasale, *The Warburg Effect: How Does it Benefit Cancer Cells?* Trends Biochem Sci, 2016. **41**(3): p. 211-218.
64. Miraki-Moud, F., et al., *Arginine deprivation using pegylated arginine deiminase has activity against primary acute myeloid leukemia cells in vivo.* Blood, 2015. **125**(26): p. 4060-8.
65. Eagle, H., *The specific amino acid requirements of a mammalian cell (strain L) in tissue culture.* J Biol Chem, 1955. **214**(2): p. 839-52.
66. Mattaini, K.R., M.R. Sullivan, and M.G. Vander Heiden, *The importance of serine metabolism in cancer.* J Cell Biol, 2016. **214**(3): p. 249-57.
67. Lunt, S.Y. and M.G. Vander Heiden, *Aerobic glycolysis: meeting the metabolic requirements of cell proliferation.* Annu Rev Cell Dev Biol, 2011. **27**: p. 441-64.
68. Kobayashi, Y., et al., *Warburg effect in Gynecologic cancers.* J Obstet Gynaecol Res, 2019. **45**(3): p. 542-548.
69. Ganapathy-Kanniappan, S., *Molecular intricacies of aerobic glycolysis in cancer: current insights into the classic metabolic phenotype.* Crit Rev Biochem Mol Biol, 2018. **53**(6): p. 667-682.

70. Madhukar, N.S., M.O. Warmoes, and J.W. Locasale, *Organization of enzyme concentration across the metabolic network in cancer cells.* PLoS One, 2015. **10**(1): p. e0117131.
71. Lieu, E.L., et al., *Amino acids in cancer.* Exp Mol Med, 2020. **52**(1): p. 15-30.
72. Kilberg, M.S., et al., *The transcription factor network associated with the amino acid response in mammalian cells.* Adv Nutr, 2012. **3**(3): p. 295-306.
73. Endo, M., et al., *The ER stress pathway involving CHOP is activated in the lungs of LPS-treated mice.* J Biochem, 2005. **138**(4): p. 501-7.
74. De Vito, A., et al., *Amino acid deprivation triggers a novel GCN2-independent response leading to the transcriptional reactivation of non-native DNA sequences.* PLoS One, 2018. **13**(7): p. e0200783.
75. Wortel, I.M.N., et al., *Surviving Stress: Modulation of ATF4-Mediated Stress Responses in Normal and Malignant Cells.* Trends Endocrinol Metab, 2017. **28**(11): p. 794-806.
76. van Galen, P., et al., *Integrated Stress Response Activity Marks Stem Cells in Normal Hematopoiesis and Leukemia.* Cell Rep, 2018. **25**(5): p. 1109-1117 e5.
77. McConkey, D.J., *The integrated stress response and proteotoxicity in cancer therapy.* Biochem Biophys Res Commun, 2017. **482**(3): p. 450-453.
78. Kilberg, M.S., J. Shan, and N. Su, *ATF4-dependent transcription mediates signaling of amino acid limitation.* Trends Endocrinol Metab, 2009. **20**(9): p. 436-43.
79. Battu, S., et al., *Amino Acid Sensing via General Control Nonderepressible-2 Kinase and Immunological Programming.* Front Immunol, 2017. **8**: p. 1719.
80. Timosenko, E., et al., *Nutritional Stress Induced by Tryptophan-Degrading Enzymes Results in ATF4-Dependent Reprogramming of the Amino Acid Transporter Profile in Tumor Cells.* Cancer Res, 2016. **76**(21): p. 6193-6204.
81. Tajan, M., et al., *Serine synthesis pathway inhibition cooperates with dietary serine and glycine limitation for cancer therapy.* Nat Commun, 2021. **12**(1): p. 366.
82. Maddocks, O.D., et al., *Serine starvation induces stress and p53-dependent metabolic remodelling in cancer cells.* Nature, 2013. **493**(7433): p. 542-6.
83. Ye, J., et al., *Pyruvate kinase M2 promotes de novo serine synthesis to sustain mTORC1 activity and cell proliferation.* Proc Natl Acad Sci U S A, 2012. **109**(18): p. 6904-9.
84. Song, Z., et al., *PHGDH is an independent prognosis marker and contributes cell proliferation, migration and invasion in human pancreatic cancer.* Gene, 2018. **642**: p. 43-50.
85. Possemato, R., et al., *Functional genomics reveal that the serine synthesis pathway is essential in breast cancer.* Nature, 2011. **476**(7360): p. 346-50.
86. Yang, M. and K.H. Vousden, *Serine and one-carbon metabolism in cancer.* Nat Rev Cancer, 2016. **16**(10): p. 650-62.
87. Batool, T., et al., *A Comprehensive Review on L-Asparaginase and Its Applications.* Appl Biochem Biotechnol, 2016. **178**(5): p. 900-23.
88. Delage, B., et al., *Arginine deprivation and argininosuccinate synthetase expression in the treatment of cancer.* Int J Cancer, 2010. **126**(12): p. 2762-72.
89. Kremer, J.C. and B.A. Van Tine, *Therapeutic arginine starvation in ASS1-deficient cancers inhibits the Warburg effect.* Mol Cell Oncol, 2017. **4**(3): p. e1295131.

90. Shima, Y., et al., *L-arginine import via cationic amino acid transporter CAT1 is essential for both differentiation and proliferation of erythrocytes.* Blood, 2006. **107**(4): p. 1352-6.
91. Glazer, E.S., et al., *Phase II study of pegylated arginine deiminase for nonresectable and metastatic hepatocellular carcinoma.* J Clin Oncol, 2010. **28**(13): p. 2220-6.
92. Beddowes, E., et al., *Phase 1 Dose-Escalation Study of Pegylated Arginine Deiminase, Cisplatin, and Pemetrexed in Patients With Argininosuccinate Synthetase 1-Deficient Thoracic Cancers.* J Clin Oncol, 2017. **35**(16): p. 1778-1785.
93. Ott, P.A., et al., *Phase I/II study of pegylated arginine deiminase (ADI-PEG 20) in patients with advanced melanoma.* Invest New Drugs, 2013. **31**(2): p. 425-34.
94. Bean, G.R., et al., *A metabolic synthetic lethal strategy with arginine deprivation and chloroquine leads to cell death in ASS1-deficient sarcomas.* Cell Death Dis, 2016. **7**(10): p. e2406.
95. Tsai, H.J., et al., *A Phase II Study of Arginine Deiminase (ADI-PEG20) in Relapsed/Refractory or Poor-Risk Acute Myeloid Leukemia Patients.* Sci Rep, 2017. **7**(1): p. 11253.
96. Tsai, H.J., et al., *Phase I study of ADI-PEG20 plus low-dose cytarabine for the treatment of acute myeloid leukemia.* Cancer Med, 2021. **10**(9): p. 2946-2955.
97. Locke, M., et al., *Inhibition of the Polyamine Synthesis Pathway Is Synthetically Lethal with Loss of Argininosuccinate Synthase 1.* Cell Rep, 2016. **16**(6): p. 1604-1613.
98. Mussai, F., et al. , *A randomised evaluation of low-dose Ara-C plus BCT-100 versus low dose Ara-C in older patients with acute myeloid leukaemia: results from the LI-1 trial.* , in *ASH*. 2021.
99. Moren, L., et al., *Metabolomic profiling identifies distinct phenotypes for ASS1 positive and negative GBM.* BMC Cancer, 2018. **18**(1): p. 167.
100. Maddocks, O.D.K., et al., *Modulating the therapeutic response of tumours to dietary serine and glycine starvation.* Nature, 2017. **544**(7650): p. 372-376.
101. Amelio, I., et al., *Serine and glycine metabolism in cancer.* Trends Biochem Sci, 2014. **39**(4): p. 191-8.
102. Yoshino, H., et al., *Characterization of PHGDH expression in bladder cancer: potential targeting therapy with gemcitabine/cisplatin and the contribution of promoter DNA hypomethylation.* Mol Oncol, 2020. **14**(9): p. 2190-2202.
103. Pacold, M.E., et al., *A PHGDH inhibitor reveals coordination of serine synthesis and one-carbon unit fate.* Nat Chem Biol, 2016. **12**(6): p. 452-8.
104. Polet, F., et al., *Reducing the serine availability complements the inhibition of the glutamine metabolism to block leukemia cell growth.* Oncotarget, 2016. **7**(2): p. 1765-76.
105. Nishihira, T., et al., *Anti-cancer therapy with valine-depleted amino acid imbalance solution.* Tohoku J Exp Med, 1988. **156**(3): p. 259-70.
106. Ohtawa, K., et al., *Apoptosis of leukemia cells induced by valine-deficient medium.* Leukemia, 1998. **12**(10): p. 1651-2.
107. Taya, Y., et al., *Depleting dietary valine permits nonmyeloablative mouse hematopoietic stem cell transplantation.* Science, 2016. **354**(6316): p. 1152-1155.
108. Jones, C.L., et al., *Inhibition of Amino Acid Metabolism Selectively Targets Human Leukemia Stem Cells.* Cancer Cell, 2018. **34**(5): p. 724-740 e4.

109. Stockard, B., et al., *Cellular Metabolomics Profiles Associated With Drug Chemosensitivity in AML.* Front Oncol, 2021. **11**: p. 678008.
110. Han, L., et al., *Dietary methionine restriction improves the impairment of cardiac function in middle-aged obese mice.* Food Funct, 2020. **11**(2): p. 1764-1778.
111. Komninou, D., et al., *Methionine restriction delays aging-related urogenital diseases in male Fischer 344 rats.* Geroscience, 2020. **42**(1): p. 287-297.
112. Lee, B.C., et al., *Methionine restriction extends lifespan of Drosophila melanogaster under conditions of low amino-acid status.* Nat Commun, 2014. **5**: p. 3592.
113. Sanderson, S.M., et al., *Methionine metabolism in health and cancer: a nexus of diet and precision medicine.* Nat Rev Cancer, 2019. **19**(11): p. 625-637.
114. Jeon, H., et al., *Methionine deprivation suppresses triple-negative breast cancer metastasis in vitro and in vivo.* Oncotarget, 2016. **7**(41): p. 67223-67234.
115. Malin, D., et al., *Methionine restriction exposes a targetable redox vulnerability of triple-negative breast cancer cells by inducing thioredoxin reductase.* Breast Cancer Res Treat, 2021. **190**(3): p. 373-387.
116. Gao, X., et al., *Dietary methionine influences therapy in mouse cancer models and alters human metabolism.* Nature, 2019. **572**(7769): p. 397-401.
117. Barve, A., et al., *Perturbation of Methionine/S-adenosylmethionine Metabolism as a Novel Vulnerability in MLL Rearranged Leukemia.* Cells, 2019. **8**(11).
118. Zhou, X., et al., *Metabolomics analysis identifies lysine and taurine as candidate prognostic biomarkers for AML-M2 patients.* Int J Hematol, 2020. **111**(6): p. 761-770.
119. Tautt, J., et al., *Sensitivity of AML leucocytes in culture to L-methioninase.* Biochem Pharmacol, 1982. **31**(15): p. 2553-6.
120. Fultang, L., et al., *Targeting Amino Acid Metabolic Vulnerabilities in Myeloid Malignancies.* Front Oncol, 2021. **11**: p. 674720.
121. Heo, Y.A., Y.Y. Syed, and S.J. Keam, *Pegaspargase: A Review in Acute Lymphoblastic Leukaemia.* Drugs, 2019. **79**(7): p. 767-777.
122. Bertuccio, S.N., et al., *Identification of a cytogenetic and molecular subgroup of acute myeloid leukemias showing sensitivity to L-Asparaginase.* Oncotarget, 2017. **8**(66): p. 109915-109923.
123. Michelozzi, I.M., et al., *Acute myeloid leukaemia niche regulates response to L-asparaginase.* Br J Haematol, 2019. **186**(3): p. 420-430.
124. Chen, T., et al., *Antiproliferative effects of L-asparaginase in acute myeloid leukemia.* Exp Ther Med, 2020. **20**(3): p. 2070-2078.
125. Chen, L. and H. Cui, *Targeting Glutamine Induces Apoptosis: A Cancer Therapy Approach.* Int J Mol Sci, 2015. **16**(9): p. 22830-55.
126. Altman, B.J., Z.E. Stine, and C.V. Dang, *From Krebs to clinic: glutamine metabolism to cancer therapy.* Nat Rev Cancer, 2016. **16**(10): p. 619-34.
127. Vanhove, K., et al., *Glutamine Addiction and Therapeutic Strategies in Lung Cancer.* Int J Mol Sci, 2019. **20**(2).
128. Kodama, M., et al., *A shift in glutamine nitrogen metabolism contributes to the malignant progression of cancer.* Nat Commun, 2020. **11**(1): p. 1320.
129. Jacque, N., et al., *Targeting glutaminolysis has antileukemic activity in acute myeloid leukemia and synergizes with BCL-2 inhibition.* Blood, 2015. **126**(11): p. 1346-56.

130. Willems, L., et al., *Inhibiting glutamine uptake represents an attractive new strategy for treating acute myeloid leukemia.* Blood, 2013. **122**(20): p. 3521-32.
131. Gallipoli, P., et al., *Glutaminolysis is a metabolic dependency in FLT3(ITD) acute myeloid leukemia unmasked by FLT3 tyrosine kinase inhibition.* Blood, 2018. **131**(15): p. 1639-1653.
132. Muscaritoli, M., et al., *Plasma amino acid concentrations in patients with acute myelogenous leukemia.* Nutrition, 1999. **15**(3): p. 195-9.
133. Mussai, F., et al., *Arginine dependence of acute myeloid leukemia blast proliferation: a novel therapeutic target.* Blood, 2015. **125**(15): p. 2386-96.
134. Song, B.H., et al., *Profiling of Metabolic Differences between Hematopoietic Stem Cells and Acute/Chronic Myeloid Leukemia.* Metabolites, 2020. **10**(11).
135. Hall, P.E., et al., *Phase II Study of Arginine Deprivation Therapy With Pegargiminase in Patients With Relapsed Sensitive or Refractory Small-cell Lung Cancer.* Clin Lung Cancer, 2020. **21**(6): p. 527-533.
136. Szlosarek, P.W., et al., *Phase 1, pharmacogenomic, dose-expansion study of pegargiminase plus pemetrexed and cisplatin in patients with ASS1-deficient non-squamous non-small cell lung cancer.* Cancer Med, 2021. **10**(19): p. 6642-6652.
137. Griessinger, E., et al., *A niche-like culture system allowing the maintenance of primary human acute myeloid leukemia-initiating cells: a new tool to decipher their chemoresistance and self-renewal mechanisms.* Stem Cells Transl Med, 2014. **3**(4): p. 520-9.
138. McKinnon, K.M., *Flow Cytometry: An Overview.* Curr Protoc Immunol, 2018. **120**: p. 5.1.1-5.1.11.
139. Yuan, M., et al., *A positive/negative ion-switching, targeted mass spectrometry-based metabolomics platform for bodily fluids, cells, and fresh and fixed tissue.* Nat Protoc, 2012. **7**(5): p. 872-81.
140. Li, J., et al., *TMTpro reagents: a set of isobaric labeling mass tags enables simultaneous proteome-wide measurements across 16 samples.* Nat Methods, 2020. **17**(4): p. 399-404.
141. Ghazaly, E.A., et al., *Repression of sphingosine kinase (SK)-interacting protein (SKIP) in acute myeloid leukemia diminishes SK activity and its re-expression restores SK function.* J Biol Chem, 2020. **295**(16): p. 5496-5508.
142. Geijsen, A., et al., *Diet quality indices and dietary patterns are associated with plasma metabolites in colorectal cancer patients.* Eur J Nutr, 2021. **60**(6): p. 3171-3184.
143. Geijsen, A., et al., *Plasma metabolites associated with colorectal cancer stage: Findings from an international consortium.* Int J Cancer, 2020. **146**(12): p. 3256-3266.
144. Jonas, J.P., et al., *Circulating metabolites as a concept beyond tumor biology determining disease recurrence after resection of colorectal liver metastasis.* HPB (Oxford), 2021.
145. Liesenfeld, D.B., et al., *Review of mass spectrometry-based metabolomics in cancer research.* Cancer Epidemiol Biomarkers Prev, 2013. **22**(12): p. 2182-201.
146. Siskos, A.P., et al., *Interlaboratory Reproducibility of a Targeted Metabolomics Platform for Analysis of Human Serum and Plasma.* Anal Chem, 2017. **89**(1): p. 656-665.

147. Haverty, P.M., et al., *Reproducible pharmacogenomic profiling of cancer cell line panels.* Nature, 2016. **533**(7603): p. 333-7.
148. Ben-David, U., et al., *Genetic and transcriptional evolution alters cancer cell line drug response.* Nature, 2018. **560**(7718): p. 325-330.
149. Cucchi, D.G.J., et al., *Ex vivo cultures and drug testing of primary acute myeloid leukemia samples: Current techniques and implications for experimental design and outcome.* Drug Resist Updat, 2020. **53**: p. 100730.
150. Thandapani, P., et al., *Valine tRNA levels and availability regulate complex I assembly in leukaemia.* Nature, 2022. **601**(7893): p. 428-433.
151. Weng, A.P., et al., *Activating mutations of NOTCH1 in human T cell acute lymphoblastic leukemia.* Science, 2004. **306**(5694): p. 269-71.
152. Takam Kamga, P., et al., *Notch Signaling Molecules as Prognostic Biomarkers for Acute Myeloid Leukemia.* Cancers (Basel), 2019. **11**(12).
153. Xu, X., et al., *Activation of Notch signal pathway is associated with a poorer prognosis in acute myeloid leukemia.* Med Oncol, 2011. **28 Suppl 1**: p. S483-9.
154. Zhang, J., et al., *Prognostic impact of δ-like ligand 4 and Notch1 in acute myeloid leukemia.* Oncol Rep, 2012. **28**(4): p. 1503-11.
155. Roca-Portoles, A., et al., *Venetoclax causes metabolic reprogramming independent of BCL-2 inhibition.* Cell Death Dis, 2020. **11**(8): p. 616.
156. Pan, D., R. Rampal, and J. Mascarenhas, *Clinical developments in epigenetic-directed therapies in acute myeloid leukemia.* Blood Advances, 2020. **4**(5): p. 970-982.
157. Weng, L., et al., *Association of branched and aromatic amino acids levels with metabolic syndrome and impaired fasting glucose in hypertensive patients.* Metab Syndr Relat Disord, 2015. **13**(5): p. 195-202.
158. Krishnaiah, S.Y., et al., *Clock Regulation of Metabolites Reveals Coupling between Transcription and Metabolism.* Cell Metab, 2017. **25**(4): p. 961-974 e4.
159. Jain, M., et al., *Analytes related to erythrocyte metabolism are reliable biomarkers for preanalytical error due to delayed plasma processing in metabolomics studies.* Clin Chim Acta, 2017. **466**: p. 105-111.
160. Cruickshank-Quinn, C., et al., *Impact of Blood Collection Tubes and Sample Handling Time on Serum and Plasma Metabolome and Lipidome.* Metabolites, 2018. **8**(4).
161. Haid, M., et al., *Long-Term Stability of Human Plasma Metabolites during Storage at -80 °C.* J Proteome Res, 2018. **17**(1): p. 203-211.
162. van Alphen, C., et al., *The influence of delay in mononuclear cell isolation on acute myeloid leukemia phosphorylation profiles.* J Proteomics, 2021. **238**: p. 104134.
163. Pastore, F., et al., *The role of therapeutic leukapheresis in hyperleukocytotic AML.* PLoS One, 2014. **9**(4): p. e95062.
164. Su, C.Y., et al., *MTAP is an independent prognosis marker and the concordant loss of MTAP and p16 expression predicts short survival in non-small cell lung cancer patients.* Eur J Surg Oncol, 2014. **40**(9): p. 1143-50.
165. Nilforoushan, N. and N.A. Moatamed, *Evaluation of MTAP immunohistochemistry loss of expression in ovarian serous borderline tumors as a potential marker for prognosis and progression.* Ann Diagn Pathol, 2020. **48**: p. 151582.

166. Jing, W., et al., *MTAP-deficiency could predict better treatment response in advanced lung adenocarcinoma patients initially treated with pemetrexed-platinum chemotherapy and bevacizumab.* Sci Rep, 2020. **10**(1): p. 843.